Enhancing Upper Limb Prostheses Through Neuromorphic Sensory Feedback

by

Luke E. Osborn

A dissertation submitted to The Johns Hopkins University in conformity with the requirements for the degree of Doctor of Philosophy.

Baltimore, Maryland

December, 2018

Abstract

Upper limb prostheses are rapidly improving in terms of both control and sensory feedback, giving rise to lifelike robotic devices that aim to restore function to amputees. Recent progress in forward control has enabled prosthesis users to make complicated grip patterns with a prosthetic hand and nerve stimulation has enabled sensations of touch in the missing hand of an amputee. A brief overview of the motivation behind the work in this thesis is given in Chapter 1, which is followed by a general overview of the field and state of the art research (Chapter 2). Chapters 3 and 4 look at the use of closed loop tactile feedback for improving prosthesis grasping functionality. This entails development of two algorithms for improving object manipulation (Chapter 3) and the first real-time implementation of neuromorphic tactile signals being used as feedback to a prosthesis controller for improved grasping (Chapter 4).

The second half of the thesis (Chatpers 5 - 7) details how sensory information can be conveyed back to an amputee and how the tactile sensations can be utilized for creating a more lifelike prosthesis. Noninvasive electrical nerve stimulation was shown to provide sensations in multiple regions of the phantom hand of amputees both with and without targeted sensory reinnervation surgery (Chapter 5). A multilayered electronic dermis (e-dermis) was developed to mimic the behavior of receptors in the skin to provide, for the first time, sensations of both touch and pain back to an am-

putee and the prosthesis (Chapter 6). Finally, the first demonstration of sensory feedback as a key component of phantom hand movement for myoelectric pattern recognition shows that enhanced perceptions of the phantom hand can lead to improved prosthesis control (Chapter 7). This work provides the first demonstration of how amputees can perceive multiple tactile sensations through a neuromorphic stimulation paradigm. Furthermore, it describes the unique role that nerve stimulation and phantom hand activation play in the sensorimotor loop of upper limb amputees.

Thesis Committee

Primary Readers

Nitish V. Thakor, PhD (Primary Advisor)
Professor
Department of Biomedical Engineering
Department of Electrical and Computer Engineering
Johns Hopkins School of Medicine

Professor and Director
Singapore Institute for Neurotechnology
Department of Electrical and Computer Engineering
Department of Biomedical Engineering
National University of Singapore

Ralph Etienne-Cummings, PhD
Professor and Chair
Department of Electrical and Computer Engineering
Johns Hopkins University

Charles E. Connor, PhD
Professor
Department of Neuroscience
Johns Hopkins University School of Medicine

Acknowledgments

I would like to thank Dr. Nitish Thakor for his guidance, encouragement, and patience over the years. Without his unwavering dogma to focus and finish I wouldn't be where I am today. Thanks to everyone in the Neuroengineering & Biomedical Instrumentation Lab for their input, criticism, and support. Joseph Betthauser for his friendship and not holding back when critiquing my figures. Győrgy Lévay for his willingness and patience to be a subject for countless hours of experiments and for his constant desire to eat wings. Guy Hotson for his senior-grad-student wisdom and inspiringly large bowls of food. Chris Hunt for his coding and Bluetooth wizard skills. Harrison Nguyen and Chris Shallal for being the liaisons to the undergrad world. Mark Iskarous for stepping up and inheriting the defacto leadership role of all things demo, sensors, lab visit, and logistics related. Darshini Balamurugan, Teja Karri, and Avinash Sharma for their curiosity and enthusiasm in picking my brain. To all the undergraduate and high school students who worked in our lab and made sure I didn't slack off. The entire Infinite Biomedical Technologies team, especially Megan Hodgson, Martin Vilariño, and Damini Agarwal, for their willingness to help out a poor graduate student at a moments notice. Dr. Rahul Kaliki for his longtime friendship, mentorship, and football organization skills. The wonderful people in the Department of Biomedical Engineering at JHU who have supported me over the last several years, but most especially Sam Bourne for his couth and always being a source of insight and relief.

I must also thank my parents for teaching me how to read and limiting their questions about when I would graduate and get a job. My siblings Paul (and Alicia), Pamela, John Mark (and Maria), Mary Gail (and Joseph), Timothy, and Laura Ruth for setting the bar so high. Ayushi Sinha for her constant emotional support and understanding all the late nights I spent in the lab. Thanks to all of those close to me who have managed to put a smile on my face and remind me that there is indeed a world outside of these laboratory walls. Thanks to all the researchers, creators, and innovators before me who developed the technology and tools I used in my research. I'd also like to thank you, the reader, for taking an interest in my work. I hope you find this thesis as wildly riveting as I do.

Dedication

To my parents who never gave up and taught me the value of dedication, patience, and hard work

Contents

List of Tables

List of Figures

1 | Introduction

1.1 Motivation

There have been great efforts in restoring movements as well as the sense of touch to upper limb amputees through a prosthetic arm. Our sense of touch is a complicated, multi-faceted phenomenon of our daily lives. Providing realistic and meaningful sensory sensations back to an amputee is a challenging problem, but one with major implications if done successfully. Decoding intended movement signals, after many years, continues to be an active area of research; however, more recent efforts have focused on restoring the sensation of touch. In this thesis, I describe my work of providing sensory feedback to upper limb amputees in an effort to create a more sophisticated, lifelike neuroprosthesis.

1.2 Original contributions

The work presented in this thesis utilizes emerging techniques to create flexible tactile sensors for sensory feedback in prosthetic hands. Furthermore, it combines neuromorphic engineering principles to mimic behavior of skin receptors to provide meaningful sensory information to amputees and the prosthesis itself. Finally, in this work I explore the role sensory feedback plays in improving

phantom hand perceptions and the sensorimotor loop for enhanced prosthesis control.

1. Developed closed-loop feedback algorithms in to improve prosthesis grasping and object manipulation
2. Demonstrated a real-time implementation of neuromorphic tactile feedback to a prosthesis for local closed-loop control during object grasping
3. Demonstrated noninvasive electrical stimulation to provide localized sensory feedback in the phantom hand of multiple amputees and quantified perceptual qualities of the stimulation
4. Conceptualized and developed a multilayered electronic dermis (e-dermis) with neuromorphic encoding to convey sensory information of mechanoreceptors and nociceptors to an amputee to enable sensations of touch and pain
5. Conceptualized and investigated the hypothesis of using sensory feedback to improve prosthesis control as a direct result of enhance phantom limb perception in amputees

1.3 Publications

The following peer-reviewed publications were generated during the course of this research [1, 9, 13–32]. For convenience, the full citations are shown below. See Google Scholar to track my publications.

Journals

1. **L. E. Osborn**, M. A. Hays, R. Bose, A. Dragomir, Z. Tayeb, G. M. Lévay, A. Bezerianos, and N. V. Thakor, "Sensory feedback enhances phantom limb perception and prosthesis control," *In Preparation*, 2019.
2. **L. E. Osborn**, A. Dragomir, J. L. Betthauser, C. L. Hunt, H. H. Nguyen, R. R. Kaliki, and N. V. Thakor, "Prosthesis with neuromorphic multilayered e-dermis perceives touch and pain," *Science Robotics*, vol. 3, no. 19, p. eaat3818, 2018. [doi]

3. J. Betthauser, C. Hunt, **L. Osborn**, M. Masters, G. Lévay, R. Kaliki, and N. Thakor, "Limb position tolerant pattern recognition for myoelectric prosthesis control with adaptive sparse representations from extreme learning," *IEEE Transactions on Biomedical Engineering*, vol. 65, no. 4, pp. 770–778, 2018. [doi]

4. D. Yang, Y. Gu, L. Jiang, **L. Osborn**, and H. Liu, "Dynamic training protocol improves the robustness of pr-based myoelectric control," *Biomedical Signal Processing and Control*, vol. 31, pp. 249–256, 2017. [doi]

5. **L. Osborn**, R. Kaliki, A. Soares, and N. Thakor, "Neuromimetic event-based detection for closed-loop tactile feedback control of upper limb prostheses," *IEEE Transactions on Haptics*, vol. 9, no. 2, pp. 196–206, 2016. [doi]

Book chapters

1. **L. E. Osborn**, M. Iskarous, and N. V. Thakor, "Sensing and control for prosthetic hands in clinical and research applications," in *Wearable Robotics*. Elsevier, 2019, *under review*.

2. **L. E. Osborn**, J. L. Betthauser, and N. V. Thakor, "Neural prostheses," in *Wiley Encyclopedia of Electrical and Electronics Engineering*. John Wiley & Sons, 2019, *in press*, pp. 1–15.

Conferences

1. M. Hays, **L. Osborn**, R. Ghosh, M. Iskarous, C. Hunt, and N. V. Thakor, "Neuromorphic vision and tactile fusion for upper limb prosthesis control," in *IEEE Neural Engineering (NER)*, 2019, pp. 1–4.

2. M. M. Iskarous, H. H. Nguyen, **L. E. Osborn**, J. L. Betthauser, and N. V. Thakor, "Unsupervised learning and adaptive classification of neuromorphic tactile encoding of textures," in *IEEE Biomedical Circuits and Systems Conference (BioCAS)*, 2018, pp. 1–4.

3. H. Nguyen, **L. Osborn**, M. Iskarous, C. Shallal, C. Hunt, J. Betthauser, and N. V. Thakor, "Dynamic texture decoding using a neuromorphic multilayer tactile sensor," in *IEEE Biomedical Circuits and Systems Conference (BioCAS)*, 2018, pp. 1–4.

4. C. L. Hunt, A. Sharma, **L. E. Osborn**, R. R. Kaliki, and N. V. Thakor, "Predictive trajectory estimation during rehabilitative tasks in augmented reality using inertial sensors," in *IEEE Biomedical Circuits and Systems Conference (BioCAS)*, 2018, pp. 1–4.

5. A. Sharma, C. L. Hunt, A. Maheshwari, **L. Osborn**, G. Lévay, R. R. Kaliki, A. B. Soares, and V. Thakor, "A mixed-reality training environment for upper limb prosthesis control," in *IEEE Biomedical Circuits and Systems Conference (BioCAS)*, 2018, pp. 1–4.

6. J. Costacurta, , **L. Osborn**, N. Thakor, and S. Sarma, "Designing feedback controllers for human-prosthetic systems using h-infinity model matching," in *2018 40th Annual International Conference of the IEEE Engineering in Medicine and Biology Society (EMBC)*, 2018, pp. 2316 – 2319. [doi]

7. J. Fu, H. Nguyen, D. Kim, C. Shallal, S. Cho, **L. Osborn**, and N. Thakor, "Dynamically mapping socket loading conditions during real time operation of an upper limb prosthesis," in *2018 40th Annual International Conference of the IEEE Engineering in Medicine and Biology Society (EMBC)*, 2018, pp. 3930 – 3933. [doi]

8. **L. Osborn**, H. Nguyen, R. Kaliki, and N. Thakor, "Prosthesis grip force modulation using neuromorphic tactile sensing," in *Myoelectric Controls Symposium (MEC)*, 2017, pp. 188–191.

9. **L. Osborn**, M. Fifer, C. Moran, J. Betthauser, R. Armiger, R. Kaliki, and N. Thakor, "Targeted transcutaneous electrical nerve stimulation for phantom limb sensory feedback," in *IEEE Biomedical Circuits and Systems (BioCAS)*, 2017, pp. 1–4. [doi]

10. J. L. Betthauser, **L. E. Osborn**, R. R. Kaliki, and N. V. Thakor, "Electrode-shift tolerant myoelectric movement-pattern classification using extreme learning for adaptive sparse representations," in *IEEE Biomedical Circuits and Systems Conference (BioCAS)*, 2017, pp. 1–4. [doi]

11. C. Hunt, R. Yerrabelli, C. Clancy, **L. Osborn**, R. Kaliki, and N. Thakor, "Pham: prosthetic hand assessment measure," in *Proceedings of Myoelectric Controls Symposium*, 2017, pp. 221–224.

12. D. Candrea, A. Sharma, **L. Osborn**, Y. Gu, and N. Thakor, "An adaptable prosthetic socket: Regulating independent air bladders through closed-loop control," in *IEEE International Symposium on Circuits and Systems (ISCAS)*, May 2017, pp. 1–4. [doi]

13. **L. Osborn**, H. Nguyen, J. Betthauser, R. Kaliki, and N. Thakor, "Biologically inspired multi-layered synthetic skin for tactile feedback in prosthetic limbs," in *IEEE Engineering in Medicine and Biology Society (EMBC)*, 2016, pp. 4622–4625. [doi]

14. J. L. Betthauser, C. L. Hunt, **L. E. Osborn**, R. R. Kaliki, and N. V. Thakor, "Limb-position robust classification of myoelectric signals for prosthesis control using sparse representations," in *2016 38th Annual International Conference of the IEEE Engineering in Medicine and Biology Society (EMBC)*, 2016, pp. 6373–6376. [doi]

15. M. Masters, **L. Osborn**, N. Thakor, and A. Soares, "Real-time arm tracking for hmi applications," in *2015 IEEE 12th International Conference on Wearable and Implantable Body Sensor Networks (BSN)*, 2015, pp. 1–4. [doi]

1.4 Thesis organization

In Chapter 2, I give an introductory overview of upper limb prostheses and the current state of research for motor control, sensors, and sensory feedback. In Chapter 3, I explore how local tactile

feedback (i.e. to the prosthesis) can be used to improve prosthesis grasping and functionality. I then present results showing how neuromorphic tactile feedback can also be used to improve prosthesis grasping in Chapter 4. In Chapter 5, I describe results on providing noninvasive sensory feedback to amputees, and in Chapter 6 I demonstrate a neuromorphic electronic dermis (e-dermis) that enables a prosthesis and amputee to perceive both touch and pain. In Chapter 7, I show results suggesting the role of sensory feedback in improving prosthesis control by enhancing phantom limb perception. Finally, in Chapter 8, I summarize the thesis and discuss future directions and possibilities.

2 | Neural Prostheses & Literature Review

Unless specified otherwise, this chapter is made up of content, with permissions and minor modifications, from the following sources.

 Adapted from:

> L. E. Osborn, J. L. Betthauser, and N. V. Thakor, "Neural prostheses," in *Wiley Encyclopedia of Electrical and Electronics Engineering*. John Wiley & Sons, 2019, ch. *in press*, pp. 1–15

Adapted from:

> L. E. Osborn, M. Iskarous, and N. V. Thakor, "Sensing and control for prosthetic hands in clinical and research applications," in *Wearable Robotics*. Elsevier, 2019, ch. *under review*

2.1 Overview

Millions of people worldwide are affected by some disability, including but not limited to limb loss, hearing loss, spinal cord injury, or visual impairment. Neural prostheses are designed to provide or replace lost functionality to these individuals. In the case of upper limb loss, simplified hook-like body powered controlled prostheses can be used; however, recent technological developments have led to anthropomorphic dexterous manipulators that require more advanced control strategies. Further, direct control of these manipulators via neural motor signals is seen as a more natural and biomimetic solution. Recent work has utilized direct neural interfacing with the brain to measure

motor commands for prosthesis control and to deliver sensory percepts to the user, either through the peripheral nervous system or the cortex. This chapter provides an introductory overview of neural prostheses and a look at the relevant state of the art in bidirectional neural prostheses, specifically incorporation of sensory feedback for prosthetic arms.

2.2 Background

It is estimated that there are more than 1.3 million Americans living with some form of limb loss [33] and more than 5.4 million Americans living with paralysis [34]. Together, these two groups represent more than 2% of the total US population. These statistics serve to justify the need for neurotechnologies such as neural prostheses, which are devices that can restore physiological motor functionality or sensation to users. Most recipients of a neural prosthesis suffer from damage to at least one motor or sensory pathway that inhibits their natural function (Fig. 2.1). Whether an individual is suffering from lost limb function or the ability to see, a neural prosthesis combines physiological processes and engineering concepts to create a functional replacement.

Neural motor prosthesis control is an area of active research devoted to aiding those with lost limb function to utilize their functioning neural transmission pathways for direct control of robotic limbs [35–37]. Neural prostheses that provide sensory feedback are also an active area of research ranging from restoration of hearing [38], vision [39], and touch [2]. Traditional neural prosthesis examples include implants for replacing functionality in the cochlea or the retina. More recently, neurotechnology advancements have made restoring both movement and the sense of touch in upper limb amputees a reality.

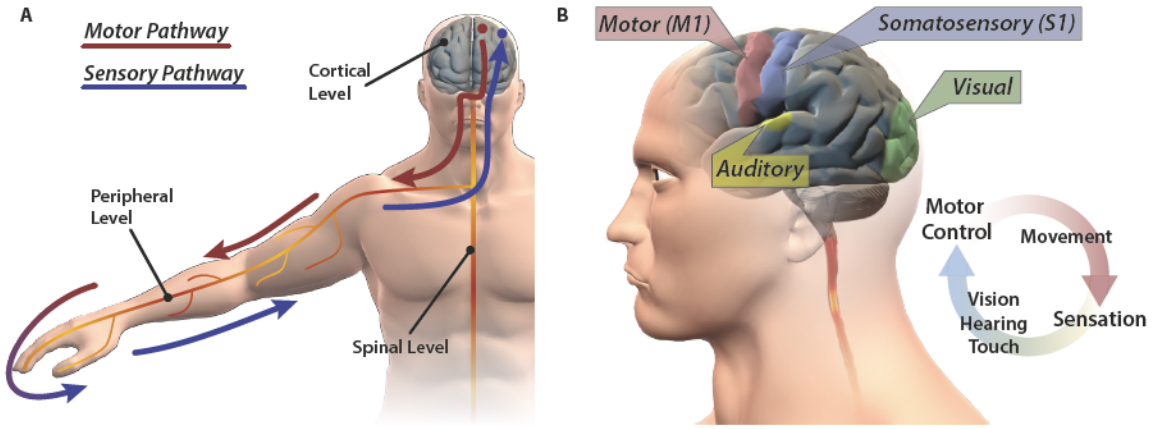

Figure 2.1: The human nervous system contains both motor and sensory pathways. (A) Voluntary body movement intent originates at the cortical level and then descends through the spinal cord and peripheral nerves to muscles. Sensory receptors throughout the body capture external information and provide feedback through ascending pathways. (B) At the cortical level, motor and sensory information is represented in different cortices of the brain. For neural prostheses, the primary motor cortex (M1) is of interest for accessing and decoding intended movement while somatosensory (S1), visual, and auditory cortex contain regions for accessing and encoding feedback. Together, the motor and sensory pathways form a continuous cycle of feedback to improve efficiency and functionality in our daily lives. Reprinted from [1].

2.3 Prosthesis fundamentals

The typical components of a neural prosthesis can be classified based on purpose and function. In these devices, there is always 1) a sensor or electrode interface with the nervous system to record or output signal data, 2) a processing unit to handle data transfer, which also includes an encoding and/or decoding algorithm to transform the data into meaningful output signals, and 3) an interface with an external device, such as a robotic limb or sensor (Fig. 2.2. An additional component commonly found in neural prostheses is hardware for wireless data and power transfer between the neural interface, the processing unit, and the external device or sensors. These components can be further defined based on the type of targeted neural function such as forward motor control for limb movement or sensory feedback to restore neural perceptions. The primary difference between motor and sensory prostheses is that for motor prostheses the neural interface captures a user's intent by measuring physiological signals, but in sensory prostheses the stimulation occurs at the neural

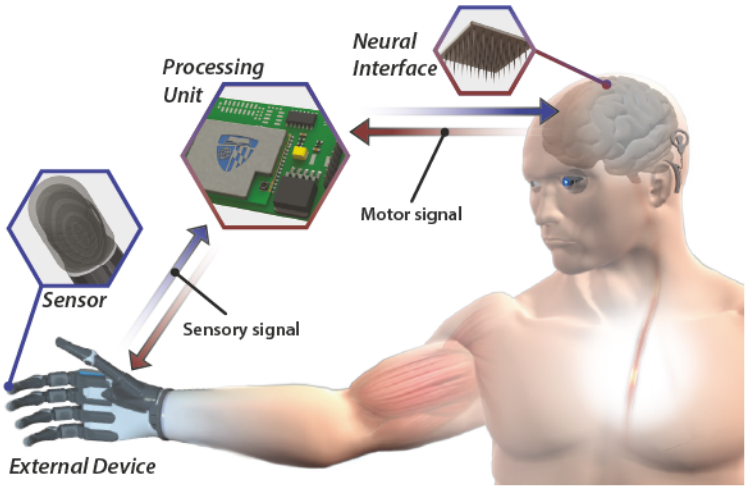

Figure 2.2: The fundamental components of neural prostheses include a neural interface, a processing unit to interpret the signal, and an external device such as a prosthetic hand with a touch sensor. Together, these make up the neural prosthesis, which connects to the nervous system and aims to restore motor, sensory, and even cognitive functionality. Whether providing sensory perception (touch, etc) or forward control (limb movement), a neural prosthesis can have a significant impact on improving functionality. The external device can provide movement (motor prosthesis) or be a sensor for capturing perception (sensory prosthesis). A bidirectional neural prosthesis, such as a prosthetic arm, includes pathways for both feedforward control and sensory feedback to the user's nervous system. Reprinted from [1].

interface to provide perception. Because of this difference, the information flow (i.e. the direction of signals) is reversed for the individual devices. In forward (i.e. motor) prosthetic devices, neural signals commonly captured by electrodes and signal conditioning circuits go from the nervous system to an external device, such as a robotic hand. In feedback (i.e. sensory) devices, a signal from the sensors on a prosthesis, such as tactile sensors, relay the sensor data back to the user's nervous system. It should be noted that in some cases sensory feedback can be sent to the processing unit for some automated control, such as in a reflex pathway to prevent object slip during grasping or even pain. Regardless, the key components of the system remain (sensor, processor, algorithm, wireless data transfer). For bidirectional neural prostheses, specifically upper limb devices, the combination of forward control with feedback presents additional challenges for both hardware and algorithms for processing and transferring signals. This chapter provides a brief overview of some of these components, but a more detailed description can be found in [1].

2.3.1 Neural interface

In both cases of motor and sensory prostheses, the neural interface can be at either the cortical level, including cranial nerves, the spinal cord level, or peripheral level of the nervous system, each bringing their own advantages and problems. At the cortical and peripheral levels, the interface can either record from or stimulate the nervous system. An important note is that typical neural interfaces to the spinal cord aim to stimulate either motor or sensory pathways. Physiological signals for motor control are usually not recorded from the spinal cord for decoding and moving an external limb due to limitations on the ability to record signals for more than a few months using piercing microelectrode arrays (MEA) and the inability to access specific motor tracts using surface electrodes [40]. However, motor pathways in the spinal cord can be stimulated to create limb movement if the corresponding pathways are still intact, such as in high level spinal cord injury (SCI) [41], or the pathways can be bypassed altogether and muscle stimulated directly [42].

At the cortical level, electrode arrays can be placed on the surface of the scalp for electroencephalography (EEG), and penetrating MEAs can target neurons in the brain and record action potentials. One commonly used MEA is the High-Density Utah Slanted Electrode Array (HD-USEA), with up to 90 individual electrodes, that can target neurons below the surface of the cortex [43]. Electrodes can also be placed on the surface of the brain directly for electrocorticography (ECoG). While EEG arrays are typically used for recording population signals from the brain, ECoG and penetrating MEAs can be used for stimulating or recording from neurons. Microwires, nerve cuffs, penetrating microelectrodes, and non-invasive electrodes on the surface of the skin can be used for interfacing with the peripheral nervous system (PNS). At the peripheral interface, the electrodes can be used to record muscle activity from electromyography (EMG) for motor control or to stimulate

peripheral nerves for sensory feedback. In addition to cuff electrodes that wrap around and stimulate an entire peripheral nerve, there are also specialized electrodes for sensory feedback, namely the longitudinally implanted intrafascicular electrode (LIFE), which penetrates the nerve to target a single fascicle [44], the transverse intrafascicular multichannel electrode (TIME), which penetrates the nerve and targets multiple fascicles [45], and the flat interface nerve electrode (FINE), which increases the surface area of target fascicles and moves central axons within the fascicle closer to the surface of the nerve [46]. A more detailed discussion of electrodes for neural interfacing, including material considerations, can be found in [47, 48] and a review of implantable technology for stimulation can be found in [49].

Sensory feedback through the neural interfacing can be achieved using either constant voltage or constant current stimulation strategies [50]; however, it is worth noting that mechanical stimulation can also be provided to peripheral nerves to elicit sensory feedback as well [51]. An overview of the type of signals captured by the various neural interfaces discussed in this section can be found in [52].

2.3.2 External hardware interface

Another fundamental component of a neural prosthesis is the external hardware. For motor prostheses, the external hardware is typically a robotic limb, a cursor on a screen, or a wheelchair controller. In the feedforward case (i.e. motor prosthesis), the external hardware is the component that carries out a user's intent (i.e. movement). For a sensory prosthesis, the processing unit connects to and processes signals from external sensors. The sensors in the feedback case (i.e. sensory prosthesis) capture parts of the environment, such as the sense of touch, which is transmitted back to the user

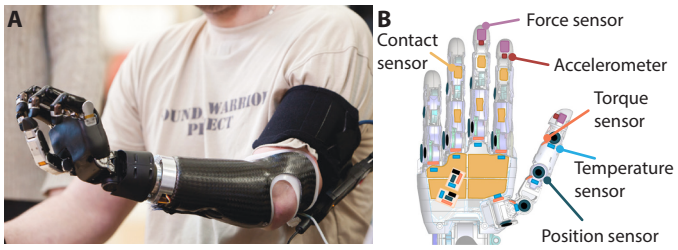

Figure 2.3: (A) The JHU/APL Modular Prosthetic Limb has 26 controllable degrees of freedom in 17 articulating joints and (B) over 100 sensors including position, force, acceleration, contact, and temperature. Images courtesy of Johns Hopkins University Applied Physics Laboratory.

(i.e. sensory perception). The external hardware is crucial to a neural prosthesis because it is the interface between the environment and the user. In both cases, the external hardware also interfaces with the processing unit and the decoding/encoding algorithms.

For bidirectional neural prostheses, the external hardware contains both motor and sensory elements. One example is the Modular Prosthetic Limb (MPL) by the Johns Hopkins University Applied Physics Laboratory (JHU/APL) [53] (Fig. 2.3A). The MPL is capable of mimicking almost every movement of a human arm. It is a sophisticated robotic limb and has been the external hardware used in several key developments for motor neural prostheses [54–56]. In addition, the MPL contains force, acceleration, torque, temperature, and position sensors (Fig. 2.3B). The MPL has also been used as a sensory prosthesis wherein tactile measurements from sensors in the hand were used to stimulate the primary somatosensory cortex (S1) in both humans [57] and non-human primates [58] to provide realistic sensory feedback.

2.4 Motor prosthesis

Cosmetic, body-powered, and myoelectric devices are the most common prosthetic hands, each making up roughly one third of devices used [59]. The focus here is on electronically powered

prosthetic hands because they present interesting control challenges. Multi-articulated prosthetic hands can be controlled by a range of physiological signals, but there are several challenges that researchers and users face when decoding intended movements, such as effects from limb position and electrode contact.

2.4.1 Movement signals & decoding

Electrical activity produced within the nervous system initiates movement. This activity is generated in the cortex and is sent through the spinal cord to the peripheral nerves and finally to the muscles which then causes muscle contractions and ultimately limb movement. For a prosthetic hand, the electrical activity that results from volitional movement is captured and sent to a controller that classifies the intended movement and outputs the correct commands to the prosthesis to drive movement. The common modalities for recording electrical activity due to intended movement from the brain are *EEG*, *ECoG*, and *action potentials*. Electrical activity from muscle movement can also be recorded from the peripheral nervous system with *EMG*, which is the most common technique for controlling upper limb prostheses, as it is noninvasive and relatively easy to set up.

Cortical and peripheral signals require delicate and usually invasive neural interfaces. For complex and dexterous prostheses in real-world applications, these decoding and control signals are still difficult to record, decode and manipulate. Surface EMG signals can be obtained noninvasively and have served very well as a practical alternative for today's myoelectrically controlled prostheses. EMG signals are easy to acquire and don't require a significant setup period. EMG can be recorded invasively using implanted electrodes to measure intramuscular activity; however, this approach has not become as common. A thorough discussion of EMG and its use in controlling prosthetic hands

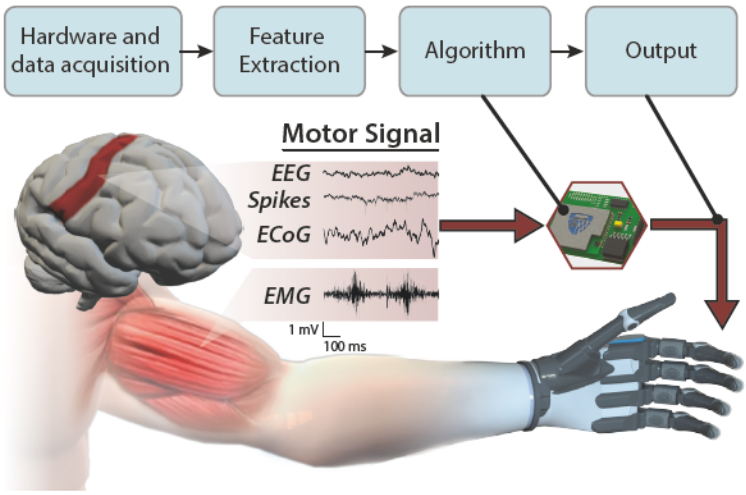

Figure 2.4: Motor neural prostheses utilize neural signals that convey user intent. One example is decoding EMG signals to determine the intended movement of a hand prosthesis. The primary motor cortex (M1) can be recorded to capture neural activity in the form of EEG, neuron spikes, or ECoG signals. EMG signals from the peripheral nervous system (PNS) can also be used to capture motor intent. The motor signal is processed to extract key features before passing through an algorithm to determine the desired movement. Reprinted from [1].

can be found in [60].

The emerging method for controlling a prosthetic hand is myoelectric pattern recognition. The idea being that when natural movements are made by an amputee, they elicit unique and reproducible neural signal patterns. Those signals are recorded and decoded into different intended hand or limb movements. The signals are then transformed into features, which are then mapped to corresponding hand movements using pattern recognition techniques (Fig. 2.4). Various machine learning techniques such as Kalman filters [3, 61], linear regression [62], neural networks [63], maximum likelihood estimation [64], and linear discriminant analysis [65] can be utilized to classify hand movements based on the neural signals. These methods can be used regardless of the neural signal being used to decode intended movements.

In general, pattern recognition techniques have been continuously improved over the past several years [14, 60, 66] and results have shown that training is a major factor in improving prosthesis

control [67]. Recently, linear regression techniques with surface EMG signals have enabled simultaneous DOF and proportional prosthesis control, which improves functionality during activities of daily living [62]. Another emerging trend is the use of high density EMG signals to create images of EMG activity for predicting hand movements [68]. Additional details on prosthesis control, including effects that degrade movement classification performance, can be found in [1, 17, 60]

2.4.2 Targeted muscle reinnervation (TMR) & osseointegration

TMR is a surgical technique where the nerves from an amputated limb are placed into healthy muscles to act as bio-amplifiers, making movement signals stronger and easier to measure [69, 70]. TMR has greatly improved the ability for prosthesis users to achieve a wider range of grips and patterns while controlling their limb [71].

A relatively new method known as osseointegration has also been shown to address several common issues such as prosthesis loading and position effects. In osseointegration, the prosthesis attaches directly to the body through a metal link that is inserted directly into the bone in the residual limb of an amputee. This intimate human-machine interface alleviates several issues such as loading effects that cause changes to surface EMG signals while also improving mobility and range of motion of the prosthesis. [72].

2.4.3 State of the art

Researchers are beginning to take advantage of new surgical techniques like TMR to develop enhanced decoding strategies [73] and achieve greater dexterity [71] for further improving prosthesis control. Another developing area is in designing control strategies that enable both simultaneous and proportional prosthesis control. Typically, users can only control 1 degree of freedom (DOF)

of their prosthesis at a time. Recently, researchers have shown promising results with simultaneous and proportional control in 2 [62] and 5 DOFs [3]. Challenges that will continue to be addressed include environmental effects such as limb position and loading. Researchers will undoubtedly turn towards more sophisticated machine learning techniques to resolve these issues.

2.5 Sensory prosthesis

Sensory feedback is also an important part for prosthetic hands. Traditionally, prosthesis users relied on visual and auditory information to monitor their prosthesis during manipulation. With the recent advancements in providing sensory feedback to users, researchers have shown that we can now complete the feedback loop by providing natural sensations back to amputees so they can actually feel with their prosthesis.

Touch is a complicated, multi-faceted sensation that works in harmony with muscle movements to enable highly sophisticated manipulation tasks and tactile perceptions. One of the challenges of providing sensory feedback is not only capturing comprehensive touch information through sensors but also in providing that information back to a user, effectively closing the loop (Fig. 2.5). Some of the most significant advancement in upper limb prostheses in the past several years have come in the form of sensory feedback to amputees. Sensory feedback can be provided by stimulating the peripheral nerves or even the somatosensory cortex directly. For peripheral nerve stimulation, relevant sensory feedback can be achieved by using noninvasive approaches, such as transcutaneous electrical nerve stimulation (TENS), or using electrodes implanted directly into the nerves. The median, ulnar, and radial nerves are the primary target when providing sensory feedback due to their coverage of the hand.

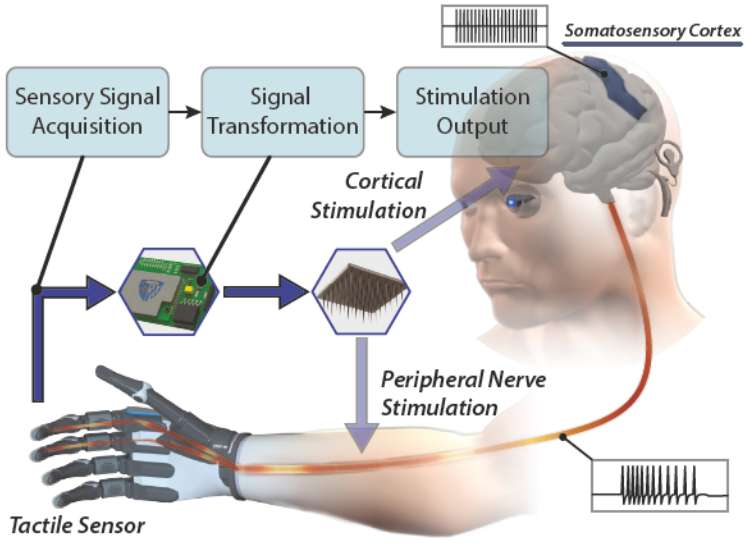

Figure 2.5: In sensory neural prostheses, some external sensor measurement, such as touch on a prosthetic hand, is recorded and sent to the processing unit. The sensor signal is transformed into unique stimulation patterns to be sent to either the peripheral nerves or the cortex. The stimulation pattern is determined by the neural target for stimulation to elicit a more natural perception. Reprinted from [1].

2.5.1 Touch sensing in humans

Before giving details on sensors used in hand prostheses, it is useful to take a brief look at the sensing capabilities of intact hands. Prosthetic hands replace lost or missing hands, so it makes sense that these devices should aim to mimic the functionality and behavior of their biological counterparts. In healthy skin, we have receptors and complex feedback loops to convey interoceptive, such as proprioception, and exteroceptive, such as pressure, temperature, and pain, perceptions. Mechanoreceptors are the primary means of our ability to perceive touch, and they are classified as either slowly adapting (SA) (Merkel cells (SA1) and Ruffini endings (SA2)) or rapidly adapting (Meissner (RA1) and Pacinian corpuscles (RA2)). SA mechanoreceptors respond to sustained loads, whereas RAs respond primarily to the transient periods of tactile loading [74].

While mechanoreceptors provide information on touch, nociceptors (free nerve endings) in the skin are responsible for conveying noxious (painful) mechanical sensations [75]. Aδ- and C-low

threshold mechanoreceptors (LTMRs) are primarily responsible for conveying sensations of temperature and it is thought that SA2 receptors, which respond to things like skin stretch, work in conjunction with muscle spindles to provide sensations of proprioception [74]. Although mechanoreceptor and afferent nerve behavior have been researched for several decades to understand their role in touch [76] and sensory-motor coordination [77], there is still active research on how sensory information is transmitted and utilized in our bodies [78].

Biological sensory receptors and pathways provide insight into the necessary components required for making sophisticated prosthetic hands that can provide meaningful, relevant, and natural sensations back to the user. A closer look at receptor behavior and how this can be modeled will be discussed in later chapters.

2.5.2 Sensors and advanced materials

More recently, there has been progress in materials science to create more sophisticated sensing modalities and electronic skins (e-skins). For prosthetic hands, an e-skin is ideal because the sensors are embodied in flexible or compliant materials. The capture of sensory information, such as touch and proprioception, is only part of an e-skin, as there are other factors that have been developed such as flexibility, compliance, self-healing, and other skin-like characteristics. Researchers have used advanced materials to create stretchable sensors [79], microstructured ferroelectric skins with pressure and temperature sensing [80], compliant prosthetic fingers that use stretchable waveguides to detect pressure [81], compliant and wireless e-skins [82], and rehealable and malleable e-skin [83].

Pressure and flexion sensors have also been developed that can both electrically and mechan-

ically heal themselves [84]. Entire pneumatic robots have also been shown to self-heal [85]. Ultraflexible organic electronics have also been constructed into skin-like material [86], and even biomimetic temperature sensitive layers [87]. More relevant to prosthetic hands, has been the development of e-skins with sensors that behave like actual mechanoreceptors. Spiking like outputs from a pressure sensor were created by ring oscillators and used to directly stimulate neurons in the somatosensory cortex of a mouse [88]. More recently, an artificial afferent was created using flexible organic electronics to mimic the function of a sensory nerve, which converted pressure into action potentials, also using ring oscillators, to stimulate motor nerves in a cockroach [89]. For a more thorough discussion of flexible electronics, advanced materials for sensors, and e-skins, see [90].

2.5.3 Sensory feedback

Tactile

For clarity, we refer to tactile as a sensation that can include perceptions of force, pressure, vibration, or texture. Groundbreaking results show the ability to provide sensory activation and sensations of pressure in the thumb, index finger, and pinky of the phantom hand of an amputee using implanted stimulating electrodes [91]. Through tactile perceptions, prosthesis users with implanted stimulating electrodes in their median and ulnar nerves have been shown to differentiate between object stiffness [91], perform fine motor movements such as pulling a stem off a cherry [2], and improve performance in functional tasks [92] and activities of daily living [72].

Touch sensations have been mapped in the phantom hand in several different studies, and each case varies in terms of the coverage obtained. Stimulation from multiple microelectrode arrays implanted in the median and ulnar nerves was shown to provide several percepts in one study [2]

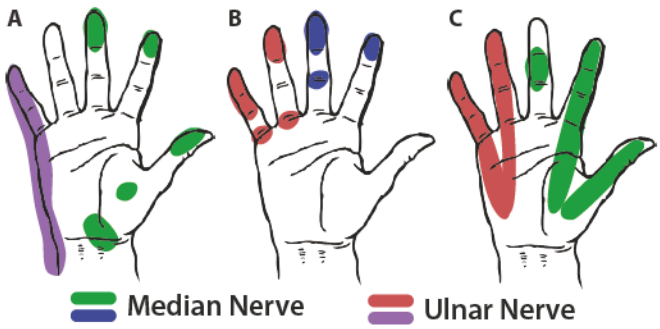

Figure 2.6: Sensory mapping of the phantom hand can provide information on the types of sensations perceived by the amputee. (A) Tactile perceptions are generally perceived in parts of the phantom hand that were once innervated by the median and ulnar nerves. Results adapted from [2]. (B) In general, sensory mapping varies in each case. For implanted stimulating electrodes, perceptions seem to be localized to smaller areas. This sensory map shows the general coverage of sensory feedback provided to amputees through electrodes implanted in the median and ulnar nerves. Individual percepts were localized to smaller regions within the larger areas. Results adapted from [3]. (C) Noninvasive stimulation of median and ulnar nerves can also provide tactile sensations and each stimulation site generally covers larger areas of the phantom hand. Results adapted from [4].

(Fig. 2.6A) and over 100 percepts in another study [3] (Fig. 2.6B). Implanted stimulating electrodes are able to target smaller nerve fascicles, as opposed to the larger nerve bundles likely activated using noninvasive approaches, which has the potential to provide more localized and a greater variety of tactile percepts in the phantom hand.

Sensations can also be provided by noninvasively electrically stimulating the peripheral nerves [4, 93, 94] (Fig. 2.6C). Despite not having direct contact with the peripheral nerve, electrical stimulation dissipates through the skin and, if positioned correctly, can reach and activate the underlying peripheral nerve bundles. Targeting the underlying nerves through the skin can be a difficult process, but targeted sensory reinnervation (TSR), a surgical technique that intentionally separates sensory nerves during surgery, can be used to enable larger spatial coverage of tactile feedback in the phantom hand [51, 95]. It was shown that subjects who had undergone TSR had a capacity to perceive sensations of grating that were similar to able-bodied subjects; however the ability of TSR subjects to identify and localize points of contact was slightly lower than the controls [96].

Although less common, it is possible to also produce tactile sensations through stimulation at the cortical level, in the somatosensory cortex [57]. This approach is a valid solution for prosthesis users who have a spinal cord injury and do not have intact peripheral nerve and spinal cord pathways for transmitting neural information.

Proprioception

One of the major forms of feedback in closed-loop manipulation with a hand is proprioception. It helps guide hand movement and complements touch feedback in that it allows an individual to create a more comprehensive understanding and representation of any movements or object manipulation. Touch information gives context of an object's features, such as surface roughness and material stiffness, while proprioceptive information helps convey object size and shape while also tracking the position of the hand. By knowing the current position of the hand through proprioception, an individual can send motor commands to make fine movements without the need for visual feedback. This type of comprehensive proprioceptive and tactile feedback is lacking in prosthetic hands.

Using implanted microelectrode arrays in the median and ulnar nerves of amputees, researchers have also identified several instances of propioceptive feedback. Multiple amputees were able to perceive different proprioceptive sensations (i.e. finger or hand movements in the phantom hand) [3]. It is unclear which afferent nerve fibers were being stimulated within the median and ulnar nerves to create these sensations, but the location of the stimulating electrode seemed to play a major role in eliciting proprioceptive sensations.

Illusory movements, sensations that the phantom hand is moving, can also be caused by vibratory feedback on the skin of amputees who have undergone TMR [97]. In multiple subjects, vibration of

the proximal reinnervated muscles elicited an illusion of hand movement, such as finger and wrist extension and flexion. This kinesthetic illusion was shown to improve movement control of their myoelectric prosthesis [97]. Although the vibration was applied to muscles, there was a perceived sensation of limb movement, which indicates the important relationship between muscle activity and sensory feedback to produce the sense of proprioception. Research has shown that proprioceptive percepts can be provided by stimulating sites in both sensory nerves and muscles, and it is most likely a combination of providing feedback to both sensory and motor neurons that will elicit more natural sensations of proprioception. The combined stimulation of muscles and sensory nerves for prorpioceptive feedback makes sense considering that SA2 mechanoreceptors provide information on skin stretch while muscle spindles convey information on limb position, which together make up our ability to localize our limb position in space without the need for visual feedback.

Now that technology has enabled tactile feedback to prosthesis users, researchers have begun to explore additional touch perceptions that can be naturally conveyed through nerve stimulation.

2.5.4 Neuromorphic models

The types of sensory feedback conveyed from a prosthetic hand to its user are still limited in that they do not fully encompass the complex nature of our sensations of touch. There is a continuous push to make prosthetic hands more life-like, and that requires sensory capabilities that enable a user to better utilize and embody their device. It is likely that future research will attempt to provide sensations of temperature, more sophisticated forms of proprioception, and combinations of other sensations back to prosthesis users. For realistic sensations to be re-created artificially, we should consider how biology produces those sensations to begin with. This leads to the use of

neuromorphic systems, which aim to mimic aspects of healthy nervous system architecture, by using digital spikes, akin to neural action potentials, to convey information. Researchers have already used a neuromorphic SA mechanoreceptor model for enabling an amputee to discriminate between textures [98]. The idea is that by using neuromorphic models, essentially modeling healthy receptor behavior as a way to stimulate peripheral nerves, more natural sensations can be produced because the stimulation is based on actual biological behavior. The limitation with this approach is that we are not yet able to stimulate individual sensory nerve fibers due to their small size. Thus, using a neuromorphic model to provide sensory feedback has not reached its full potential yet. At this point, the nerve stimulation is representative of the activity of a population of receptors, which can then by used to stimulate a nerve fascicle or bundle. However, researchers have already developed extremely sophisticated models that very accurately predict and replicate actual mechanoreceptor behavior. Using physiological data from afferents in non-human primates, SA1, RA1, and RA2 receptors have been modeled, with millisecond precision [99].

2.5.5 State of the art

A major part of providing sensory information from a prosthetic hand back to the user is understanding how that feedback is perceived by the user. Researchers are using traditional psychophysical experiments to quantify sensory perceptions and identify how different parameters influence perceptions of intensity [100]. Furthermore, an amputee is able to adapt to sensations in the phantom hand, such as a repeated tapping, in a similar way as someone adapts to sensations in an intact limb [101]. Differences in stimulating electrode (invasive vs noninvasive) is also a question worth considering in terms of how sensations change. Implanted stimulating electrodes to elicit sensory feedback are more stable than noninvasive approaches since they consistently stimulate the same

regions after implantation [3, 57]. Combined with understanding user perception of feedback, researchers have looked at how feedback influences the neural signals of an amputee [4], which could also be used to help better understand the quality of sensory perceptions from nerve stimulation. The effect of the stimulation on neural signals may offer insight into how information is processed in the somatosensory cortex after an amputation or spinal cord injury. This effect will help continue to push knowledge for improving not only prostheses but brain-machine interfaces in general.

TSR surgery has already enhanced the ability of researchers to provide sensory feedback to the peripheral nerves of amputees. There is often natural regrowth of peripheral nerves in an amputated limb, but this growth is somewhat arbitrary in that the nerve fibers may end up close to the surface of the skin, in the soft tissue, or deeper within the arm. With TSR, surgeons intentionally separate the afferent nerve fascicles and place them so that their growth into the soft tissue will make it easier for providing sensory feedback.

3 | Closed-Loop Tactile Feedback in Upper Limb Prostheses

This chapter is made up of content, with permissions and minor modifications, from [16].

> L. Osborn, R. Kaliki, A. Soares, and N. Thakor, "Neuromimetic event-based detection for closed-loop tactile feedback control of upper limb prostheses," *IEEE Transactions on Haptics*, vol. 9, no. 2, pp. 196–206, 2016. [doi]

3.1 Overview

In this chapter, we utilize tactile information to provide active touch feedback to a prosthetic hand. First, we developed fingertip tactile sensors for producing biomimetic spiking responses for monitoring contact, release, and slip of an object grasped by a prosthetic hand. We convert the sensor output into pulses, mimicking the rapid and slowly adapting spiking responses of receptor afferents found in the human body. Second, we designed and implemented two neuromimetic event-based algorithms, *Compliant Grasping* and *Slip Prevention*, on a prosthesis to create a local closed-loop tactile feedback control system (i.e. tactile information is sent to the prosthesis). Grasping experiments were designed to assess the benefit of this biologically inspired neuromimetic tactile feedback to a prosthesis. Results from able-bodied and amputee subjects show the average number of objects

that broke or slipped during grasping decreased by over 50% and the average time to complete a grasping task decreased by at least 10% for most trials when comparing neuromimetic tactile feedback with no feedback on a prosthesis. Our neuromimetic method of closed-loop tactile sensing is a novel approach to improving the function of upper limb prostheses.

3.2 Introduction

Prosthetic hands are important tools for improving the lives of upper limb amputees; however, most of these devices lack the ability to determine and understand the sense of touch. This lack of tactile feedback can cause issues such as unstable grasping of objects as many amputees are forced to rely primarily on visual feedback to ensure their prosthetic limb is behaving appropriately. Relying primarily on visual feedback with no tactile input can be rather burdensome for an amputee when it comes to picking up, holding, or manipulating objects with their prosthesis. In healthy hands, numerous mechanoreceptors within the skin allow for our sense of touch and make up the closed-loop tactile feedback system that provides us with valuable information regarding our environment [102, 103].

Many of the prosthetic arms today are controlled using myoelectric (EMG) signals [66, 104–106]. Recent advances in EMG prosthesis control have allowed for functional improvements [107], and new EMG pattern recognition techniques have shown promise for a more natural control of a prosthesis [67, 108]. These EMG control methods are useful for creating prosthetic systems with more intuitive control, but amputees still face the problem of no tactile feedback in their control strategies. This lack of touch information can give rise to issues such as accidentally breaking or dropping an object as the prosthesis user is unable to determine the amount of grip force being used

or when the object comes into contact with the prosthesis.

Knowledge gained through active touch sensing plays an important role in many manipulation tasks [109–112], and research suggests that using information such as grip force and pressure can help improve the functionality and grasping control of prosthetic hands [6, 113–117]. Advancements in closed-loop prosthesis control include improving grasp force sensitivity by incorporating force-derivative feedback in a prosthetic hand to help regulate grasping force [115], a nonlinear force controller for estimating and reducing the force fluctuations during grasping [118], and even a hybrid force-velocity sliding mode controller for preventing excessive grasping force [119]. Recent progress has shown the benefit of providing visual force feedback to prevent slip during grasping [120] as well as using an adaptive sliding mode prosthesis control to help prevent grasped object slip and deformation [116].

Current approaches fail to take into account the biological aspects of tactile sensing, specifically the behavior of mechanoreceptors in identifying onset and offset of object contact. This type of behavior is vital for stable grasping as we rely heavily on active touch sensing to gain information of an object [121, 122]. We use the mechanoreceptors for active touch sensing as a means to better understand a task, whether that is holding an object or discriminating a fine texture [122]. In healthy skin, the transient behavior of rapidly adapting (RA) receptors is believed to send information to the peripheral nervous system regarding the onset of object contact and release while the sustained response of the slowly adapting type 1 (SA1) receptors is thought to convey information regarding the amount of static grip force (Fig. 3.1) [5, 121]. It has been shown that by using these event-based responses along with numerous other inputs we are able to manipulate and grab objects with high precision and reliability [102]. Drawing inspiration from biology, an event-based approach could

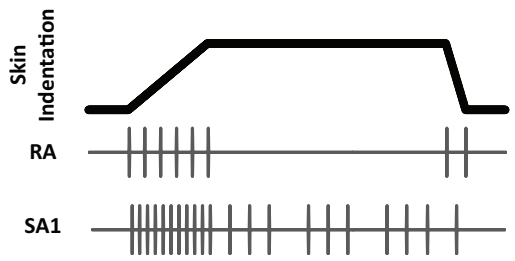

Figure 3.1: Adaptation of results from [5], this schematic shows the amount of skin indentation (top) and typical RA (middle) and SA1 (bottom) responses. RA receptors respond during the transient periods of indentation to help indicate contact and release while SA1 receptors exhibit a response during sustained indentation. ©2016 IEEE.

be engineered as a neuromimetic system to enable active touch sensing for a prosthesis that relies on object contact and release events made evident through spiking behavior.

Neuromimetic systems aim to imitate some aspect of brain function using analogous neural elements, such as spiking activity [123, 124]. Neurologically inspired approaches have been employed for visual information processing [125] and object recognition [126] as well as for modeling neural circuits, eye movements, and other sensory systems [127–130]. Here we model a tactile sensing system using RA 'event-based' responses to determine object contact and slip in conjunction with SA1 type information of sustained grasping force to create a neuromimetic control method for a prosthetic system. We hypothesize that this bioinspired approach will create a closed-loop tactile feedback system that can prevent object damage and slip during grasping with a prosthesis.

One study showed how different feedback modalities can influence a person's ability to detect and correct for an object slipping. The response time in healthy humans for preventing object slip by using EMG signals ranged from 1.51 – 1.75 s, depending on the feedback modality [131]. However, during grasping, the natural reflex pathway in healthy adults is capable of responding between 50 - 70 ms after the onset of slip occurs [132, 133]. The disconnect between muscle contractions and prosthesis movements for an upper limb amputee introduces an inherent delay when compared to

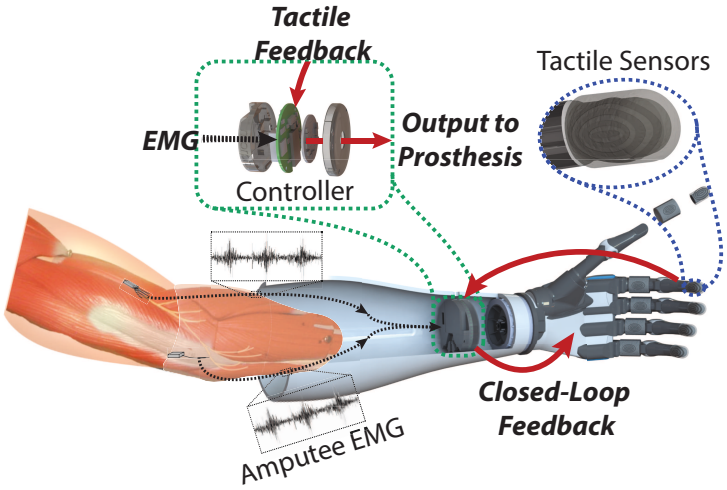

Figure 3.2: System diagram showing the closed-loop nature of the tactile feedback system. The prosthesis control unit receives both amputee EMG signals and tactile information before sending out a command to the terminal device. ©2016 IEEE.

the automatic skeletal muscle response triggered by efferent nerve fibers in the peripheral nervous system [103, 132, 134]. Thus, there is a need for a closed-loop tactile feedback system for prostheses with the ability to make quick, accurate adjustments in real-time during grasping, similar to our very own reflex pathway.

In this work we 1) present compliant force sensors to monitor grasping forces as active tactile sensory inputs to a prosthesis control unit, and 2) implement our neuromimetic force based control algorithms, *Compliant Grasping* and *Slip Prevention*, on the prosthesis controller to create an active closed-loop tactile feedback system for improving grasping functionality of a prosthetic hand, as outlined by Fig. 3.2. In this work, tactile feedback is sent directly to the prosthesis controller and not the user.

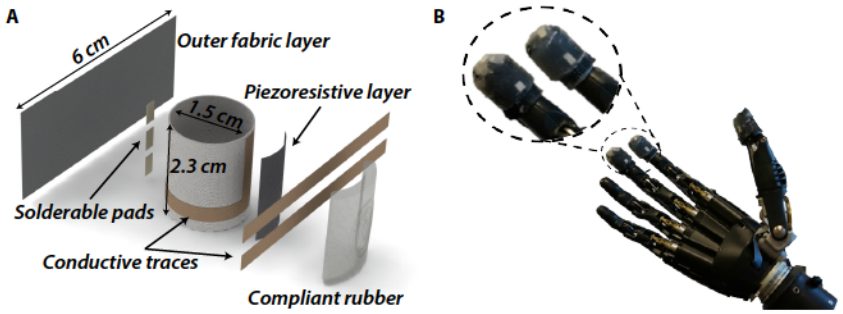

Figure 3.3: (A) Textile sensor cuff design, which includes flexible and stretchable materials that allow the sensor to be placed on a prosthesis phalanx. Conductive traces act as the sensing elements and are protected by an outer fabric layer along with a rubber coating. (B) Sensor cuffs are placed on the tips of the thumb, index, and middle fingers of the prosthesis. ©2016 IEEE.

3.3 Materials and ethods

3.3.1 Textile force sensor

We have designed and built a customized textile force sensitive resistor (FSR) to measure applied loads during grasping with a prosthetic hand. The sensors are based on previous designs with stretchable textiles [135] and designed specifically for the fingertips of a prosthetic hand. Sensor cuffs, as seen in Fig. 3.3B, are made up of stretchable conductive textile traces (LessEMF, Latham, USA) placed on a textile backing and covered by a stretchable outer layer. A 3 mm rubber layer (Dragon Skin 10, Smooth-On, USA) is used to add compliance to the grasping surface of the prosthesis. The sensors were previously characterized and verified for use in prosthetic applications, particularly during grasping tasks [136].

The textile FSRs are designed to easily fit on the phalanx of an existing prosthesis, removing any need for special disassembly or mechanical manipulation of the device. For this work, the sensor cuff is placed on the thumb, index, and middle distal phalanges of the bebionic3 prosthetic hand, as shown in Fig. 3.3B. The relationship between the applied surface load and the sensor output is described in [136].

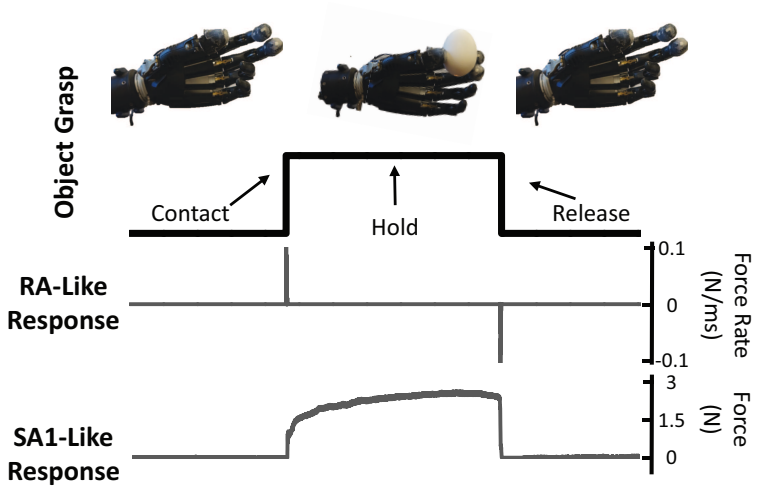

Figure 3.4: A grasp-hold-release event with tactile feedback. The top plot shows the onset, hold, and release of an object grasped by a prosthetic hand. The RA-like tactile response (middle) produces a small cluster of positive spikes during the onset of object contact and negative spikes during object release. The SA1-like response (bottom) simultaneously measures sustained grip force. ©2016 IEEE.

3.3.2 Neuromimetic algorithms

The normal force measured by the sensors is used as an analog to skin indentations that produce RA and SA1 responses. Rapid changes in the applied force, as measured by the sensors, are translated to an RA-like spiking response to indicate object contact and release, as seen in Fig. 3.4. This is achieved by measuring the rate of change of the force signal and characterizing positive changes as the onset of object contact and negative changes as object release. In addition, the absolute value of a sustained applied load is simultaneously measured by the sensor to capture SA1-like information of a steady-state force or indention (Fig. 3.4). In our approach, these signals serve as the active tactile inputs for the neuromimetic prosthesis grasping algorithms.

Compliant Grasping control

This control strategy determines when the prosthetic hand contacts an object and modulates the hand's response to the user's EMG signal during a grasping task based on the applied force from the

fingertip sensors to promote a stable prosthesis grip without overexerting forces on an object. Our approach to compliant grasping is to create a device to implement a feed-forward EMG gain control model that uses an RA-like sensor response, $R(t)$, to determine object contact and the static SA1-like sensor response, $S(t)$, to determine the absolute grip force. The RA-like sensor response, $R(t)$, is modeled as a high pass filtered signal of the SA1-like sensor response, $S(t)$, and approximated using Newton's quotient

$$R(t) = \frac{S(t + \Delta t) - S(t)}{\Delta t}$$

where Δt is the time between measurements. This creates the spiking response that can be used for determining the onset of object contact and release. Object contact is defined as a threshold crossing by the RA or SA1-like sensor response

$$R(t) \geq \beta \qquad \text{or} \qquad S(t) \geq \eta$$

with $\beta = 0.08$ N/ms and $\eta = 0.1$ N, which were found experimentally to be outside of the normal force rate fluctuations of the sensor and the minimum force needed for sensor activation, respectively [136]. After object contact during a grasping task, the prosthesis control unit actively modulates the user's EMG signals by applying a gain reduction, α, which is dependent on the SA1-like sensor response, $S(t)$. This is outlined in Fig. 3.5 and is given by the piecewise function

$$\alpha = \begin{cases} e^{-\gamma S(t)} & S(t) < 8 \text{ N} \\ \gamma & S(t) \geq 8 \text{ N} \end{cases}$$

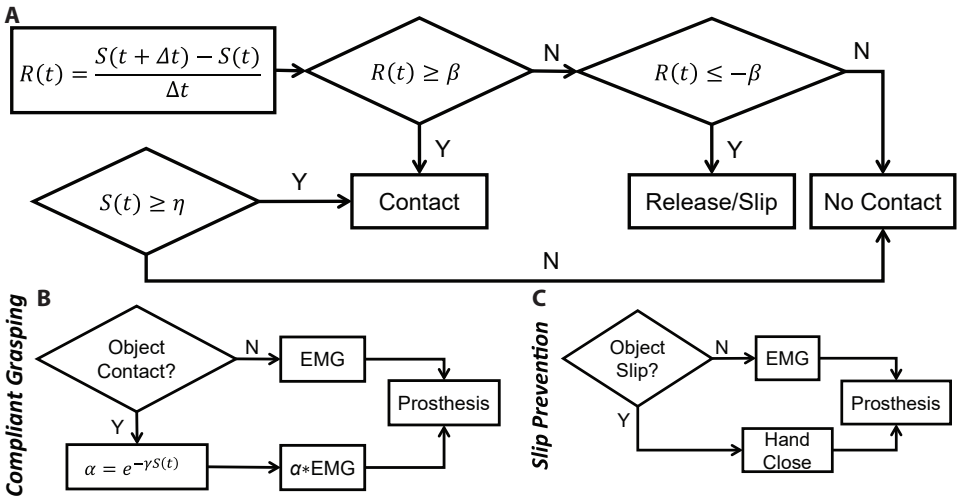

Figure 3.5: (A) The neuromimetic touch feedback algorithm uses the RA-like sensor response, $R(t)$, which is found by passing the force signal ($S(t)$) through a high pass filter and comparing it to the threshold β, to determine the onset of object contact, release, and slip. (B) The *Compliant Grasping* strategy uses object contact to dynamically modulating the user's EMG gain, α, to help prevent grasping objects with excessive force, and (C) uses the same neuromimetic RA-like response to monitor and correct for object slip. ©2016 IEEE.

where γ is the EMG gain threshold of 20%. To find γ we took the average EMG amplitude of several maximum effort contractions and found the percentage of the signal needed to maintain prosthesis control. The 8 N threshold was chosen to ensure continuity of the gain reduction function, α, as it is the intersection of the two parts of the piecewise function. Because the prosthetic hand operates using proportional control, a reduced EMG signal will result in an appropriately reduced hand reaction. The exponential decrease of the EMG gain was found heuristically to allow for finer manipulation with smaller grasping forces, which makes it ideal when handling delicate objects that are easily crushed, compared to an inversely proportional or inverse sigmoidal decaying function. Fig. 3.6 shows the actual EMG gain output from the prosthesis controller based on the measured force signal during active *Compliant Grasping* feedback control. The goal of this algorithm is to allow the user to make fine force adjustments, due to the decreasing EMG gain, after contacting an object without the worry of over grasping and breaking the object.

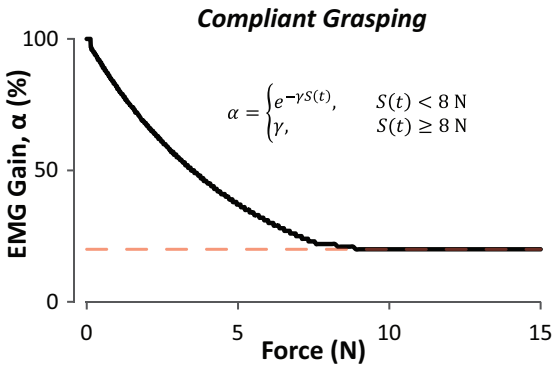

Figure 3.6: The true EMG gain measured from the prosthesis controller during a prosthesis grasping task with increasing grip force and *Compliant Grasping*. To prevent the EMG signal from shrinking to zero, a lower threshold of 20% is placed on the gain. ©2016 IEEE.

Slip Prevention **control**

During prosthesis grasping it is useful to have a stable grip on the target object. For this case, we introduce a neuromimetic *Slip Prevention* algorithm that uses the RA-like sensor response, $R(t)$, to determine the offset (*i.e.* slip) of object contact. While object contact is determined by a positive increase in $R(t)$, as described in the previous section, object release is determined by a *negative* change in $R(t)$.

$$R(t) \geq \beta \quad \Rightarrow \quad \text{Object Contact}$$

$$R(t) \leq -\beta \quad \Rightarrow \quad \text{Object Release}$$

A negative change in the grip force, less than $-\beta$, indicates movement or release between the prosthesis and grasped object interface and triggers the prosthesis to close for time τ. The value of τ is chosen as 45 ms, which is similar to actual grip force adjustment times found in humans [132]. This time was also verified experimentally as enough time for the prosthesis motors to respond to the hand close signal. The algorithm is continuously monitoring $S(t)$, so the total time of hand

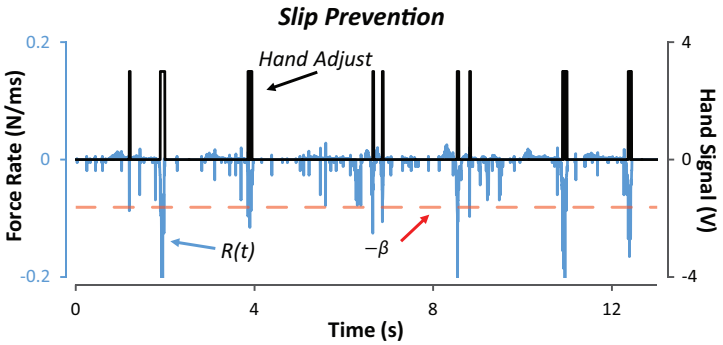

Figure 3.7: The *Slip Prevention* control strategy uses the biomimetic RA-like sensor response, $R(t)$, spikes to monitor for object slip. Instances of slip are identified using this neuromimetic approach by measuring the rate of change of the grip force. An instance of slip triggers the prosthesis to close to prevent an object from slipping from its grasp. ©2016 IEEE.

closure, T, is increased by τ for every instance of slip, n, and can be modeled using the update equation

$$T^i = T^{i-1} - \Delta t + \sum_{j=1}^{n} \tau_j^i$$

where Δt is the elapsed time between iterations, i, and is dependent on the prosthesis control unit sampling rate. The prosthesis receives a close signal for time T^i, which will increase with increasing instances of slip, n. This algorithm is outlined in Fig. 3.5, and its output is shown in Fig. 3.7, which portrays the RA-like sensor response, $R(t)$ and the corresponding signal to close the prosthesis.

In the event that the user intends to release a grasped object from the prosthesis an intentional EMG "open" signal will override the automatic hand closure reflex signal from the *Slip Prevention* algorithm.

3.4 Experimental methods

To evaluate the use of active tactile feedback during prosthesis operation, we developed a series of grasping experiments that require a human subject to pick up and handle objects with a bebionic3

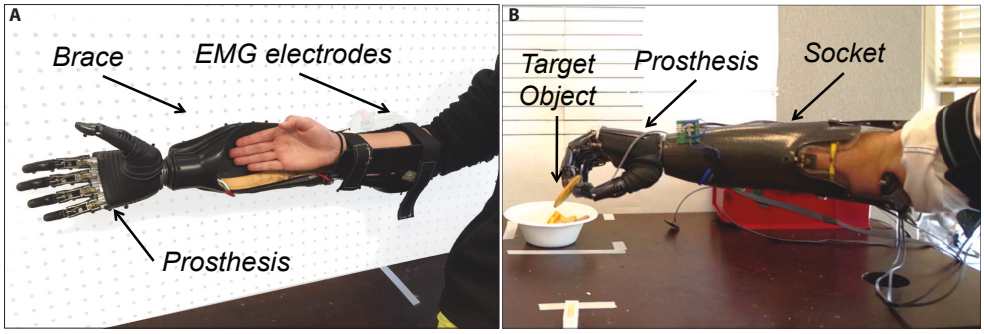

Figure 3.8: (A) A custom brace is used for operation of a prosthetic hand by able-bodied subjects. A pair of Ottobock electrodes (Myobock, Ottobock, Austin, USA) are placed on the forearm of the subject to collect the EMG signals. (B) The amputee participants used their personal prosthetic socket with embedded Ottobock EMG electrodes. ©2016 IEEE.

prosthetic hand. To evaluate the algorithms with an adequate sample size, 10 able-bodied subjects participated in the experiments. To evaluate the touch feedback system with actual prosthesis users, 2 transradial amputees, one of whom is a bilateral amputee and the other a unilateral amputee, participated in experiments. All subjects consented to participate in the experiments, which were approved by the Johns Hopkins Medicine Institutional Review Board.

3.4.1 Hardware and data collection

To operate the prosthesis, able-bodied subjects wore a customized brace, Fig. 3.8A, while the amputee participants used their personal prosthetic sockets, Fig. 3.8B. A tripod grip (Fig. 3.9) was used by all subjects during the grasping tasks and the EMG signals used to control the prosthesis were collected using a pair of Ottobock electrodes (Myobock, Ottobock, Austin, USA) placed on the forearm of the subject. The same pair of electrodes was used for all able-bodied subjects and the amputee subjects used personal Ottobock EMG electrodes that were already embedded within their socket.

Fingertip sensors were placed on the thumb, index, and middle fingers of the prosthesis, as

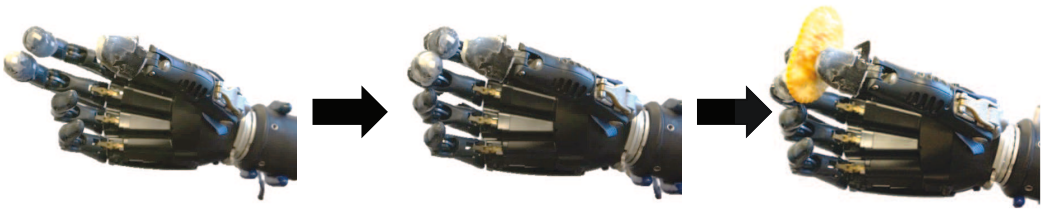

Figure 3.9: A tripod grip is used by the prosthesis for all grasping tasks. For this grip, the thumb as well as the index and middle fingers are used to grasp an object. ©2016 IEEE.

seen in Fig. 3.3B. Each sensor contains a sensing element at the distal end and tip of the finger, and they communicate directly with the prosthesis controller (Infinite Biomedical Technologies, USA) at 260 Hz. To test the individual touch feedback strategies, an external switch was placed on the prosthesis controller to change between the *Compliant Grasping* and the *Slip Prevention* algorithms. This allows each algorithm to be evaluated independently of the other. Data were sent via serial communication between the prosthesis controller and a PC and analyzed using LabVIEW (National Instruments, USA). Every experiment was recorded using a Sony Nex-5R digital camera for monitoring time and object movement during the experiments. A paired *t*-test with confidence interval (COI) of 95% was used for analyzing whether the data reject the null hypothesis when compared to each other.

3.4.2 Able-bodied experiments

Two different tasks were designed to test the functionality of the *Compliant Grasping* and *Slip Prevention* algorithms. Each able-bodied subject performed the tasks using 1) an unmodified bebionic3 prosthetic hand, 2) the prosthesis with the neuromimetic feedback for compliant grasping and slip control, and finally 3) the prosthesis with the finger sensors deactivated. There is no cosmesis, a skin-like glove, on the unmodified prosthesis. The reason for the final case with deactivated sensors is to investigate the effect of the sensors' material on the system's performance during grasping.

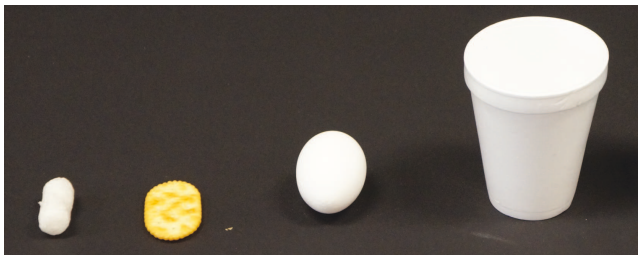

Figure 3.10: The items used for the *Compliant Grasping* task. From left to right: packing foam, cracker, hollow egg, and a polystyrene cup. These common objects, most of which have been used in previous grasping studies, were chosen due to their delicate nature [6–8].

Each subject was allowed to train with the prosthesis, both unmodified and with sensors attached, for up to a total of 15 minutes to learn basic operation and control of the device before starting the experiments.

Compliant Grasping

Common objects that are relatively easy to break were chosen for this task and are shown in Fig. 3.10. Most of these items have been used in previous prosthesis and robotic grasping tasks [6–8]. To ensure repeatability, we quantified the mass of the items as well as the amount of force required to break each item, as seen in Table 3.1. For this experiment, an object is considered broken when it exceeds its yield strength and undergoes plastic deformation [137]. Each trial consists of picking up and moving 5 items of the same type approximately 25 cm. Every able-bodied subject completed a single trial of five movements for each object type. The trials were repeated for the unmodified prosthesis, the prosthesis with the neuromimetic touch feedback algorithms, and the prosthesis with deactivated sensors. The order of trials was randomized and the number of broken objects as well as the time to complete a trial were measured.

Table 3.1: Items used in the grasping tasks. ©2016 IEEE.

Item	Mass (g)	Force to Break (N)
Foam	0.19 ± 0.01	>1
Cracker	3.1 ± 0.1	>2
Cup	3.2 ± 0.1	>2
Egg	5.7 ± 0.7	>8

Slip Prevention

To induce slip, weight is added to an empty polypropylene cylinder, held by the subject, in either 1 N increments (up to 5 N) or a single increment of 3.8 N. The two methods of weight addition allow for measuring the effect of small (1 N) and large (3.8 N) changes in the grasped object's weight. The weights are dropped from the top of the cylinder every time and fall approximately 12 cm to the bottom of the cylinder. The vertical distance moved by the grasped cylinder and the number of times it slipped completely from the prosthesis' grasp were measured using the high definition digital video camera at 30 fps. Each able-bodied subject performed each weight addition trial 3 times.

3.4.3 Amputee experiments

To evaluate the neuromimetic tactile feedback system with actual prosthesis users, 2 transradial amputees participated in the experiments. Both amputee subjects used their own prosthetic system, which included the socket, electrodes, a prosthesis control unit, and a bebionic3 prosthetic hand. Both subjects regularly use their bebionic3 hand without a cosmesis during daily activities and have been using a prosthesis for 3 years or more.

The amputee subjects performed the same *Compliant Grasping* and *Slip Prevention* tasks as described in 3.4.2 and 3.4.2, respectively, and did so using 1) their unmodified bebionic3 prosthesis,

2) the prosthesis with the neuromimetic feedback for compliant grasping and slip control, and finally 3) the prosthesis with the finger sensors deactivated.

For the *Compliant Grasping* task, both amputee subjects performed 4 trials of every object movement with the unmodified prosthesis, the prosthesis with the neuromimetic tactile feedback, and the prosthesis with deactivated sensors. For the *Slip Prevention* task, one amputee subject performed each weight addition trial 4 times. The bilateral amputee subject did not participate in this grasping task.

3.5 Results

The results from the grasping tasks are separated by able-bodied and amputee subjects. The data collected from the two different grasping tasks are separated in order to evaluate the two neuromimetic algorithms independently. All error bars in the following plots represent the standard error of the mean and a paired *t*-test is used for analyzing the statistical significance of the able-bodied subject results. A statistical analysis was not performed for the amputee subjects' results because of the small sample size, which was also the case in [107].

3.5.1 Compliant Grasping

For both subject types, the average number of broken items, as a percentage of the total number of items moved, is shown in Fig. 3.11. An object is considered broken if its elastic limit is exceeded and it undergoes plastic deformation during the grasp [137]. In general, the unmodified prosthesis broke the most number of items, and the number of broken objects decreases significantly with the use of compliant fingertip sensors and feedback. Fig. 3.12 shows the normalized time for

completing a trial based on the target object. To allow comparison across the subjects of a group, the time to complete a trial for an object was normalized against the completion time of using the unmodified prosthesis for that same object.

Able-bodied subjects

The number of broken objects (Fig. 3.11A) dropped from 44%, 32%, 2%, and 4% while using the unmodified prosthesis to 16%, 10%, 0%, and 2% while using the prosthesis with deactivated sensors for the foam pieces, crackers, cups, and eggs, respectively, for able-bodied subjects. The failure rate for the foam and crackers decreased further to 10% and 8% while there was no change for the cups and eggs with the *Compliant Grasping* algorithm. There is a statistical significance ($p < 0.05$) between the results from the unmodified prosthesis and those from the neuromimetic closed-loop tactile feedback. There is a statistical significance observed between results from the deactivated sensors and those with the tactile feedback for the foam ($p = 0.01$) and crackers ($p = 0.04$) but not for the other two items.

Using the unmodified prosthesis resulted in the longest trial completion times for the able-bodied subjects. The normalized completion time changed from 0.89, 0.82, 0.85, and 0.73 with the deactivated sensors to 0.78, 0.67, 0.82, and 0.72 while using the neuromimetic touch feedback for the foam, crackers, cups, and eggs, respectively (Fig. 3.12A). There is a statistically significant difference ($p < 0.05$) between results from using the prosthesis and the *Compliant Grasping* algorithm. This is also true for the results from the deactivated sensors and the tactile feedback for the foam and crackers but not for the cups ($p = 0.19$) or the eggs ($p = 0.72$).

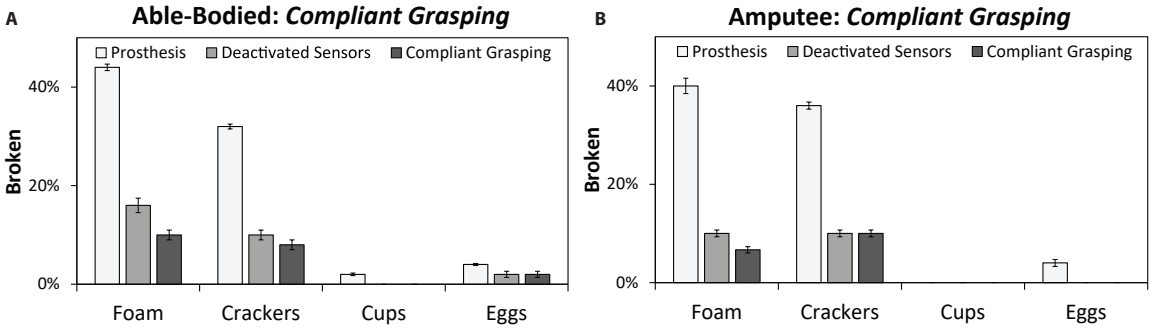

Figure 3.11: The average number of broken objects during the *Compliant Grasping* tests for the (A) able-bodied and (B) amputee subjects. ©2016 IEEE.

Amputee subjects

The number of broken objects decreased from 40%, 36%, and 4% while using a prosthesis to 10%, 10%, and 0% while using a prosthesis with deactivated sensors to grab the foam, crackers, and eggs, respectively, for the amputee subjects (Fig. 3.11B). Utilizing the tactile feedback with the *Compliant Grasping* algorithm further decreased the broken foam to 7% while the number of broken crackers and eggs stayed the same. No cups were broken by the amputees on any trial.

The normalized completion times while using the prosthesis with the deactivated sensors are 0.95, 0.82, 1.09, and 1.34 for the foam, crackers, cups, and eggs, respectively. These times are reduced to 0.90, 0.84, 0.94, and 1.06 while using active touch feedback control, as seen in Fig. 3.12B.

3.5.2 Slip prevention

The average distance slipped by the cylinder during the small (1 N) or large (3.8 N) weight addition for the *Slip Prevention* grasping task was measured and is shown in Fig. 3.13. All instances of slip were less than 1 s in duration. Fig. 3.14 shows the failed trials, which are defined as the cylinder slipping entirely from the grasp of the prosthesis during weight addition.

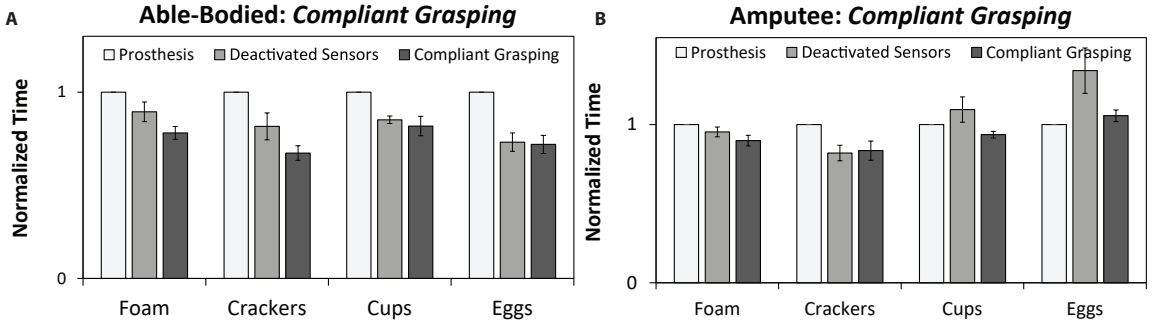

Figure 3.12: The normalized time to complete a *Compliant Grasping* tests for the (A) able-bodied and (B) amputee subjects. Trial completion times are normalized using the average time to complete a task for a particular item using the unmodified prosthesis. Both plots show a decrease in the time required to complete item movements while using tactile feedback as an input for the control algorithm, with the exception of the eggs for the amputee subjects. ©2016 IEEE.

Able-bodied subjects

The average distance slipped while using a prosthesis is 8.3 mm and 25.5 mm for the small (1 N) and large (3.8 N) weight additions, respectively. These values are reduced to 1.2 mm and 6.1 mm while using deactivated sensors on the prosthesis and further reduced to 0.8 mm and 3.8 mm while using the *Slip Prevention* algorithm (Fig. 3.13A). 9% of the trials resulted in complete slip (*i.e.* failure) while using the prosthesis during small weight increments and 38% for the large weight increment. Both of these failure rates reduced to 3% with the presence of the deactivated sensors and were reduced even further to 0% with the neuromimetic algorithm to prevent slip (Fig. 3.14). There is a statistically significant result ($p < 0.05$) between all trials with the unmodified prosthesis and those utilizing the *Slip Prevention* algorithm; however, this is not the case when comparing the results from the prosthesis with deactivated sensors and *Slip Prevention*. The resulting p values for this comparison (deactivated sensors vs *Slip Prevention*) from the slip distance data for the small and large weight increments are 0.24 and 0.19, respectively.

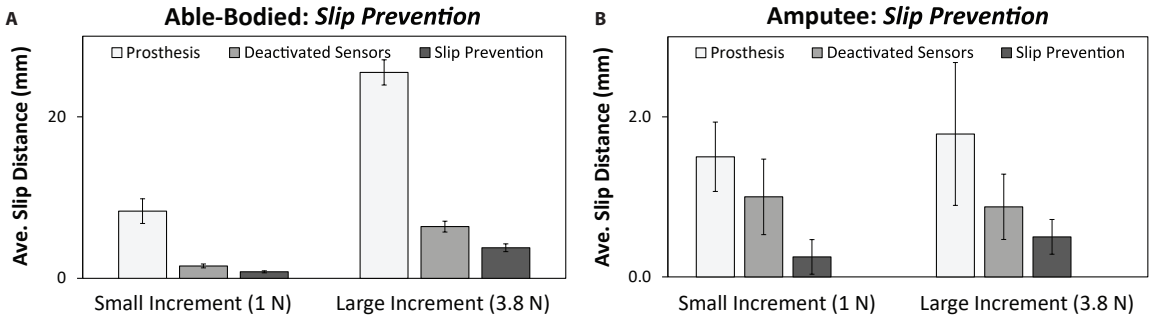

Figure 3.13: The average distance the grasped cylinder slipped during the *Slip Prevention* tests for the (A) able-bodied and (B) amputee subjects. ©2016 IEEE.

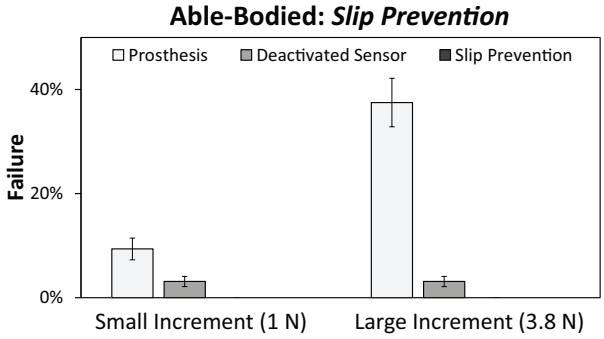

Figure 3.14: The number of times, as a percentage of the total number of trials, the grasped cylinder fell from the prosthesis during the *Slip Prevention* tests for the able-bodied subjects. There were no failed trials during experiments with the amputee subject.

Amputee subject

While using the unmodified prosthesis, small and large weight additions resulted in an average slip distance of 1.5 mm and 1.8 mm, respectively, for the amputee subject. The presence of the deactivated sensors reduced the slip distance to 1.0 mm and 0.9 mm for the small and large weight additions, respectively, while using the neuromimetic *Slip Prevention* resulted in distances of 0.3 mm and 0.5 mm for the same weight increments (Fig. 3.13B). There were no instances of failed trials during this task.

3.6 Discussion

This system is the first to incorporate active neuromimetic touch feedback algorithms on a prosthetic hand. Using event-based spiking activity from force sensors on the fingertips of the prosthesis, results from the *Compliant Grasping* and *Slip Prevention* algorithms suggest the benefit of using such an event-based approach for closed-loop control of a prosthetic hand.

3.6.1 Compliant Grasping

In general, the *Compliant Grasping* control strategy appears to benefit the user by reducing the number of broken objects during grasping. From Fig. 3.11, it is clear that the lack of tactile feedback makes it difficult to grab delicate objects without breaking them, which has been seen in other studies as well [112, 115, 120], while the presence of the neuromimetic tactile feedback system reduces the likelihood of objects breaking. Interestingly, the deactivated sensors also reduced the number of broken items compared to the unmodified prosthesis, but to a lesser degree. This is likely caused by the compliant nature of the sensor surface, thus helping distribute any grasping loads over a larger surface area and in turn reducing the pressure applied to an object during grasping.

Able-bodied subjects

The reduction of broken objects when using the deactivated fingertip sensors (Fig. 3.11A) highlights the effect of the compliant sensor surfaces on the grasping performance of the prosthesis; however, the presence of the active neuromimetic tactile feedback showed even better performance, specifically for the more delicate objects. Similarly with the normalized completion time, the *Compliant Grasping* algorithm has the best performance (Fig. 3.12A). This enhanced performance can

be attributed to the RA-like event-based responses for determining the onset of object contact. The knowledge of initial contact allows the tactile feedback system to effectively reduce the prosthesis grasping force through EMG modulation, which is a function of the SA1-like sensor response as described in 3.3.2.

The likelihood of breaking delicate objects during prosthesis grasping was reduced by using a force derivative feedback in [115] as well as visual force feedback in [120]; however, this neuromimetic tactile feedback approach results in higher success rates for grasping delicate objects.

Amputee subjects

Similarly, there is a reduction in failure rates when handling the objects with the deactivated sensors on the prosthesis and a further reduction with the neuromimetic algorithm (Fig. 3.11B). It is interesting to note that the cup was never broken by an amputee subject nor were there any failures with the closed-loop tactile feedback for the eggs. One possible reason for this is that the amputee subjects are much more experienced using their devices and are able to control it with more precision than a naive user, thus they are more capable of handling objects that require slightly higher force to break ($F > 8$ N); however, the presence of the neuromimetic tactile feedback was still beneficial to improve grasping of objects, specifically those that are very delicate (*i.e* $F \leq 2$ N to break).

There are slight decreases in completion time for all manipulation tasks, except for with the egg, while using the *Compliant Grasping* feedback strategy (Fig. 3.12B). One amputee subject claimed that he was so comfortable operating his prosthesis in an unmodified state, without any cosmesis or covering, on a daily basis that adding the fingertip sensors caused observable changes in how he used the device, particularly in how quickly he would pick up objects. As a result,

the active neuromimetic tactile feedback still provides the added benefit of reducing the likelihood of breaking objects but may not have a profound effect on the time to complete a grasp as many experienced prosthesis users are already proficient regarding the time required to grab and move an object. While this may be the case in general, we still observe reduced completion times for the three most delicate objects with the presence of the active tactile feedback.

3.6.2 Slip prevention

During the *Slip Prevention* task, the spiking neuromimetic feedback allowed the system to noticeably reduce the amount of slip during weight addition to the grasped object (Fig. 3.13). Although the sensors do not isolate the changes in tangential loading during slip, a negative spike in $R(t)$ indicates an instance of object slip and leads to a hand reaction to stop the object from falling (Fig. 3.7), not unlike the healthy reflex pathway. This *Slip Prevention* method relies solely on the RA-like sensor signal to monitor and correct for rapid changes in the grip force caused by a slipping object. This is similar to actual human behavior where adjustments in grip forced are caused by changes in the vertical load of the grasped object [132]. Interestingly, it has been shown that the grip force adjustment is proportional to the magnitude of the vertical load perturbation but is not related to the preexisting grip force [132]. By drawing parallels with biology, our neuromimetic *Slip Prevention* tactile feedback algorithm has demonstrated ability to reduce object slip during grasping with a prosthesis.

Previous studies have shown the ability to prevent object slip [7, 131]. A series of experiments that tested ability of a user to produce EMG signals to stop a simulated slip showed mean user response times greater than 1.5 s with a success rate not exceeding 30% [131]. Although the ex-

perimental conditions differ, the neuromimetic feedback system showed greater ability in reducing slip failure rates suggesting the importance of prompt reaction times. One prosthesis experiment of 20 slip trials resulted in only 1 failure [7]. It should be noted that these experiments were performed without human subjects and with a limited range of detectable forces. Although the *Slip Prevention* algorithm didn't result in any slip failures, one possible area of investigation would be the performance of the system over a much larger range of slip conditions, such as slip speed.

Able-bodied subjects

There is a significant reduction in the distance slipped by the grasped object while using a prosthesis with the deactivated sensors; however, there is a further reduction with the *Slip Prevention* feedback control (Fig. 3.5.2). The compliant nature of the sensors appears to have the a major impact on preventing slip. This is likely due to the increased surface area and friction introduced by the compliant material of the sensor itself; however, the closed-loop *Slip Prevention* algorithm is still beneficial, although not significantly so ($p > 0.05$), in that it is able to further reduce the amount of object slip by monitoring the $R(t)$ sensor signal for instances of grip force perturbations. More importantly, the active touch feedback successfully prevented any instant of major or complete object slip (Fig. 3.14).

Amputee subject

There is an obvious decrease in the slip distance when the deactivated sensors or on the prosthetic hand, again likely due to their larger coefficient of friction than the plastic prosthesis phalanges, and a further decrease when using the *Slip Prevention* feedback (Fig. 3.13B). Because of the relatively small sample size, any statistical backing of these results is unclear; however, these results follow a

similar trend to those seen with the able-bodied subjects. The overall small magnitude of the slipped distance as well as the lack of any slip failures can be attributed to the amputee's natural desire to "over grasp" the cylinder. When asked about his grasping tendencies, the unilateral amputee indicated that it is common for him to naturally use a larger grip force than necessary, especially with a sturdy object such as the cylinder used in this experiment, to overcompensate for the lack of feedback that is used to prevent object slip. This being the case, small amounts of slip were still observed and were reduced when using the event-based neuromimetic algorithm for tactile feedback. This suggests that despite an amputee's best efforts to properly grasp an object there are still instances of accidental object slip, which could be mitigated with the addition of a biologically inspired neuromimetic *Slip Prevention* system.

3.6.3 Active touch sensing

The tactile feedback sent to the prosthesis controller directly influences the behavior of the limb in order to better complete the current task. Whether handling delicate objects (*Compliant Grasping*) or trying to keep grasped objects steady (*Slip Prevention*), the sensory information from the fingertips plays a key role in the decisions made by the controller. The primary goal being that the control of the prosthesis is updated to whatever manner best suits the current task. This aspect of the system is analogous to the natural behavior in healthy grasping in which rapid and reliable cues are used to control our behavior during such a task [122].

This neuromimetic tactile feedback system attempts to use active touch sensing to further improve how a prosthetic limb operates by drawing parallels to healthy biological systems, specifically our ability to reliably and comfortably manipulate and grab objects.

3.6.4 General considerations

Careful consideration must be made before making any comparisons between able-bodied and amputee subjects as the two groups are inherently different, but there are a few interesting aspects to note. One is the reduction in time to complete the *Compliant Grasping* task. Able-bodied subjects show larger improvements with the addition of the automatic event-based tactile feedback algorithm; however this can likely be attributed to the fact that they are naive prosthesis users and have a larger room for improvement compared to experienced prosthesis users. Experienced prosthesis users are more likely to be efficient in terms of their ability to use the unmodified prosthesis, as discussed in 3.6.1. Amputee subjects are typically more comfortable with operating a prosthesis and so any changes to the device they are already comfortable using could result in reduced performance as the modifications are unfamiliar. Despite this possibility, the active touch feedback was still able to improve prosthesis grasping.

Another aspect between the two groups is the large difference in the object slip distance. The distance slipped during able-bodied trials tends to be an order of magnitude higher than for the amputee subject. This is likely due to the higher grasping force of the amputee, as mentioned in 3.6.2. This could also be attributed to the able-bodied subjects being naive users who are unfamiliar with efficient prosthesis grasping techniques. In fact, data from the SA1-like sensor response, $S(t)$, shows that the grasping force for these trials was indeed higher for the amputee subject than it was for the able-bodied subjects. In addition, this could potentially be attributed to the different torques produced at the distal end of the prosthesis with the addition of weight. Because the brace worn by the able-bodied subjects extends further than the user's arm, a torque is produced by the terminal device, the prosthesis, and any added weight, which creates an upward force on the arm of the

subject. This could potentially cause the user to quickly stabilize his or her arm with an opposing force, which would effectively move the prosthesis upward and could allow for additional slip of the grasped object.

The physical presence of the fingertip sensors improves the prosthesis grasping functionality. The compliant nature of the sensors' surface provides increased surface area during grasping while also increasing the friction between the prosthesis and the target object. A similar effect was found in [6] where a majority of prosthesis grasping improvements were found to be linked with the compliant nature of the sensors used in the tactile feedback control. This fact is not surprising as it has been shown that the compliant nature and mechanical deformation of human finger pads work in tandem with the mechanoreceptors in the human skin and are used to enhance human grasping [138–140].

Studies have shown the benefit of vibrotactile feedback to a user for preventing object slip [112, 131]. However, there is a delay with this type of feedback before a user's reaction. Given the short time scale of this particular application ($< 1s$), it is necessary for direct, closed-loop feedback to the prosthesis controller in order for reaction quick enough to prevent object slip or damage. There is a possible benefit of combining our neuromimetic feedback to the prosthesis controller with feedback to the user; however, it will likely require that the feedback to the prosthesis controller trigger the primary response due to the time delay of feedback to the user before a reaction.

Grasping and the sense of touch is an extremely complicated biological system that is only a portion of the even more complicated neuromuscular system. Our active neuromimetic tactile feedback system by no means attempts to model all the neurological aspects of tactile feedback during grasping, instead our method focuses on using two key elements to convey grasping information –

RA and SA1 mechanoreceptor responses. Using this as a model, we can extract meaningful information regarding the onset of object contact and release to create an event-based detection system for improving prosthesis grasping.

Subjective evaluation

Both amputee subjects were interviewed after the experiments to provide feedback on the proposed method. One subject noted that there was no significant perceived difference in their ability to pick up or move objects between the various experiments. This subject did indicate that the physical presence of the sensors felt awkward in the sense that it changed the thickness of the fingertips and was different than what this subject is used to. This subject indicated that a feedback system like this could be useful if it was seamlessly integrated with the prosthetic system without affecting the user's normal operation of the device. The biggest drawback for this subject was the added thickness of the fingertips due to the presence of the sensors. The subject did agree though that the presence of the compliant tactile sensors offered a benefit for reducing broken objects. Likewise, the other subject describe a sensation of being able to "feel" the presence of the compliant sensors and their ability to reduce the number of broken objects during grasping. This subject indicated that although no feedback was given to the user, the compliant nature of the sensors and the feedback to the prosthesis appeared to make it easier while grabbing delicate objects.

3.7 Conclusion

Our novel approach uses RA and SA1-like sensor responses to create a neuromimetic event-based tactile feedback system, which is shown to offer improvements in grasping over a traditional open

loop prosthesis system. The primary goal of this investigation is to provide tactile feedback to a prosthetic hand by drawing inspiration from nature. In doing so, we have successfully shown the added benefit of implementing neuromimetic tactile feedback algorithms, *Compliant Grasping* and *Slip Prevention*, for not only enhancing ability of prosthesis users to pick up and manipulate delicate objects but to also reduce accidental slip in objects that are being perturbed by changes in weight. This neuromimetic approach offers a new insight into the improvements that can be made towards prosthesis functionality by using natural human neurological function as a platform.

4 | Grip Force Modulation Using Neuromorphic Tactile Sensing

This chapter is made up of content, with permissions and minor modifications, from [25].

Reprinted, with permission, from the Myoelectric Controls Symposium and the Institute of Biomedical Engineering at the University of New Brunswick:

> L. Osborn, H. Nguyen, R. Kaliki, and N. Thakor, "Prosthesis grip force modulation using neuromorphic tactile sensing," in *Myoelectric Controls Symposium (MEC)*, 2017, pp. 188–191

This article can be found at https://tinyurl.com/y9274qs7 or at http://www.unb.ca/research/institutes/biomedical/mec/_resources/docs/Past%20MEC%20Proceeding/MEC17FullProceedings.pdf

4.1 Overview

In this chapter, we use tactile signals to improve prosthesis grasping. The difference from the last chapter is that here we look at how using a neuromorphic representation of touch can be incorporated into a prosthesis. This is the first time a neuromorphic tactile signal is used used for real-time control. The lack of tactile feedback is not a new problem for prosthesis users, but how tactile information is handled can have a significant impact on the performance of the system. As pros-

thetic limbs become more advanced, there has been a push towards developing systems that are biologically inspired to more closely mimic how the healthy human system operates. Tactile information is represented by slowly adapting (SA) and rapidly adapting (RA) mechanoreceptors in the skin. In this work we utilize a leaky integrate and fire neuron model with spike rate adaption for representing tactile information in a prosthetic hand. The model is tuned to exhibit realistic firing rates corresponding to the grip force measured by sensors on the fingertips of the prosthesis. We investigate the use of the simulated neuron spike rate in an EMG gain modulating function to limit the amount of grip force applied by a prosthetic hand during grasping of a delicate object. We compare this method with the use of the grip force as an input to the EMG gain modulating function as well as to grasping with no tactile feedback. Results show a reduction in the percentage of broken objects during grasping from 27.5% with no feedback to 14% with grip force feedback and 14.5% when using the neuromorphic spiking of the LIF neuron. This demonstrates the feasibility of using a neuromorphic representation of tactile information for improving prosthesis functionality in real-time.

4.2 Introduction

The sense of touch offers a multitude of functionality such as exploring intricate objects, performing complex finger movements, or even providing comfort to loved ones. The seemingly unparalleled performance of tactile sensation gives rise to our instinctive behavior to reach out and explore new objects or surroundings with our hands. Our sense of touch helps provide information on texture, shape, weight, and temperature, which we rely on for understanding objects [141, 142]. Together with the visual system, the tactile information we process through our peripheral nervous system

helps us paint a more complete picture of our surroundings [77].

One problem faced by people with upper limb loss is the lack of tactile information in most commercial prosthetic limbs available today [143]. Although recent developments in myoelectric (EMG) prosthesis control have shown improvements in pattern recognition control strategies [31, 67, 107], a major component of creating fully functioning upper limb prostheses is tactile feedback. This has led to progress in novel closed-loop tactile feedback control algorithms [16, 116, 144], sensory feedback via peripheral nerve stimulation [2, 91, 92, 98], and even the social aspect of touch for prostheses [145].

As technology moves towards more human-like prosthetic arms it is necessary to develop faster, more efficient, and more natural ways of processing tactile information to be used for sensory stimulation. Early work with sensory feedback of tactile information used force sensor information to drive peripheral nerve stimulation where increased grip force translated to increased stimulation frequency, which was used for object discrimination [91] and grip force modulation [2]. More recently, an Izhikevich neuron stimulation model was implemented using signals from a tactile sensing prosthetic finger for texture discrimination [98, 146]. In an effort to provide more biologically inspired responses to tactile information during prosthesis grasping, recent work has also shown functionality improvements using event-based triggers to respond to contact and slip during grasping [16].

There is a trend towards developing neuromorphic devices and models to mimic the natural behavior of biological systems to improve efficiency and performance over traditional methods. Recent examples include the vestibular system [130], eye saccades [128], cortical neurons [123], visual information processing [125], touch [147], and other sensory systems [148]. For the purpose of tactile feedback in upper limb prostheses a neuromorphic approach includes modeling of

the slowly adapting (SA) and rapidly adapting (RA) mechanoreceptors found in our skin. The goal being that this approach will offer more efficient transmission of relevant tactile information, similar to a healthy peripheral nervous system, to the prosthesis controller as well as for driving nerve stimulation for sensory feedback. Recent efforts towards improving tactile feedback systems specifically for prostheses using a more biologically inspired approach include novel synthetic skin designs [30], the previously mentioned neuron modeling [98], and event-based signal processing [16]. Previous work using models to simulate tactile afferent patterns have investigated implementation of the models with little emphasis on real-time functionality [149–152]. In this work we investigate the ability of a prosthesis controller to functionally interpret a neuromorphic model of tactile information using a leaky integrate-and-fire neuron with spike rate adaption to estimate grip force and prevent breaking a delicate object during a prosthesis grasping task.

4.3 Model & Methods

One particular model that is commonly used to simulate the behavior of SA and RA mechanoreceptors is the leaky integrate and fire (LIF) neuron model [149–153]. In its basic form, a neuron is modeled as a leaky integrator of the input current $I(t)$

$$\tau_m \frac{dv}{dt} = v_r - v(t) + RI(t) \tag{4.1}$$

where $v(t)$ represents the membrane potential at time t, and τ_m is the membrane time constant. R is the membrane resistance. This is a simple RC circuit where the leakage is due to the resistor and the integration of $I(t)$ is from the capacitor in parallel. When the membrane potential reaches a spiking threshold, v_{th}, it is reset instantaneously to a lower value, v_r.

For this work we implemented an LIF neuron model with spike rate adaption, which introduces a hyperpolarizing current that makes the neuron less likely to fire once it has previously fired. This adapted model is used to create the neuromorphic response and represent a more realistic neuron spiking behavior. The model can be written as

$$\tau_m \frac{dv}{dt} = v_r - v(t) + RI(t) - g(t)\left(v(t) - E_k\right) \tag{4.2}$$

where the refractory conductance of the neuron is given by $g(t)$ and E_k is the reversal potential for the spike rate adaption. The change of the conductance is given as

$$\tau_g \frac{dg}{dt} = -g(t) \tag{4.3}$$

where τ_g is the conductance refractory period. The conductance is incremented by Δg after each spike. A more detailed and complete discussion of this model and its extensions can be found in [153].

To create a neuromorphic tactile feedback system, we use the output of force sensors as the input stimulus, $I(t)$, to the model. The model is tuned so that the maximum firing rate is 100 Hz, which occurs when the grip force of the prosthesis is 20 N. This model represents a SA type neuron due to its sustained response to a given input. The neuromorphic tactile feedback method presented here differs from our previous work in that it uses more realistic, continuous neuron model dynamics to simulation spiking behavior. The neuron firing rate of the mechanoreceptor model is used to determine grip force, which is then used to prevent accidental damage to delicate objects during grasping. Our previous work utilized event-based spikes to trigger the onset, offset, and changes in

force but used the raw sensor signal for determining grip force [16].

The sensors are placed on the thumb, index, and middle fingertips of a bebionic3 prosthetic hand (Steeper, Leeds, UK) (Fig. 4.1A). The sensors are force sensitive resistors made up of stretchable textiles. The sensors are cuffs designed to fit over the phalanges of a prosthetic hand. The cuff contains conductive textiles (LessEMF, Latham, USA), which are used to sandwich a piezoresistive layer (Eeonyx, Pinole, USA). A 3mm silicone rubber layer (Dragon Skin 10, Smooth-On, Macungie, USA) is on the outer surface of the cuff to provide realistic fingertip compliance to the cuff (Fig. 4.1B. These sensors have been previously developed and used for measuring grip force on a prosthetic hand [16, 136]. Each fingertip cuff has 3 sensing elements. A custom control board, with an ARM Cortex-M processor, developed by Infinite Biomedical Technologies (Baltimore, USA) is used to interface with the prosthesis and read in the fingertip force sensor signals. The grip force is found by summing the output of the sensing elements. Electromyography (EMG) electrodes (Infinite Biomedical Technologies, Baltimore, USA) are used to record motor neuron activity in the forearm from the prosthesis user to control the hand. The neuromorphic model is implemented using MATLAB (MathWorks, Natick, USA). The sensor signals are relayed via bluetooth communication to MATLAB from the prosthesis controller. The sensor signals are sampled and sent to MATLAB at 200 Hz while the EMG electrodes are sampled at 1 kHz. The system diagram is shown in Fig. 4.2.

An EMG gain modulating function that uses tactile information is implemented on the prosthesis controller to limit the amount of grip force applied during grasping. This exponential decaying function, the *Compliant Grasping* algorithm, was presented and described in detail in [16]. We adapted the algorithm for this work to limit the maximum grip force to 10 N before forcing the

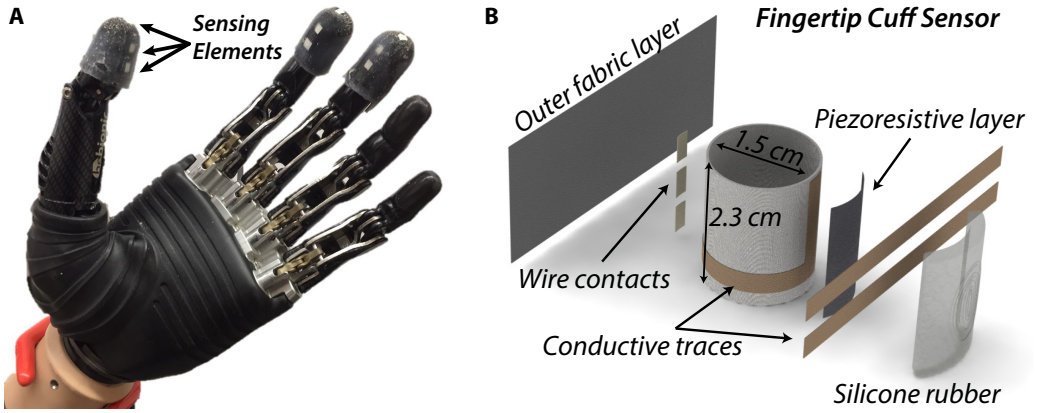

Figure 4.1: (A) The fingertip cuff sensors are placed on the thumb, index, and middle fingers of the bebionic3 prosthesis. Each sensor cuff contains three sensing elements, whose values are recorded by the prosthesis controller. (B) The cuff is made up of conductive and piezoresistive textiles as well as silicone rubber.

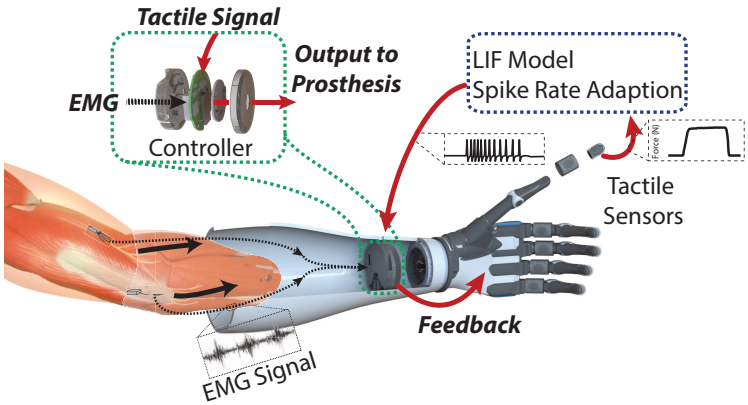

Figure 4.2: The system diagram shows the flow of information and tactile signal processing for an upper limb prosthesis. The prosthesis grip force serves as the input to the neuromorphic model. The prosthesis controller processes both EMG and tactile signals, which allows for efficient modulation of the information being sent to the prosthesis as feedback. In this work, the feedback to the prosthesis is a modulated EMG gain that is dependent on the spike rate of the neuromorphic model.

EMG signal to zero. EMG modulation was only applied to the electrode signal that closed the prosthesis. Two algorithm conditions were investigated in this work. The first uses the measured grip force as the input to the EMG modulating function, which is similar to the approach in [16]. The second method uses the output of the neuromorphic model and the neuron firing rate as the input to the EMG modulating function. The goal here is to investigate the ability of a prosthesis to utilize neuromorphic input as a way to successfully modulate a user's EMG signal to improve grasping of delicate objects.

4.4 Experiments & Results

To evaluate the neuromorphic tactile feedback system the prosthetic hand was mounted on a stand and controlled by the user's forearm EMG signals. Three male subjects participated in this experiment, a bi-lateral upper limb amputee and two able-bodied individuals. The participants controlled the prosthesis to grab, hold, and release a delicate object presented by the experimenter. The experiment was approved by the Johns Hopkins Medicine Institutional Review Board. The goal was to not break the object, a cracker (m $= 1.8 \pm 0.11$ g, force to break > 8 N), during grasping. Each user was allowed to practice with the system for up to 10 minutes before starting the experiment. Three different conditions were tested: 1) no tactile feedback, 2) grip force (GF) tactile feedback and 3) neuromorphic spike rate (SR) tactile feedback. Each trial consisted of 10 presentations of the delicate object, and the number of broken objects was recorded. Up to 10 trials of each condition were performed in a random order. Results from all participants are similar and were combined to provide a larger data set. As described in the previous section, both of the tactile feedback conditions reduced the amplitude of the EMG signal to close the prosthesis, effectively limiting the

hand's ability to exert a large grip force, similar to what has been described in [16] and [6].

The neuromorphic response to the tactile signal during grasping is shown in Fig. 4.3. This figure shows a representative grasp, hold, and release for a single trial from the experiment. The spike rate of the neuron is found using a 60 ms sliding window and is used in the EMG gain modulation algorithm for limiting the amount of grip force applied by the prosthesis. The results from the prosthesis grasping task are shown in Fig. 4.4. The number of broken objects are recorded and the average percentage of broken objects for each testing condition are shown in Fig. 4.4. With no tactile feedback, 27.5% of the objects broke during grasping. Using the total grip force as an input to the EMG gain modulation function, 14% of the grasped objects broke whereas 14.5% of the objects broke when using the neuromorphic spiking behavior from the neuron model as the input for EMG gain modulation. The error bars in Fig. 4.4 represent the standard error of the mean.

4.5 Discussion

The LIF neuron model with spike rate adaption performs as expected by producing biologically relevant signals with realistic dynamics as shown by Fig. 4.3. The ability to represent tactile information using a neuromorphic approach will help further prosthesis technology by allowing for transmission of larger amounts of data in a more efficient manner, similar to how the human body acquires and processes information. The spike rate adaption component of the traditional LIF model provides more realistic neuron behavior by adjusting the neuron conductance with sustained stimulation. This adaption is seen in the prosthesis implementation by the decreasing firing rate during the sustained grip force in Fig. 4.3.

The neuromorphic approach to processing tactile information shows improved performance over

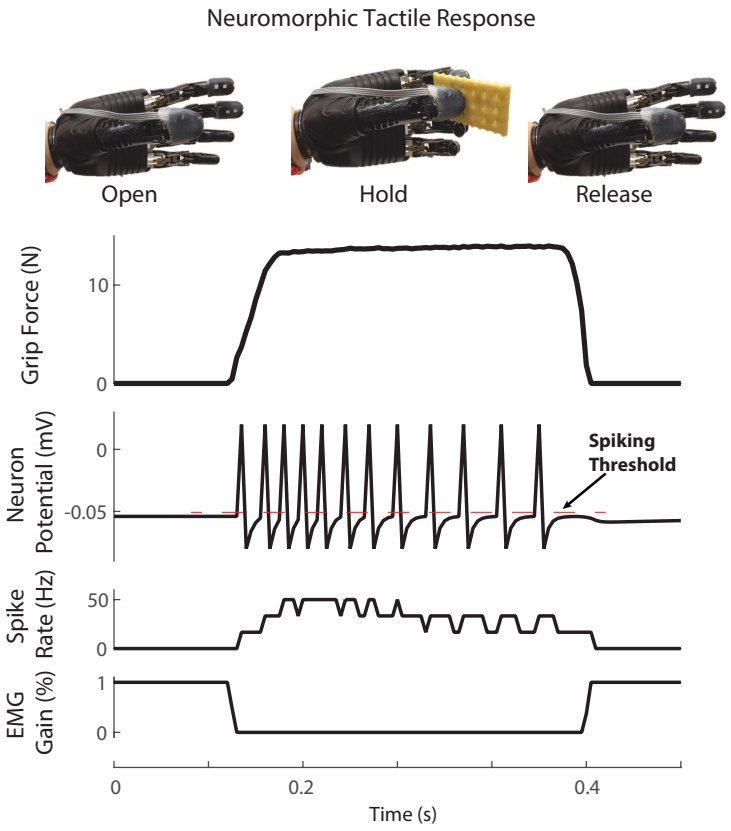

Figure 4.3: The grip force and corresponding neuromorphic spiking response during an actual prosthesis grasping task are shown by the top two curves, respectively. Spikes are counted when the neuron potential crosses the threshold, v_{th}. The neuron spike rate and the modulate EMG gain are shown by the bottom two curves, respectively. For the neuromorphic tactile feedback, the spike rate is used as the input to the EMG gain modulation algorithm. This data is taken from a single grasping task and is representative of the data set.

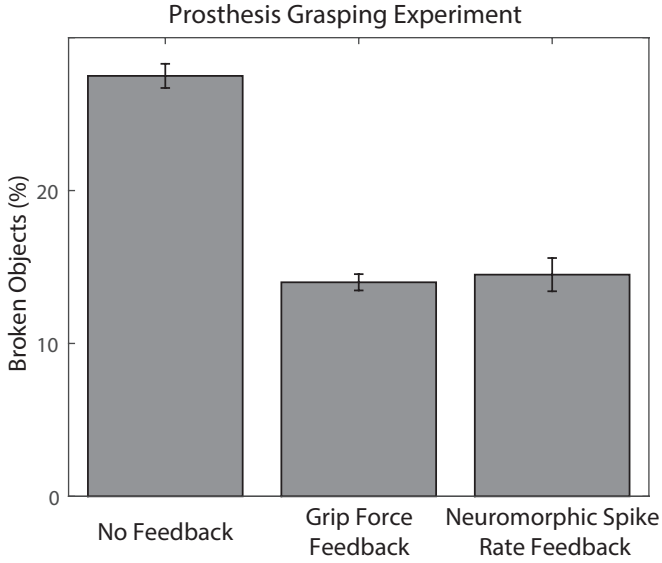

Figure 4.4: Results from the prosthesis grasping task show improvements while using tactile feedback. The use of grip force or neuromorphic spike rate show improvements over the case of no tactile feedback. The neuromorphic approach shows similar improvements as the more traditional method of using grip force as a feedback input.

no tactile feedback. With no form of tactile feedback, the prosthesis grasping task resulted in 27.5% of the objects being broken during the experiment. Including grip force information as part of an EMG modulating strategy drastically improves this number by reducing it to 14%, which is similar to results seen in [16] and [6]. The average percentage of broken objects is 14.5% while using only the firing rate of the LIF neuron with spike rate adaption for modulating the EMG gain. This is a significant finding in that it demonstrates the ability of the prosthesis hardware to efficiently process the spiking response and transform it into EMG gain modulation. Additional user testing under more scenarios is necessary to better understand the system's performance. The results presented here have major implications for future prosthetic limbs incorporating sensory feedback to the user. Providing realistic neuron activity to the prosthesis will help streamline the information flow from sensors back into the nervous system of the user.

4.6 Conclusion

The goal of this work is to demonstrate the feasibility of a neuromorphic tactile feedback system for use in a prosthetic arm. The results from the prosthesis grasping task suggest the ability to use a purely neuromorphic representations of a tactile signal for improving grasping of delicate objects. This is one of the first implementations of a neuron model to represent tactile information for real-time processing by a prosthetic limb. The highlight of this work is the use of a neuromorphic tactile feedback system based on a LIF neuron model with spike rate adaption for real-time functional improvements in a prosthesis. This will play an important role for future prosthetic technology as limbs become more sophisticated and attempt to mimic the human body in both utility and performance.

5 | Targeted Sensory Feedback in Upper Limb Amputees

This chapter is made up of content, with permissions and minor modifications, from [26].

L. Osborn, M. Fifer, C. Moran, J. Betthauser, R. Armiger, R. Kaliki, and N. Thakor, "Targeted transcutaneous electrical nerve stimulation for phantom limb sensory feedback," in *IEEE Biomedical Circuits and Systems (BioCAS)*, 2017, pp. 1–4. [doi]

5.1 Overview

In this chapter, we investigate the use of noninvasive, targeted transcutaneous electrical nerve stimulation (TENS) of peripheral nerves to provide sensory feedback to two amputees, one with targeted sensory reinnervation (TSR) and one without TSR. In the previous chapters we discussed the role of local tactile feedback (i.e. to the prosthesis) in improving grasping function. A major step in developing a closed-loop prosthesis is providing the sense of touch back to the amputee user. We investigated the effect of targeted nerve stimulation amplitude, pulse width, and frequency on stimulation perception. We discovered that both subjects were able to reliably detect stimulation patterns with pulses less than 1 ms. We utilized the psychophysical results to produce a subject specific stimulation pattern using a leaky integrate and fire (LIF) neuron model from force sensors on a prosthetic hand during a grasping task. For the first time, we show that TENS is able to provide graded sensory

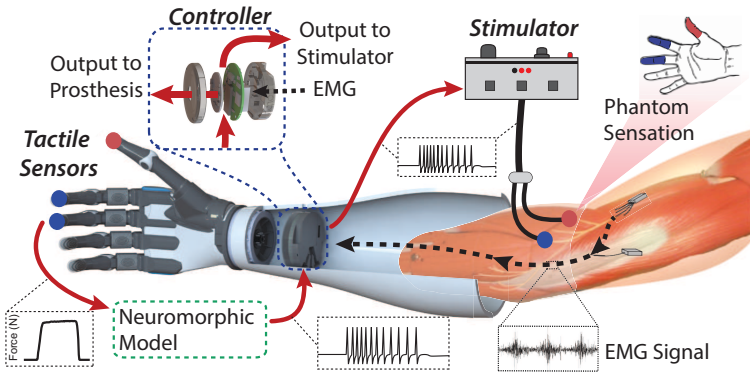

Figure 5.1: Schematic of targeted transcutaneous electrical nerve stimulation on the residual limb of an amputee for sensory feedback to the phantom limb. Multiple peripheral nerve sites can be stimulated on an amputee to elicit activation of specific regions of the phantom hand. Sensor outputs from a prosthetic hand can be mapped to specific nerve stimulation sites and a neuromorphic tactile signal used to drive stimulation for closed-loop sensory feedback for amputees. ©2017 IEEE.

feedback at multiple sites in both TSR and non-TSR amputees while using behavioral results to tune a neuromorphic stimulation pattern driven by a force sensor output from a prosthetic hand.

5.2 Introduction

An overarching goal for upper limb prosthetic technology is a system with both forward motor control and sensory feedback through the use of nerve stimulation to elicit sensations in the missing hand of the user (Fig. 5.1). Touch sensation plays a vital role in our ability to explore texture, manipulate objects, or even use tools. The sensations we perceive from cutaneous afferents allow us to understand and infer seemingly complex details of an object such as shape, weight, or temperature [142]. Two major issues resulting from upper limb amputation are the loss of both motor control signals and sensory information. Significant developments with myoelectric (EMG) prosthesis control, specifically pattern recognition strategies, have shown promise in restoring intuitive hand movements to amputees [27, 67, 73]. There has been a great deal of recent progress in sensor development [30, 136] and local closed-loop tactile feedback strategies for improving prosthesis grasping [16, 25, 116], and even sensory feedback through direct nerve stimulation [92, 98, 100].

In addition to advances in prosthesis hardware and control methods, novel surgical methods have emerged, including targeted motor and sensory reinnervation [51, 69, 95]. In targeted reinnervation surgery, amputated efferent or afferent peripheral nerves that once innervated muscles or skin in the missing limb are rerouted to muscle or skin in the residual limb [51]. The muscle with the reinnervated peripheral nerves produces EMG signals that correspond to the original motor commands of the missing limb [51]. Targeted muscle reinnervation allows for more intuitive and higher dimensional motor control [51]; targeted sensory reinnervation can enable more intuitive noninvasive sensory feedback as cutaneous interactions with the reinnervated sites are perceived to localize to the missing limb [69]. In a previously reported case study, transcutaneous electrical nerve stimulation (TENS) of a targeted reinnervation site was used to activate regions of an amputee's phantom hand [69]. In a recent advancement of the targeted sensory reinnervation (TSR) surgery, individual nerve fascicles of the median and ulnar nerves were routed to regions of an amputee's residual limb away from motor regions to create more distinction and separation between activated sensory regions of the phantom hand [95]. In this work we attempt to understand the sensory perception created by using noninvasive TENS of the median and ulnar nerves in the residual limb of two transhumeral amputees. We investigate the use of TENS as a viable method for sensory feedback in 1) an amputee with TSR surgery and 2) an amputee with no TSR surgery through sensory mapping and psychophysics to determine stimulation thresholds. Finally, we build upon our previous work [25] to create a subject specific neuromorphic stimulation pattern, driven by the output from force sensors on a prosthetic hand, using a leaky and integrate fire (LIF) neuron model.

Table 5.1: Subject characteristics. ©2017 IEEE.

Subject	**A1**	**A2**
Gender	Female	Male
Age	43	29
Amputation Side	Right	Left
Amputation Level	Transhumeral	Transhumeral
Amputation Type	TSR	No TSR
Time Since Amputation	1.5 yr	5 yr

5.3 Methods & Experiments

Two transhumeral amputee subjects participated in this study. One subject (A1) had undergone targeted sensory and muscle reinnervation surgery 1.5 years prior to the study and the other subject (A2) was amputated (5 years prior) without any targeted reinnervation. In both cases, amputation was a result of severe sepsis. Both users have operated myoelectric prostheses but neither had undergone electrical stimulation for sensory feedback. Characteristics of each subject are shown in Table 5.1. To understand the mapping between peripheral nerves in the residual limb and activation in the phantom hand of each subject, we used an Ag-AgCl probe with a 2 mm tip to electrically stimulate regions of the residual limb. The anterior region, which was the target of the TSR surgery, of the residual limb was scanned with the stimulating probe for subject A1 and both anterior and posterior sides of subject A2's residual limb were scanned. An outline of a hand was used for each subject to indicate which regions were activated during electrical stimulation. Figure 5.2 shows the stimulation sites and activation regions in the phantom hand for subject A1 and Fig. 5.3 shows the mapping for subject A2. For both subjects, the median and ulnar nerves were targeted for stimulation. In general, the subjects reported sensations of tingling and occasional pressure in the activated regions on the phantom hand.

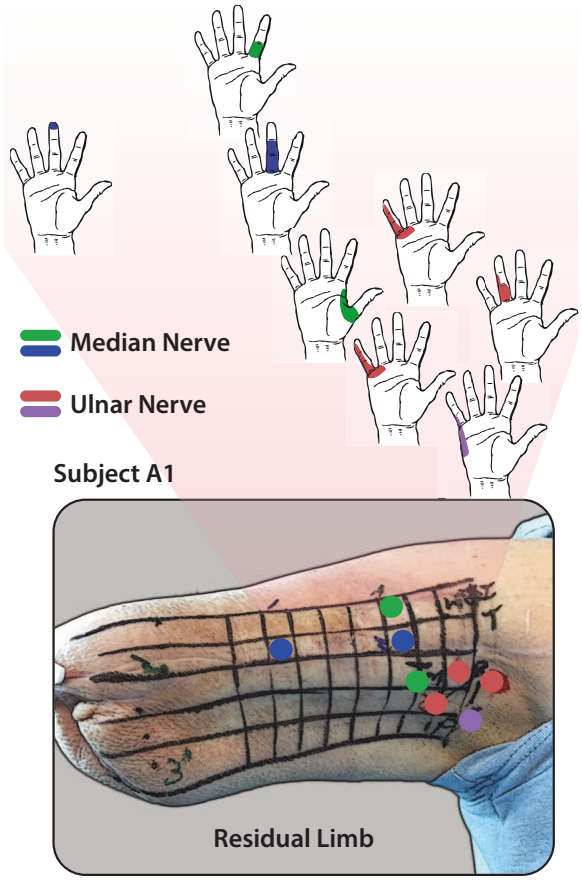

Figure 5.2: Phantom hand activation mapping for stimulation of the median and ulnar nerve areas for subject A1. Targeted reinnervation of median and ulnar nerves to the anterior part of the residual limb provides distinct mapping to various parts of the phantom hand. ©2017 IEEE.

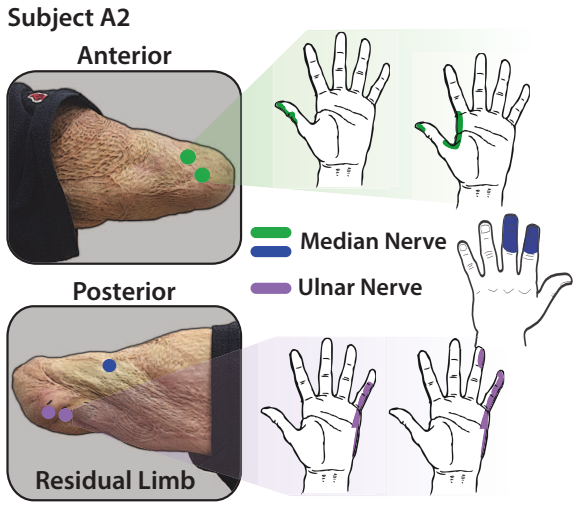

Figure 5.3: Phantom hand activation mapping for stimulation of identified median and ulnar nerve areas for subject A2. Although targeted reinnervation was not performed on this subject at the time of amputation, natural reinnervation occurred in the residual limb but with less order than in the case of subject A1. ©2017 IEEE.

5.3.1 Perception Experiments

To better understand how noninvasive peripheral nerve stimulation can be utilized for sensory feedback in prosthetic limbs we performed psychophysical experiments to determine detection thresholds by varying pulse width and frequency of the stimulation pattern. In this study, a monophasic, single channel, isolated constant current stimulator (DS3, Digitimer, England) was used. A 5 mm disposable Ag-AgCl electrode was placed on the skin over a region corresponding to a specific activation area of the phantom hand. For subject A1 the middle finger (median nerve) of the phantom hand was stimulated and the pinky finger (ulnar nerve) was stimulated for subject A2. These regions were chosen because they caused very distinct and comfortable activation of the phantom hand for the subjects. Unless otherwise noted, an electrical stimulation amplitude of 1.0 mA was used for all experiments.

To understand the sensory perception of the nerve stimulation we performed two experiments. 1) Stimulation detection to determine the minimum levels of detectable stimulation for the targeted activation sites and 2) discrete vs continuous frequency detection to determine the levels of stimulation that result in the sensation of a continuous perception in the targeted activation sites. The subject was seated in front of a computer monitor that displayed a visual cue when stimulation was on. For each experiment, the targeted nerve site was stimulated for 2 s. For the first experiment the subject verbally indicated if he/she felt the stimulation. The stimulation frequency and amplitude were held constant while the pulse width was modulated. For the second experiment the subject verbally indicated if he/she perceived the stimulation as being discrete or continuous. The stimulation amplitude and pulse width were held constant while the frequency was modulated. Every stimulation pattern was randomized and presented at least 5 times for each experiment. Psychometric functions were

fit to the data using a sigmoid link function:

$$\frac{1}{1+e^{-(x-\alpha)/\beta}} \tag{5.1}$$

where α is the detection threshold and β is the discrimination sensitivity. Both parameters were found using the curve fitting toolbox in MATLAB (MathWorks, USA).

5.3.2 Neuromorphic Sensor Model

As a demonstration, we implemented a leaky integrate and fire neuron model on customized prosthesis hardware (Infinite Biomedical Technologies, USA) to create a subject specific neuromorphic spiking output from previously developed force sensors on a bebionic3 prosthetic hand (Steeper, UK) [136]. Subject A2 performed a grasping task with the prosthetic hand where he picked up, held, and released an object. The prosthesis was controlled using subject A2's EMG signals. The pulse width and frequency of the neuromorphic output was based on the stimulation detection thresholds for subject A2. In this demonstration, the neuromorphic tactile signal was used as feedback to the prosthesis controller but not the subject to demonstrate feasibility. The neuromorphic model is given by

$$\tau_m \frac{dv}{dt} = v_r - v(t) + RI(t) - g(t)\left(v(t) - E_k\right) \tag{5.2}$$

where $I(t)$ is the model input current from the prosthesis grip force, $v(t)$ represents the neuron's membrane potential at time t, and τ_m is the membrane time constant. R is the membrane resistance. When the neuron potential reaches a spiking threshold, v_{th}, it is reset instantaneously to a lower value, v_r. The refractory conductance of the neuron is given by $g(t)$ and E_k is the reversal potential for the model's spike rate adaption. The use of this model is discussed in more detail in our previous

work [25]. The pulse width and maximum frequency of the neuromorphic tactile signal is tuned to subject A2's stimulation perceptions. The prosthesis grip force is mapped to frequency because subject A2 reported that he perceived increase in stimulation intensity with increasing frequency. For more details on this model and its parameters see [25]. All experiments were approved by the Johns Hopkins Medicine Institutional Review Boards and the subjects provided informed consent before participating, and all data was collected and analyzed using MATLAB.

5.4 Results

The results from the stimulation detection experiment for both subjects are shown in Fig. 5.4. The detection threshold is defined as the pulse width where the probability of feeling the stimulation is 0.5. Subject A1 has a detection threshold of 2.1 ms and 4.6 ms for stimulation with an amplitude of 1.0 mA and frequency of 20 Hz and 2 Hz, respectively. Subject A2 has a detection threshold of 0.78 ms and 0.94 ms for a stimulation frequency of 20 Hz and 2 Hz, respectively. Figure 5.5 shows the shift in detection threshold for subject A1 when the stimulation amplitude is increased from 1.0 mA to 1.2 mA. The increased stimulation amplitude causes a decrease (leftward shift) in the detection threshold. The results from the second experiment, with a corresponding neuromorphic tactile response, are shown in Fig. 5.6. The frequency of the stimulation is modulated while the pulse width is held constant at 5 ms, which is well above the stimulation detection threshold for both subjects. Subject A1 has a threshold for perceiving a stimulation as continuous at 9.7 Hz while the threshold for subject A2 is 21 Hz. The neuromorphic tactile signal from the prosthesis grasping task is shown in Fig. 5.7. Based on the psychophysical results for subject A2, each spike from the neuromorphic tactile sensing output has a pulse width of 1 ms and the maximum spiking frequency

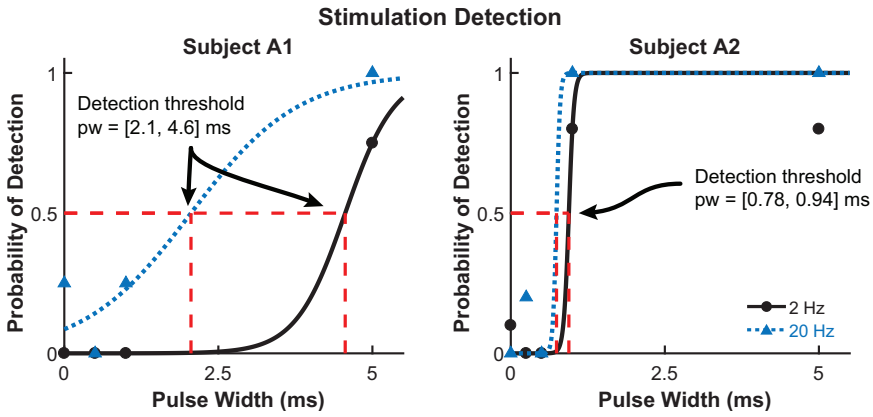

Figure 5.4: Stimulation detection for subjects A1 (left) and A2 (right). Multiple stimulation pulse widths (pw) and frequencies were used for each subject. From the fitted psychometric functions, the detection threshold for subject A1 is 2.1 ms and 4.6 ms for a stimulation frequency of 2 Hz and 20 Hz, respectively. The detection threshold for subject A2 is 0.78 ms and 0.94 ms for a stimulation frequency of 2 Hz and 20 Hz, respectively. The coefficient of determination, R^2, is > 0.91 for every psychometric function fit. ©2017 IEEE.

is mapped to 20 Hz, which corresponds to a grip force of 20 N.

5.5 Discussion

This work presents a unique look at how noninvasive TENS can be used to provide sensory feedback to both TSR and non-TSR transhumeral amputees. Targeted TENS provides distinct sensory activation in the phantom limb (Figs. 5.2 and 5.3) for both subjects. The TSR subject (A1) seemed to have more localized regions of phantom hand activation compared to the non-TSR subject (A2). This is likely due to the intentional placement of peripheral nerve fascicles in the anterior portion of subject A1's residual limb. For subject A2, median and ulnar nerve sites naturally reinnervated the skin but without any external guidance, causing less structure or ordering of the nerve sites. However, this does not mean that a non-TSR amputee is not a good candidate for targeted TENS for sensory feedback.

The minimum level of stimulation needed for reliable detection shown in Fig. 5.4 offers valuable insight to designing a fully closed-loop system. The frequency of the stimulation seems to

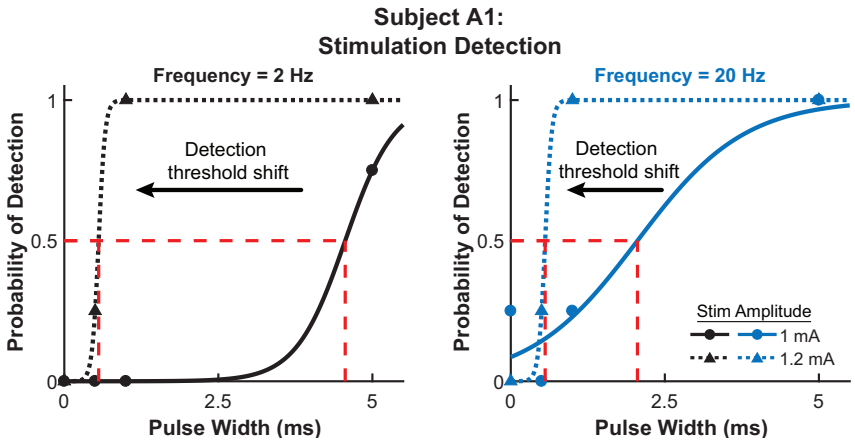

Figure 5.5: Detection threshold shift due to varying stimulation amplitude for subject A1 at a frequency of 2 Hz (left) and 20 Hz (right). Slight increase in stimulation amplitude from 1 mA to 1.2 mA for subject A1 causes a leftward shift in the detection threshold. The higher amplitude lowers the detection threshold to 0.56 ms for both 2 Hz and 20 Hz stimulation. Every psychometric function has an $R^2 > 0.91$. ©2017 IEEE.

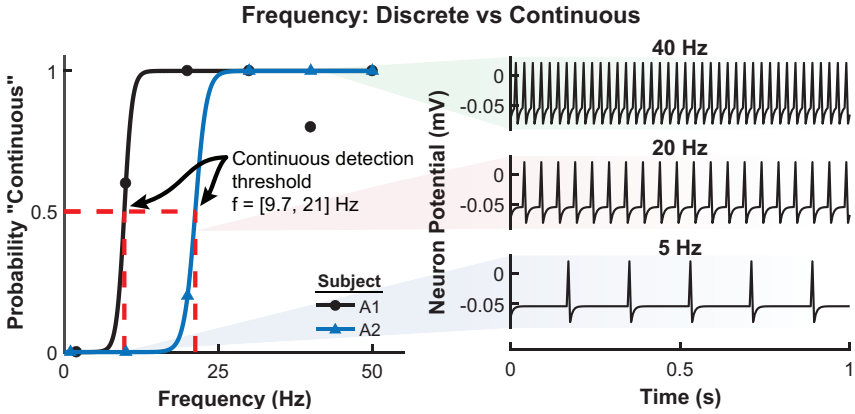

Figure 5.6: Perception of discrete or continuous stimulation for subjects A1 and A2 (left) with corresponding prosthesis neuromorphic output (right). The stimulation amplitude for subject A1 is 1.0 mA and 1.4 mA for subject A2. The frequency (f) threshold for perceiving a stimulation as continuous is 9.7 Hz for subject A1 and 21 Hz for subject A2. The fitted psychometric functions have an $R^2 > 0.90$. The neuromorphic tactile response represents points along the psychometric function at a particular frequency. ©2017 IEEE.

influence the detection threshold if the stimulation amplitude is low enough. Results in Fig. 5.5 show that both psychometric functions shift leftward (reduces the detection threshold) to 0.56 ms with slightly increased amplitude. For subject A2 (Fig. 5.4) it appears that the amplitude used was high enough for the detection thresholds to converge, a phenomenon seen for subject A1 after the stimulation amplitude was increased. Another important value is the threshold for perceiving a stimulation pattern as a discrete or continuous activation (Fig. 5.6). This is crucial for noninvasive

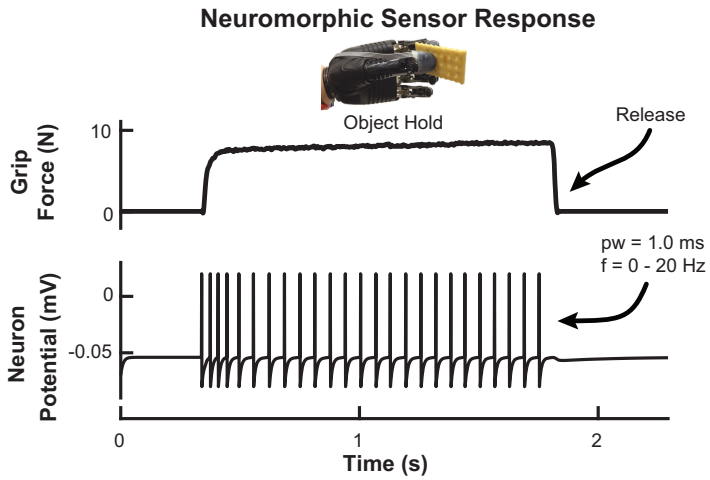

Figure 5.7: Neuromorphic tactile signal during the prosthesis grasping task. The LIF neuron model produces spikes, using stimulation and frequency detection thresholds for subject A2 to determine the pulse width (1 ms) and frequency range (0 - 20 Hz). This spiking output form the prosthesis sensors can then be used as feedback on the residual limb to create the closed-loop prosthesis. ©2017 IEEE.

electrical stimulation due to the low-pass filtering effects of skin and soft tissue on the residual limb. This threshold is 9.7 Hz and 21 Hz for subjects A1 (TSR) and A2, respectively. This threshold can be influenced by a variety of factors such as electrode placement, depth of nerve site in the skin, or skin conductance. The neuromorphic tactile response that would correspond to the psychometric function is also shown in Fig. 5.6. The psychometric function shows how the neuromorphic response from the prosthesis would be perceived by the user. The neurmorphic sensor model combined with prosthesis hardware gives subject specific stimulation patterns during object grasping to enable more advanced feedback (Fig. 5.7).

5.6 Conclusion

We showed how results from TENS on amputees can be utilized to tune a real-time neuromorphic output based on the grip force of a prosthetic hand. By understanding the detection thresholds for subject A2, we successfully implemented the LIF neuron model on prosthesis hardware to create a spiking output that is specific for the user (Fig. 5.7), which in this case is defined by the minimum

stimulation pulse width (1 ms) and frequency range needed for discrete stimulation pulse detection (0 - 20 Hz). Our goal is to further understand how noninvasive methods can be used for providing sensory feedback and how we can combine this with existing prosthesis sensors and hardware to create a fully closed-loop prosthetic system, as shown in Fig. 5.1.

6 | Multilayered e-Dermis for Perceiving Touch and Pain

This chapter is made up of content from [9].

L. E. Osborn, A. Dragomir, J. L. Betthauser, C. L. Hunt, H. H. Nguyen, R. R. Kaliki, and N. V. Thakor, "Prosthesis with neuromorphic multilayered e-dermis perceives touch and pain," *Science Robotics*, vol. 3, no. 19, p. eaat3818, 2018. [doi]

Supplementary material for this article can be found at http://robotics.sciencemag.org/content/suppl/2018/06/18/3.19.eaat3818.DC1

6.1 Overview

In this chapter, we utilize our findings from previous chapters for providing sensory feedback and expand it to include sensations of touch and pain. The human body is a template for many state-of-the-art prosthetic devices and sensors. Perceptions of touch and pain are fundamental components of our daily lives that convey valuable information about our environment while also providing an element of protection from damage to our bodies. Advances in prosthesis designs and control mechanisms can aid an amputee's ability to regain lost function but often lack meaningful tactile feedback or perception. Through transcutaneous electrical nerve stimulation (TENS) with an amputee, we discovered and quantified stimulation parameters to elicit innocuous (non-painful) and

noxious (painful) tactile perceptions in the phantom hand. Electroencephalography (EEG) activity in somatosensory regions confirms phantom hand activation during stimulation. We invented a multilayered electronic dermis (e-dermis) with properties based on the behavior of mechanoreceptors and nociceptors to provide neuromorphic tactile information to an amputee. Our biologically inspired e-dermis enables a prosthesis and its user to perceive a continuous spectrum from innocuous to noxious touch through a neuromorphic interface that produces receptor-like spiking neural activity. In a Pain Detection Task (PDT), we show the ability of the prosthesis and amputee to differentiate non-painful or painful tactile stimuli using sensory feedback and a pain reflex feedback control system. In this work, an amputee can use perceptions of touch and pain to discriminate object curvature, including sharpness. This work demonstrates possibilities for creating a more natural sensation spanning a range of tactile stimuli for prosthetic hands.

Special thanks to Andrei Dragomir for his assistance in analyzing the EEG data in this chapter. There are several supplementary videos for this chapter. Each reference to a video contains a hyperlink to the actual clip.

6.2 Introduction

One of the primary functions of the somatosensory system is to provide exteroceptive sensations to help us perceive and react to stimuli from outside of our body [74]. Our sense of touch is a crucial aspect of the somatosensory system and provides valuable information that enables us to interact with our surrounding environment. Tactile feedback, in conjunction with proprioception, allows us to perform many of our daily tasks that rely on the dexterous manipulation of our hands [154]. Mechanoreceptors and free nerve endings in our skin give us the means to perceive tactile

sensation [154]. The primary mechanoreceptors in the glabrous skin that convey tactile information are Meissner corpuscles, Merkel cells, Ruffini endings, and Pacinian corpuscles. The Merkel cells and Ruffini endings are classified as slowly adapting (SA) and respond to sustained tactile loads. Meissner and Pacinian corpuscles are rapidly adapting (RA) and respond to the onset and offset of tactile stimulation [74, 76]. More recently, research has shown the role of fingertips in coding tactile information [155] and extracting tactile features [78].

A vital component of our tactile perception is the sense of pain. Although often undesired, pain provides a protection mechanism when we experience a potentially damaging stimulus. In the event of an injury, increased sensitivity can even render innocuous stimuli as painful [156]. Nociceptors are dedicated sensory afferents in both glabrous and non-glabrous skin responsible for conducting tactile stimuli that we perceive as painful [156]. Nociceptors, free nerve endings in the epidermal layer of the skin act as high threshold mechanoreceptors (HTMRs) and respond to noxious stimuli through Aβ, Aδ, and C nerve fibers [74], which enables our perception of tactile pain. It was discovered that Aδ fiber HTMRs respond to both innocuous and noxious mechanical stimuli with an increase in impulse frequency while experiencing the noxious stimuli [157]. It is also known that mechanoreceptor activation along with nociceptor activation helps inhibit our perception of pain, and our discomfort increases when only nociceptors are active [75], which helps explain our ability to perceive a range of innocuous and noxious sensations. Although novel approaches have improved prosthesis motor control [73], comprehensive sensory perceptions are not available in today's prosthetic hands.

The undoubted importance of our sense of touch, and lack of sensory capabilities in today's prostheses, has spurred research on artificial tactile sensors and restoring sensory feedback to those

with upper limb loss. Novel sensor developments utilize flexible electronics [79, 158, 159], self-healing [84, 160] and recyclable materials [83], mechanoreceptor-inspired elements [88, 161], and even optoelectronic strain sensors [81], which will likely impact the future of prosthetic limbs. Local force feedback to a prosthesis is known to improve grasping [16], but in recent years there has been a major push towards providing sensory feedback to the prosthesis and the amputee. Groundbreaking results show that implanted peripheral nerve electrodes [2, 3, 91, 100] as well as noninvasive electrical nerve stimulation methods [26] can successfully elicit sensations of touch in the phantom hand of amputees.

Recent approaches aim to mimic biological behavior of tactile receptors using advanced skin dynamics [99] and what are known as neuromorphic [98] models of tactile receptors for sensory feedback. A neuromorphic system aims to implement components of a neural system, for example the representation of touch through spiking activity based on biologically driven models. One reason for utilizing a neuromorphic approach is to create a biologically relevant representation of tactile information using actual mechanoreceptor characteristics. Neuromorphic techniques have been used to convey tactile sensations for differentiating textures using SA-like dynamics for the stimulation paradigm to an amputee through nerve stimulation [98] and for feedback to a prosthesis to enhance grip functionality [25]. While important, methods of sensory feedback have been limited to sensations of pressure [91], proprioception [3], and texture [98] even though our perception of tactile information culminates in a sophisticated, multifaceted sensation that also includes stretch, temperature, and pain.

Current forms of tactile feedback fail to address the potentially harmful mechanical stimulations that could result in damage to cutaneous tissue, or, in this context, the prosthesis itself. We

investigate the idea that a sensation of pain could benefit a prosthesis by introducing a sense of self-preservation and the ability to automatically release an object when pain is detected. Specifically, we implement a pain reflex in prosthesis hardware that mimics the functionality of the polysynaptic pain reflex found in biology [10, 162, 163]. Pain serves multiple purposes in that it allows us to convey useful information about the environment to the amputee user while also preventing damage to the fingertips or cosmesis, a skin-like covering, of a prosthetic hand. It is worth noting that an ideal prosthesis would allow the user to maintain complete control and overrule pain reflexes if desired. However, in this paper we focus on the ability to detect pain through a neuromorphic interface and initiate an automated pain reflex in the prosthesis.

We postulate that the presence of both innocuous and noxious tactile signals will help in creating more advanced and realistic prosthetic limbs by providing a more complete representation of tactile information. We developed a multilayered electronic dermis (e-dermis) and neuromorphic interface to provide tactile information to enable the perception of touch and pain in an upper limb amputee and prosthesis. We show closed-loop feedback to a transhumeral amputee through transcutaneous electrical nerve stimulation (TENS) to elicit either innocuous or painful sensations in the phantom hand based on the area of activation on a prosthesis (Fig. 6.1). Furthermore, we identify unique features of peripheral nerve stimulation, specifically pulse width and frequency, that play key roles in providing both innocuous and noxious tactile feedback. Quantifying the differences in perception of sensory feedback, specifically innocuous and noxious sensations, adds dimensionality and breadth to the type and amount of information that can be transmitted to an upper limb amputee, which aids in object discrimination. Finally, we demonstrate the ability of the prosthesis and the user to differentiate between safe (innocuous) and painful (noxious) tactile sensations during grasp-

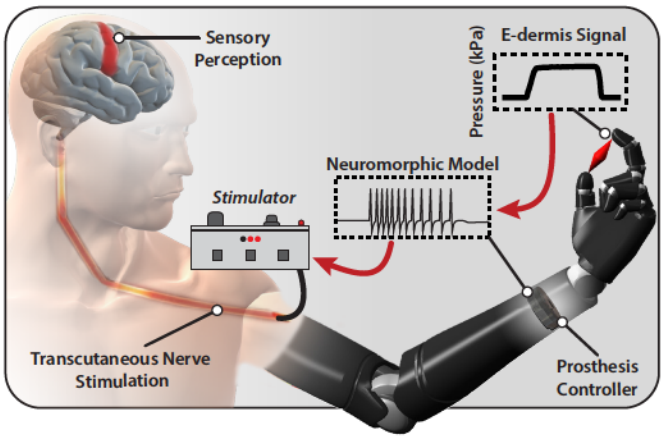

Figure 6.1: Prosthesis system diagram. Tactile information from object grasping is transformed into a neuromorphic signal through the prosthesis controller. The neuromorphic signal is used to transcutaneously stimulate peripheral nerves of an amputee to elicit sensory perceptions of touch and pain. Reprinted with permission from AAAS [9].

ing and appropriately react using a prosthesis reflex, modeled as a polysynaptic withdrawal reflex, to prevent damage and further pain.

6.3 Results

6.3.1 Biologically inspired e-dermis

Mechanoreceptors in the human body are uniquely structured within the dermis and, in the case of Meissner corpuscles (RA1) and Merkel cells (SA1), lie close to the epidermis boundary [74]. RA1 receptors are often found in the dermal papillae, which lend to their ability to detect movement across the skin, and SA1 receptors tend to organize at the base of the epidermis. However, in glabrous skin the HTMR free nerve endings extend into the epidermis (i.e. the outermost layer of skin) [74]. We used this natural layering of tactile receptors to guide the multilayered approach of our e-dermis (Fig. 6.2A) to create sensing elements to capture signals analogous to those detected by mechanoreceptors (dermal) and nociceptors (epidermal) in healthy glabrous skin (Fig. 6.2B). The sensor was designed using a piezoresistive (Eeonyx, Pinole, USA) and conductive fab-

rics (LessEMF, Latham, USA) to measure applied pressure on the surface of the e-dermis. A 1 mm rubber layer (Dragon Skin 10, Smooth-On, Easton, USA) between the artificial epidermal (top) and dermal (bottom) sensing elements provides skin-like compliance and distributes loads during grasping. There are 3 tactile pixels, or taxels, with a combined sensing area of approximately 1.5 cm^2 on each fingertip. The sensor layering resulted in variation of the e-dermis output during loading (Fig. 6.2C). The change in resistance in the tactile sensor was greater for the epidermal layer, enabling higher sensitivity. During grasping of an object, the e-dermis sensing layers, which were calibrated for a range of 0 – 300 kPa, exhibited differences in behavior. These differences can be used for extracting additional tactile information such as pressure distribution and object curvature (Fig. 6.2D-E).

6.3.2 Touch and pain perception

To provide sensory feedback, we used targeted TENS to extensively map and understand the perception of a transhumeral amputee's phantom limb during sensory feedback, a method we previously demonstrated in multiple amputees [26]. Although the participant did not undergo any targeted muscle or sensory reinnervation during surgery, there was a natural regrowth of peripheral nerves into the remaining muscles, soft tissue, and skin around the amputation. The median and ulnar nerves were identified on the amputee's left residual limb and targeted for noninvasive electrical stimulation because these nerves innervated relevant areas of the phantom hand. The participant received more than 25 hours of sensory mapping in addition to over 150 trials of sensory stimulation experiments to quantify the perceptual qualities of the stimulation. Extensive mapping of the residual limb showed localized activation of the amputee's phantom hand (Fig. 6.3A).

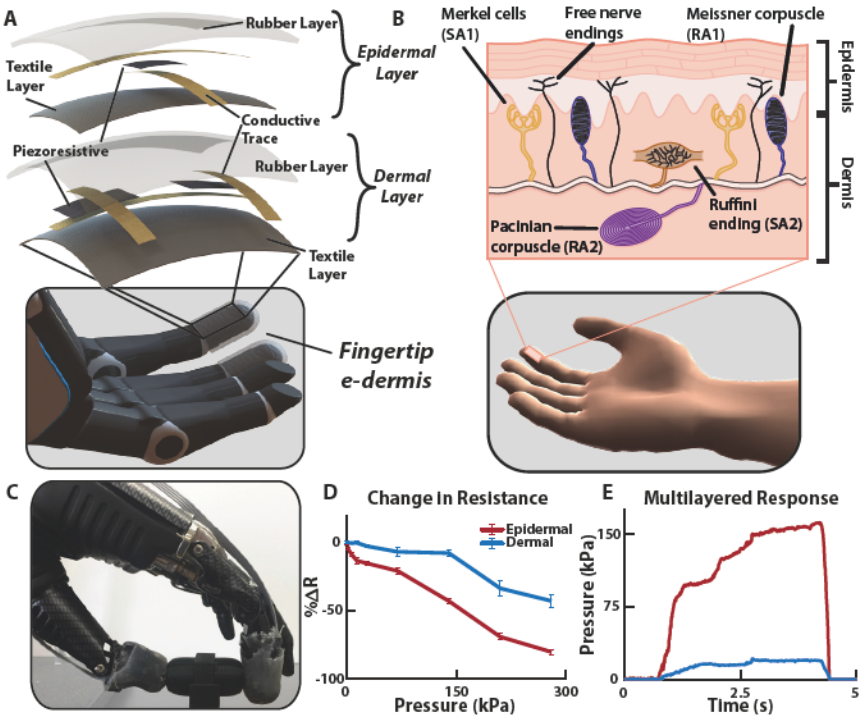

Figure 6.2: Multilayered e-dermis design and characterization. (A) The multilayered e-dermis is made up of conductive and piezoresistive textiles encased in rubber. A dermal layer of two piezoresistive sensing elements are separated from the epidermal layer, which has one piezoresistive sensing element, with a 1 mm layer of silicone rubber. The e-dermis was fabricated to fit over the fingertips of a prosthetic hand. (B) The natural layering of mechanoreceptors in healthy glabrous skin makes use of both rapidly (RA) and slowly adapting (SA) receptors to encode the complex properties of touch. Also present in the skin are free nerve endings (nociceptors) that are primarily responsible for conveying the sensation of pain in the fingertips. (C) The prosthesis with e-dermis fingertip sensors grasps an object. (D) The epidermal layer of the multilayered e-dermis design is more sensitive and has a larger change in resistance compared to the dermal layer. (E) Differences in sensing layer outputs are captured during object grasping and can be used for adding dimensionality to the tactile signal. Reprinted with permission from AAAS [9].

The amputee identified multiple unique regions of activation in his phantom hand from the electrical stimulation. The participant did not report any sensory activation, other than the physical presence of the probe, of his residual limb at the stimulation sites. He indicated that the dominating perceived sensation during stimulation occurred in his phantom hand, which is supported by our previous work [26]. Cutaneous receptors on the residual limb respond to physical stimuli whereas the electrical stimulation activates the underlying peripheral nerves to activate the phantom hand. Psychophysical experiments showed the amputee's perception of changes in stimulation pulse width and frequency on his median and ulnar nerves (Fig. 6.3B-C). In general, the stimulation was perceived primarily as pressure with some sensations of electrical tingling (paresthesia) (Fig. 6.3D).

Sensory feedback of noxious tactile stimuli was delivered using TENS to an amputee and the perception quantified. The results show that changes in both stimulation frequency and pulse width influence the perception of painful tactile sensations in the phantom hand (Fig. 6.3E). The relative discomfort of the tactile sensation was reported by the user on a modified comfort scale ranging from -1 (pleasant) to 10 (very intense, disabling pain that dominates the senses) (Table 6.1). In this experiment, the highest perceived pain was rated as a 3, which corresponded to uncomfortable but tolerable pain. The most painful sensations were perceived at relatively low frequencies between 10 and 20 Hz. Higher frequency stimulation tends towards more pleasant tactile sensation, which is contrary to what might be expected when increasing stimulation frequency [164]. In addition, very low frequencies generally resulted in innocuous activation of the phantom hand whereas frequency that are closer to the discrete detection boundary (15 – 30 Hz) resulted in the most noxious sensations in the activated region. We used electroencephalography (EEG) signals to localize and obtain an affirmation of the stimulus associated pain perception. The stimulation caused activation

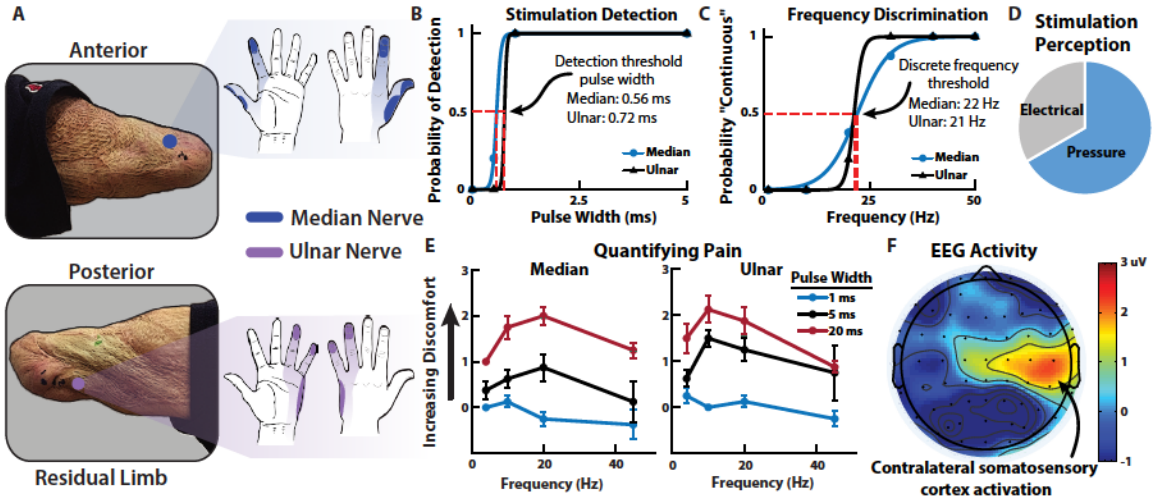

Figure 6.3: Sensory feedback and perception. (A) Median and ulnar nerve sites on the amputee's residual limb and the corresponding regions of activation in the phantom hand due to TENS. (B) Psychophysical experiments quantify the perception of the nerve stimulation including detection and (C) discrete frequency discrimination thresholds. In both cases the stimulation amplitude was held at 1.4 mA. (D) The perception of the nerve stimulation was largely a tactile pressure on the activated sites of the phantom hand although sensations of electrical tingling also occured. (E) The quantification of pain from nerve stimulation shows that the most noxious sensation is perceived at higher stimulation pulse widths with frequencies in the 10 - 20 Hz range. (F) Contralateral somatosensory cortex activation during nerve stimulation shows relevant cortical representation of sensory perception in the amputee participant (movie S1). Reprinted with permission from AAAS [9].

in contralateral somatosensory regions of the amputee's brain, which corresponded to his left hand (Fig. 6.3F) [165]. EEG activation during stimulation is significantly higher ($p<0.05$) than baseline activity, confirming the perceived phantom hand activation experienced by the user (Fig. 6.4, movie S1).

6.3.3 Neuromorphic transduction

As mentioned previously, a neuromorphic system attempts to mimic the behavior found in the nervous system. Based on the results from the sensory mapping of the participant, the neuromorphic representation of the tactile signal was developed to enable the sensation of both touch and pain. To enable direct sensory feedback to an amputee through peripheral nerve stimulation, the e-dermis signal was transformed from a pressure signal into a biologically relevant signal using a neuromor-

Table 6.1: Scaled comfort response. The table shows the scale used by the amputee subject during TENS to quantify the amount of pain or discomfort associated with stimulation patterns. An option for pleasant or enjoyable sensation (-1) was included because some stimulation patterns evoke this perception. The responses include no pain (0) all the way up to very intense pain (10). The highest response from the amputee subject was 4, which was recorded only for the most intense stimulation that elicited a painful perception. The scale is a modified version of a standard pain scale used in clinical environments to quantify chronic or acute pain in patients.

Group	Rating	Description
Pleasant	-1	Pleasant or enjoyable
Neutral	0	No pain
Minor	1	Very light barely noticeable pain, like a bite or itch
	2	Minor pain, like lightly pinching skin
	3	Uncomfortable but tolerable pain
Moderate	4	Very noticeable pain, like an accidental cut
	5	Slightly strong, uncomfortable pain. You can adapt to it over time
	6	Strong, deep pain, like a toothache or the sting from a bee. It's so strong you can't adapt to it
	7	Strong, deep, piercing pain, such as a sprained ankle when you stand on it wrong
Severe	8	Strong, deep piercing pain that is almost dominating your senses
	9	Strong, deep, piercing pain so strong it dominates your sense
	10	Same as 9 but pain completely dominates your senses, effectively disabling you

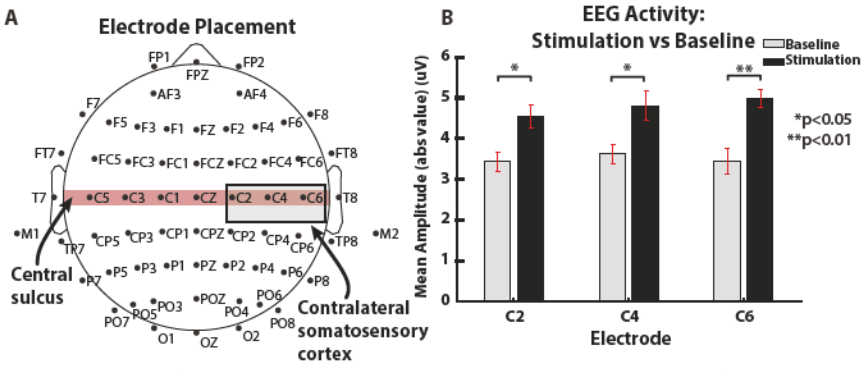

Figure 6.4: EEG activation. 64 channel EEG was used to collect neural activation from the amputee participant during nerve stimulation. (A) The standard 64 channel electrode placement covers the central sulcus. The primary somatosensory cortex is in the postcentral gyrus just posterior to the central sulcus (34). (B) Electrodes C2, C4, and C6 show cover the primary somatosensory cortex region and show significantly more activity during nerve stimulation.

phic model. The aim for the neuromorphic model was to capture elements of our actual neural system, in this case to represent the neural equivalent of a tactile signal for feedback to an amputee. To implement the biological activity from tactile receptors, namely the spiking response in the peripheral nerves due to a tactile event, we utilized the Izhikevich model of spiking neurons [146], which provides a neuron modeling framework based on known neural dynamics while maintaining computational efficiency and easily allowing for different neuron behaviors from parameter adjustments. The Izhikevich model has been used in previous work for providing tactile feedback to an amputee through nerve stimulation [98]. In our work, mechanoreceptor and nociceptor models produced receptor-specific outputs, in terms of neuron voltage, based on the measured pressure signal on the prosthesis fingertips. The mechanoreceptor model combined characteristics of SA and RA receptors through the regular and fast spiking Izhikevich neurons, respectively, to convey more pleasant tactile feedback to the amputee. The nociceptor model utilized fast spiking Izhikevich neuron dynamics to mimic behavior of the free nerve endings.

When an object was grasped by the prosthesis, a higher number of active taxels indicated a larger distribution of the pressure on the fingertip, which was conveyed in the neuromorphic transduction as an innocuous (i.e. non-painful) tactile sensation. Changes in the tactile signal were captured in the neuromorphic transduction by changes in stimulation frequency and pulse width to correspond to the appropriate perceived levels of touch or pain during sensory feedback. Based on the results from the psychophysical experiments and the quantification of pain, the perception of noxious tactile feedback was achieved through the nociceptor model (see Materials and Methods, Section 6.5.7).

To demonstrate the neuromorphic representation of a tactile signal, three different objects were used, each of equal width but varying curvature, to elicit different types of tactile perception in the

prosthesis during grasping (Fig. 6.5A). The objects follow a power law shape where the radius of curvature (R_c) was modified using the power law exponent n, which ranges between 0 and 1 and effectively defines the sharpness of the objects (see Materials and Methods, Section 6.5.9). The power law exponents used were $^1/_4$, $^1/_2$, and 1 and correspond to Object 1, Object 2, and Object 3, respectively. The response of the fingertip taxels during object loading captured differences in object curvature based on the relative activation of all sensing elements (Fig. 6.5B-C, movie S2). As expected, the epidermal layer was the most activated taxel during loading and absorbed the largest pressure. The sharp edge of Object 3 produced a highly localized pressure source on the epidermal layer of the e-dermis, which triggered the neuromorphic nociceptor model (see Materials and Methods, Section 6.5.7) (Fig. 6.5D).

6.3.4 Prosthesis tactile perception and pain reflex

As an extension of the body, a prosthetic hand should exhibit similar behavior and functionality of a healthy hand. The perception of both innocuous touch and pain are valuable at both the local (i.e. the prosthetic hand) and the global (i.e. the user) levels. At the local level, a reflex behavior from the prosthesis to open when pain is detected can help prevent unintended damage to the hand or cosmesis. It should be noted that in an ideal prosthesis this reflex would be modulated by the user based on the perceived pain. To demonstrate a local closed-loop pain reflex, a prosthetic hand, with a multilayered e-dermis on the thumb and index finger, grasped, held, and released one of the previously described objects (Fig. 6.6A-C). The sensor signals were used as feedback to the embedded prosthesis controller to enable differentiation of the various objects and determine pain. We used pressure distribution (Fig. 6.7A), contact rate (Fig. 6.7B), and the number of activated sensing elements per finger (Fig. 6.7C) as input features in a linear discriminant analysis (LDA)

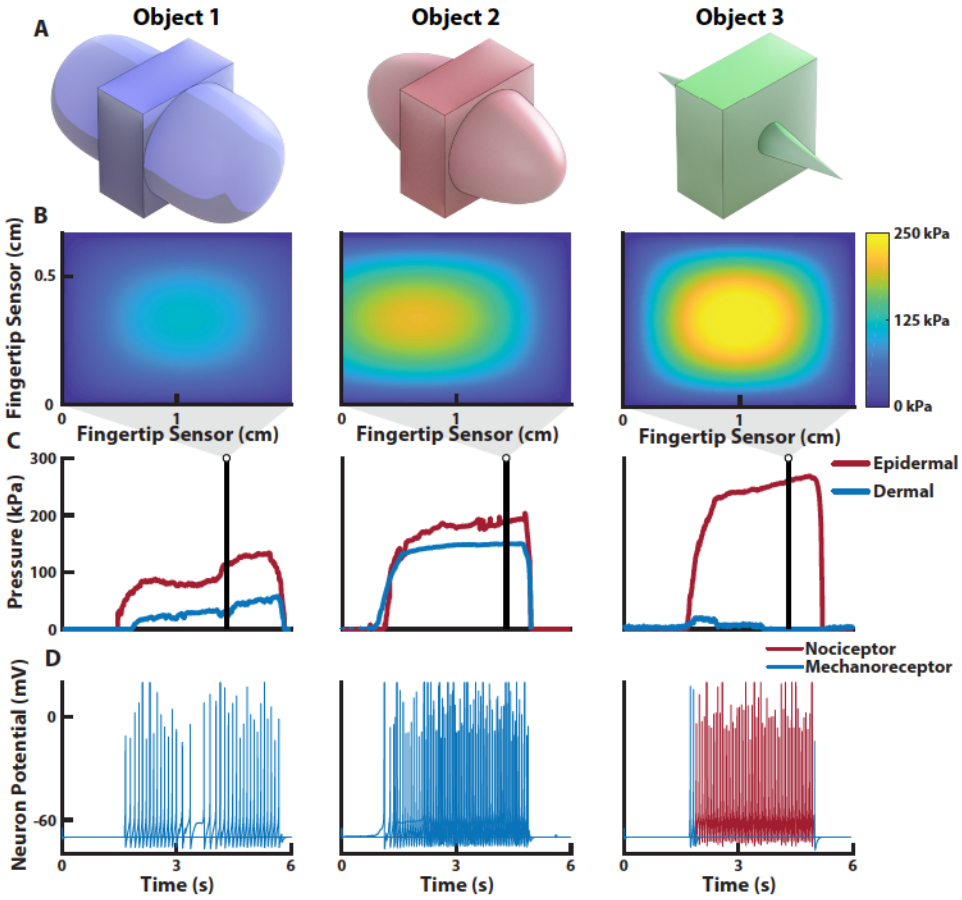

Figure 6.5: E-dermis and neuromorphic tactile response from different objects. (A) Three different objects, with equal width but varying curvature, are used to elicit tactile responses from the multilayered e-dermis. (B) The pressure heatmap from the fingertip sensor on a prosthetic hand during grasping of each object and (C) the corresponding pressure profile for each of the sensing layers. (D) The pressure profiles are converted to the input current, I, for the Izhikevich neuron model for sensory feedback to the amputee user (movie S2). Note the highly localized pressure during the grasping of Object 3 and the resulting nociceptor neuromorphic stimulation pattern, which is realized through changes in both stimulation pulse width and the neuromorphic model parameters. Reprinted with permission from AAAS [9].

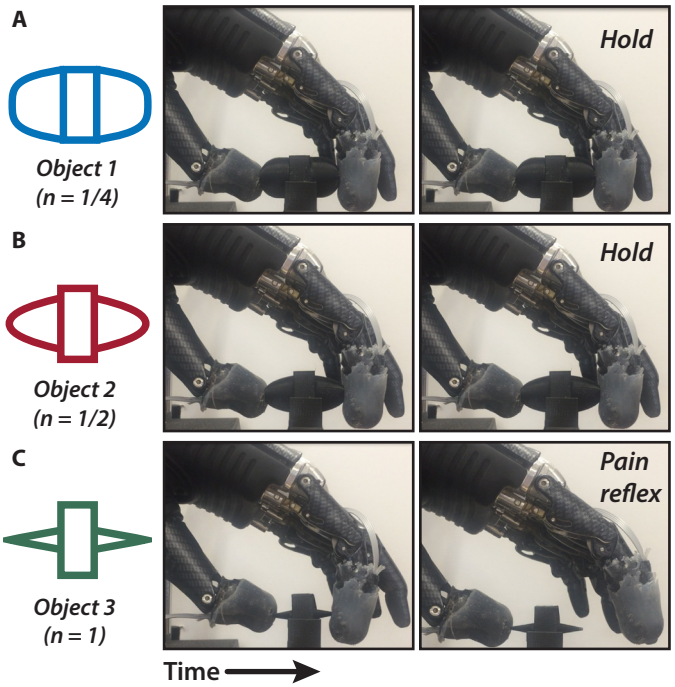

Figure 6.6: To demonstrate the ability of the prosthesis to determine safe (innocuous) or unsafe (painful) objects, we performed the pain detection task (PDT). The objects are (A) Object 1, (B) Object 2, and (C) Object 3, each of which are defined by their curvature. In the case of a painful object (Object 3), the prosthesis detects the sharp pressure and releases its grip through its pain reflex (movie S3). Reprinted with permission from AAAS [9].

algorithm for object detection.

In the online Pain Detection Task (PDT), the prosthesis grabs, holds, and releases an object (movie S3). In this work, the curvature of Object 3 was assumed to be considered painful during grasping. When pain was detected, a prosthesis pain reflex caused the hand to open, releasing the object. Results showed the prosthesis' ability to reliably detect which object is being grasped (Fig. 6.8A). The prosthesis had a high likelihood of perceiving pain while grasping Object 3 and a significantly less likelihood of perceiving pain for Objects 2 and 1 ($p<0.001$) (Fig 6.8B). The reaction time for the prosthesis to complete a reflex after perceiving pain was recorded and was similar to reaction times in healthy humans from previously published data [10] (Fig. 6.8C).

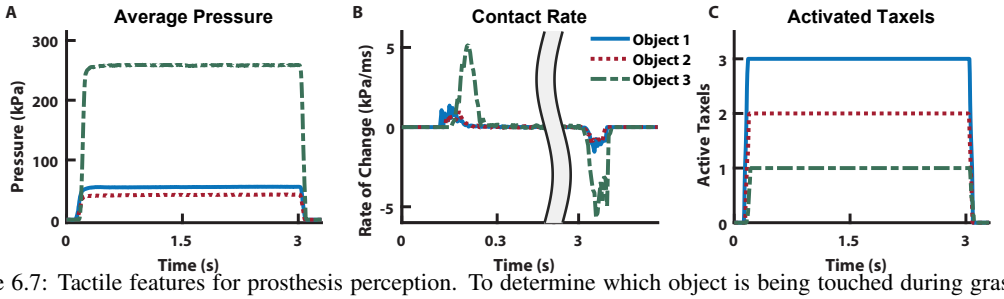

Figure 6.7: Tactile features for prosthesis perception. To determine which object is being touched during grasping, we implemented LDA to discriminate between the independent classes. As input features into the algorithm, we used (A) sensor pressure values, (B) the rate of change of the pressure signal, and (C) the number of active sensing elements during loading. Reprinted with permission from AAAS [9].

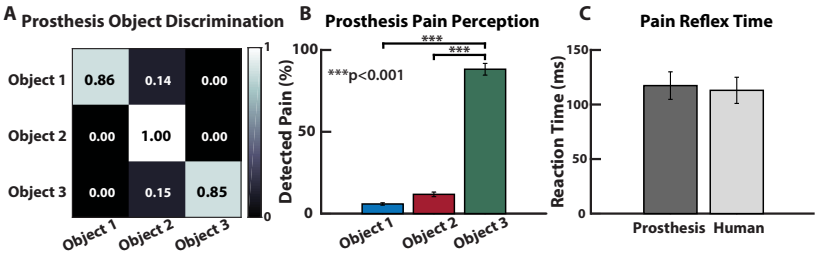

Figure 6.8: Real-time prosthesis pain perception. (A) The LDA classifier's accuracy across the various conditions and (B) the percentage of trials where the prosthesis perceived pain during the online PDT. Note the high percentage of detected pain during the PDT for Object 3. (C) Pain reflex time of the prosthesis, using the rate of change of the pressure signal to determine object contact and release, compared to previously published data of pain reflex time in healthy adults [10]. Reprinted with permission from AAAS [9].

6.3.5 User tactile perception

With the added ability to perceive both innocuous and noxious tactile sensations in a single stimulation modality, an amputee user can utilize more realistic tactile sensations to discriminate between objects with a large or small (sharp) radius of curvature. The participant demonstrated his ability to perceive both innocuous and noxious tactile sensations by performing several discrimination tasks with a prosthetic hand. The neuromorphic tactile signal was passed from the prosthesis controller directly to the stimulator to provide sensory feedback to the amputee. The participant could reliably detect, with perfect accuracy, which of the fingers of the prosthesis were being loaded (Fig. 6.9A). To demonstrate the ability of the prosthesis and user to perceive differences in object shape through variation in the comfort levels of sensory feedback, each of the three objects were presented to the

prosthesis. Sensory feedback to the thumb and index finger regions of the phantom hand enabled the participant to perceive variations in the object curvatures, which was realized through changes in perceived comfort of the sensation. The results show an inversely proportional relationship between the radius of curvature of an object and the perceived discomfort of the tactile feedback (Fig. 6.9B). In addition to being able to perceive variation in sharpness of the objects as conveyed by the discomfort in the neuromorphic tactile feedback, the participant could reliably differentiate between the three objects with high accuracy (Fig. 6.9C). Finally, the participant performed the PDT with his prosthesis (movie S4). The prosthesis pain reflex control was implemented during the grasping task, which resulted in the prosthesis automatically releasing an object when pain was detected (see Materials and Methods). During actual amputee use, the prosthesis pain reflex registered over half of the Object 3 movements as painful, significantly more than for the other objects ($p<0.05$) (Fig. 6.9D).

Responses from a subjective survey of the perception of the sensory stimulation show that the amputee felt as if the tactile sensations were coming directly from his phantom hand. In addition, the participant stated that he could clearly feel the touch of objects on the prosthetic hand and that it seemed that the objects themselves were the cause of the touch sensations that he was experiencing during the experiments.

6.4 Discussion

6.4.1 Perceiving touch and pain

Being able to quantify the perception of innocuous and noxious stimuli for tactile feedback in amputees is valuable in that it enables the replacement of an extremely valuable piece of sensory in-

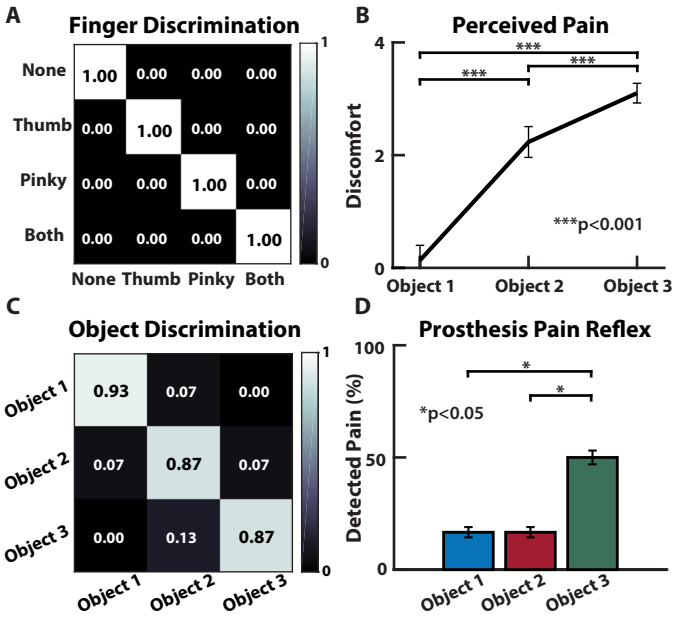

Figure 6.9: Innocuous (mechanoreception) and noxious (nociception) prosthesis sensing and discrimination in an amputee. (A) The amputee could discriminate which region of his phantom hand was activated, if at all. (B) Perception of pain increases with decreasing radius of curvature (i.e. increase in sharpness) for the objects presented to the prosthetic hand. (C) Discrimination accuracy shows the participant's ability to reliably identify each object presented to the prosthesis based purely on the sensory feedback from the neuromorphic stimulation. (D) Results from the PDT during user controlled movements, with pain reflex enabled. Reprinted with permission from AAAS [9].

formation: pain. Not only does pain play a role in providing tactile context about the type of object being manipulated, but it also acts as a mechanism for protecting the body. One could argue that this protective mechanism is not necessary in a prosthesis because it is merely an external tool or piece of hardware to an amputee user. We postulate that being able to capture noxious stimuli is actually more valuable to a prosthesis because it does not possess the same self-healing characteristics found in healthy human skin, although recent research has shown self-healing materials that could be used for future prosthetic limbs [85, 160]. To enable an artificial sense of self-preservation, a noxious tactile signal is useful for the prosthesis to ensure it does not exceed the limits of a cosmetic covering or the hand itself. As prosthetic limbs become more sophisticated and sensory feedback becomes more ubiquitous, there will be a need to increase not just the resolution of tactile information but also the amount of useful information being passed to the user. We have identified how changing

stimulation pulse width and frequencies enables a spectrum of tactile sensation that captures both innocuous and noxious perceptions in a single stimulation modality.

Our extensive phantom hand mapping, psychophysics, and EEG results support the use of TENS as providing relevant sensory information to an amputee. The EEG results are limited in that they do not provide detailed information on how changes in stimulation patterns are perceived, but they do show activation in sensory regions of the brain indicating relevant sensations in the amputee. Furthermore, the results from the user survey showed that sensory feedback helped the amputee better perceive his phantom hand and that objects being grabbed by the prosthesis were perceived as being the source of the sensation, which helps support the neuromorphic stimulation as a valid approach for providing relevant sensory feedback. The results from the PDT showed the ability of the prosthesis to detect pain and reflex to release the object. Object 3 was overwhelmingly detected as painful, due to its sharp edge (Fig. 6.8B). The high success rate for detecting and preventing pain for the benchtop PDT is likely due to the controlled nature of the prosthesis grip. The likelihood of detecting Object 3 as painful decreased and the chances of pain being detected for the other objects increased during the PDT with a user controlled prosthesis (Fig. 6.9D); however, pain detection and reflex were still significantly more likely for Object 3 ($p<0.05$). This shift in pain detection is likely due to the amputee's freedom to pick up the objects with his prosthesis in any way he chose. The variability in grasping orientation and approach for each trial resulted in more instances where Object 3 was not perceived as painful by the prosthesis. The ability to handle objects in different positions and orientations raises an interesting point in that the amount of pain produced is not an inherent property of an object, rather it is dependent on the way in which it is grasped. A sharp edge may still be safely manipulated without pain if the pressure on the skin does not exceed the

threshold for pain. To reliably encode both touch and pain for prostheses, tactile signals should be analyzed in terms of pressure as opposed to grip force.

The prosthesis pain reflex presented here is autonomous, but one possibility is to use the amputee's electromyography (EMG) signal as an additional input to the reflex model to enable modulation of the pain sensitivity perceived by the prosthesis. In this work, the pain sensation was not severe enough to generate a significant EMG reflex signal, so the reflex decision was made by the prosthesis instead of the user. The time for a user to process sensory feedback and produce a voluntary contraction is over 1 s [131], which is why we implemented an autonomous prosthesis pain reflex to achieve a response time closer to what is found in biology (Fig. 6.8C). Biologically, this autonomous response is equivalent to a fast spinal reflex compared to the slower cortical response for producing a voluntary EMG signal for controlling limb movement.

Another major implication of this work is in the quantification of the perceived noxious and innocuous tactile sensations during transcutaneous electrical nerve stimulation of peripheral afferents. One might assume that an increase in discomfort would be associated with an increase in delivered charge; however, we found that the most painful sensations during tactile feedback to an amputee delivered through TENS were primarily dictated by an increase in stimulation pulse width as well as stimulation frequency. Specifically, frequencies that were near the discrete detection boundary (15 – 30 Hz) were perceived as more painful than higher frequencies. Changes in stimulation frequency seemed to have the largest influence on the perceptions of touch and pain while pulse width affected intensity of the sensation (Fig. 6.3E). Furthermore, we demonstrated real-time discrimination between object curvature based purely on perceived discomfort in tactile feedback, which was associated with sharpness of the objects by the participant.

6.4.2 Neuromorphic touch

The ability of the participant to discriminate objects, specifically those that cause pain, is rooted in the neuromorphic tactile transduction and corresponding nerve stimulation. The psychophysical results illuminate the unique stimulation paradigms necessary to elicit tactile sensations that correspond to both mechanoreceptors and nociceptors in the phantom hand of an amputee.

More sophisticated neuron models exist and could be used to capture behavior of individual receptors and transduction [99]; however, the limitation of hardware prevents the stimulation of individual afferent nerve fibers. The Izhikevich model is simplistic in its dynamics but still follows basic qualities of integrate-and-fire models with voltage non-linearity for spike generation and extremely low computational requirements, which allow for the creation of a wide variety of neuron behaviors [146]. The advantage of the neuromorphic representation of touch in our work is that we can transform signals from the multilayered e-dermis directly into the appropriate stimulation paradigm needed to elicit the desired sensory percepts in the amputee participant. Specifically, the combination of mechanoreceptor and nociceptor outputs enables additional touch dimensionality while maintaining a single modality of feedback, both in physical location and stimulation type. This combination allows the user to better differentiate between the objects based on their unique evoked perceptions for each object (Fig. 6.9B-C).

The limitation of this work is the small study sample. Although this work is a case study with a single amputee, the extensive psychophysical experiments and stability (Fig. S1 and S2) of the results over several months show promise that other amputees would experience a similar type of perception from TENS, a technique we have previously validated for activating relevant phantom

hand regions in multiple amputees [26]. However, the psychophysics will likely have slight differences based on age and condition of the amputation. The results are promising in that the stimulation parameters used to elicit pain or touch followed the same trend in both median and ulnar nerve sites of the amputee (Fig. 6.3E). A major implication of this work is the idea that both innocuous and noxious touch can be conveyed using the same stimulation modality. In addition, we showed that it is not necessarily a large amount of injected charge into the peripheral nerves that elicits a painful sensation. Rather, a unique combination of stimulation pulse width and frequency at the discrete detection boundary appears to create the most noxious sensations. Additional amputee participants who are willing to undergo nerve stimulation, sensory mapping, and psychophysical experiments to the quantify their perceived pain would be needed to allow us to generalize the clinical significance to a wider amputee population. Our findings have applications not only in prosthetic limb technology but for robotic devices in general, especially devices that rely on tactile information or interactions with external objects. The overarching idea of capturing meaningful tactile information continues to become a reality as we can now incorporate both innocuous and noxious information in a single channel of stimulation. Whether it is used for sensory feedback or internal processing in a robot, the sense of touch and pain together enable a more complete perception of the workspace.

This study illustrates, through demonstration in a prosthesis and amputee participant, the ability to quantify and utilize tactile information that is represented by a neuromorphic interface as both mechanoreceptor and nociceptor signals. Through our demonstration of capturing and conveying a range of tactile signals, prostheses and robots can incorporate more complex components of touch, namely differentiating innocuous and noxious stimuli, to behave in a more realistic fashion. The sense of touch provides added benefit during manipulation in prostheses and robots, but the sense

of pain enhances their capabilities by introducing a novel sense of self preservation and protection.

6.5 Materials and methods

6.5.1 Objectives and study design

Our objectives were to show that 1) a prosthetic hand was capable of perceiving both touch and pain through a multilayered e-dermis and 2) an amputee was capable of perceiving the sense of both touch and pain through targeted peripheral nerve stimulation using a neuromorphic stimulation model.

6.5.2 Participant recruitment

All experiments were approved by the Johns Hopkins Medicine Institutional Review Board. The amputee participant was recruited from a previous study at Johns Hopkins University in Baltimore, MD. At the time of the experiments, the participant was a 29-year-old male with a bilateral amputation 5 years prior, due to tissue necrosis from septicemia. The participant has a transradial amputation of the right arm and a transhumeral amputation of the left arm. The left arm was used for all sensory feedback and controlling the prosthesis in this work. The participant consented to participate in all the experiments and to have images and recordings taken during the experiments used for publication and presentations. After 2 months of sensory mapping, the experiments were performed on average once every 2 weeks over a period of 3 months with follow up sessions after 2, 5, and 8 months. EEG data was collected in one session over a period of 2 hours.

6.5.3 Sensory feedback

The sensory feedback experiments consisted of TENS of the median and ulnar nerves using monophasic square wave pulses. We performed mapping of the phantom hand using a 1 mm beryllium copper (BeCu) probe connected to an isolated current stimulator (DS3, Digitimer Ltd., UK). An amplitude of 0.8 mA and frequency of 2 – 4 Hz were used while mapping the phantom hand. Anatomical and ink markers were used, along with photographs of the amputee's limb, to map the areas of the residual limb to the phantom hand. For all other stimulation experiments, we used a 5 mm disposable Ag-Ag/Cl electrode. A 64-channel EEG cap with Ag-Ag/Cl electrodes (impedance < 10 kΩ) was used for the EEG experiment. The participant was seated and stimulation electrodes were placed on his median and ulnar nerves. Each site was stimulated individually for a period of 2 s followed by a 4 s delay with 25% jitter before the next stimulation. There was a total of 60 stimulation presentations with varying pulse width (1-20 ms) and frequencies (4 – 45 Hz) with an amplitude of 1.6 mA. A time window of 450 ms starting at 400 ms after stimulation was used to average EEG activity across trials and compared to baseline activity using methods similar to those in [166].

6.5.4 Psychophysical experiments

Psychophysical experiments were performed to quantify the perception of TENS on the median, radial, and ulnar nerves of the amputee. Experiments included sensitivity detection (varying pulse width at 20 Hz), detection of discrete versus continuous stimulation (varying frequency with pulse width of 5 ms), and scaled pain discrimination. For the pain discrimination experiment the participant used a discomfort scale that ranged from pleasant or enjoyable (-1) to no pain (0) to very intense pain (10) (Table 6.1). Stimulation current amplitude was held at 2 mA while frequency and

pulse width were modulated to quantify the effect of signal modulation on perception in the participant's phantom hand. Every electrical stimulation was presented as a 2 s burst with at least 5 s rest before the next stimulation. Experiments were conducted in blocks up to 5 min with a break up to 10 min between each block. Every stimulation condition was presented up to 10 times and at least 4 times. Psychometric functions were fit using a sigmoid link [26].

6.5.5 E-dermis fabrication

The multilayered e-dermis was constructed from piezoresistive transducing fabric (Eeonyx, USA) placed between crossing conductive traces (stretch conductive fabric, LessEMF, USA), similar to the procedure described in previous work [136]. The piezoresistive material is pressure sensitive and decreases in resistance with increased loading. The intersection of the conductive traces created a sensing taxel, a tactile element. Human anatomy expresses a lower density of nociceptors, compared to mechanoreceptors, in the fingertip [167]. So, we designed the epidermal layer as a 1 x 1 sensing array while the dermal layer was a 2 x 1 array (Fig. 6.2A). The size of the prosthesis fingertip and the available inputs to the prosthesis controller limited the number of sensing elements to 3 per finger. The piezoresistive and conductive fabrics were held in place by a fusible tricot fabric with heat activated adhesive. A 1 mm layer of silicone rubber (Dragon Skin 10, Smooth-On, USA) was poured between two sensing layers. After the intermediate rubber layer cured, the textile sensors were wrapped into the fingertip shape and a 2 mm layer of silicone rubber (Dragon Skin 10, Smooth-On, USA) was poured as an outer protection and compliance layer, which is known to benefit prosthesis grasping [16]. The e-dermis was placed over the thumb, index, and pinky phalanges of a prosthetic hand.

6.5.6 Prosthesis control

A bebionic prosthetic hand (Ottobock, Duderstadt, Germany) was used for the experiments. Prosthesis movement was controlled using a custom control board, with an ARM Cortex-M processor, developed by Infinite Biomedical Technologies (IBT) (Baltimore, USA). The board was used for interfacing with the prosthesis, reading in the sensor signals, controlling the stimulator, and implementing the neuromorphic model. During the user controlled PDT, the amputee used his own prosthesis , a bebionic hand with Motion Control wrist and a UtahArm 3+ arm with elbow (Motion Control Inc, Salt Lake City, USA). The amputee controlled his prosthesis using a linear discriminant analysis (LDA) algorithm on an IBT control board for EMG pattern recognition. The electrodes within his socket were bipolar Ag-Ag/Cl EMG electrodes from IBT.

6.5.7 Neuromorphic models

We implemented artificial mechanoreceptor and nociceptor models to emulate natural tactile coding in the peripheral nerve. We tuned the model to match the known characterization of TENS in the amputee to elicit the appropriate sensation. Constant current was applied during stimulation and both pulse width and spiking frequency were modulated by the model. Higher grip force was linked to increased stimulation pulse width and frequency, which was perceived as increased intensity in the phantom hand. Innocuous tactile stimuli resulted in shorter pulse widths (1 ms or 5 ms) whereas the noxious stimuli produced a longer pulse width (20 ms), a major contributor to the perception of pain through TENS as shown by the results. To create the sensation of pain, we varied the parameters of the model in real-time based on the output of the e-dermis. We converted the e-dermis output to neural spikes in real-time by implementing the Izhikevich neuron framework [146] in the embedded

C++ software on the prosthesis control board. The output of the embedded neuromorphic model on the control board was used to control the stimulator for sensory feedback. The neuromorphic mechanoreceptor model was a combination of SA and RA receptors modelled as regular and fast spiking neurons. The nociceptor model was made up of Aδ neurons, which were modeled as fast spiking neurons to elicit a painful sensation in the phantom hand. It should be noted that the fast spiking neuron model was perceived as noxious with an increase in pulse width, which allows us to use the same Izhikevich neuron for both mechanoreceptors and nociceptors. The e-dermis output was used as the input current, I, to the artificial neuron model. The evolution of the membrane potential v and the refractory variable u are described by Eq. 6.1 and 6.2. When the membrane potential reaches the threshold vth the artificial neuron spikes. The membrane potential was reset to c and the membrane recovery variable u was increased by a predetermined amount d (Eq. 6.3). The spiking output was used to directly control the TENS unit for sensory feedback.

$$\frac{dv}{dt} = Av^2 + Bv + C - u + \frac{I}{RC_m} \tag{6.1}$$

$$\frac{du}{dt} = a\left(bv - u\right) \tag{6.2}$$

$$\text{if } \left(v \geq v_{th}\right), \text{then } \begin{cases} v \leftarrow c \\ u \leftarrow u + d \end{cases} \tag{6.3}$$

Because we are not directly stimulating individual afferents in the peripheral nerves we tuned the model to represent behavior of a population of neurons. The parameters used for the different

receptor types were: $A = 0.04/\text{Vs}$; $B = 5/\text{s}$; $C = 140\,\text{V/s}$; $C_m = 1\,\text{F}$; $R = 1$; $b = 0.2/\text{s}$; $c = -65$ mV; $d = 8$ mV/s; $v_{th} = 30$ mV; and

$$a = \begin{cases} 0.02/\text{s}, & \text{Regular spiking (RS)} \\ 0.01/\text{s}, & \text{Fast spiking (FS)} \end{cases}$$

R is dimensionless in this model. The fast spiking neurons fire with high frequency with little adaptation, similar to responses from nociceptors during intense, noxious stimuli [157]. In the model, fast spiking is represented by a very fast recovery (a). Values for the parameters were taken from [98] and [146].

We limited the spiking frequency of the neuromorphic model to 40 Hz and 20 Hz for the mechanoreceptor and nociceptor models, respectively. The transition of the neuromorphic model from mechanoreceptors to nociceptors relies on the pressure measured at the fingertips of the prosthesis, the number of active sensing elements, and the standard deviation of the pressure signal across the active taxels. The prosthesis fingertip pressure (P) is used to determine the neuromorphic stimulation model for sensory feedback. Highly localized pressure above a threshold β triggers the FS model whereas the RS model is used in cases of more distributed fingertip pressure. The following pseudocode explains how the stimulation model is chosen, where $\beta = 150\,\text{kPa}$, n is the number of active taxels, and pw is the stimulation pulse width:

if $(P \geq \beta \,\&\, n < 2)$, then $\big(nociceptor\,(A\delta)\,(FS\colon\ pw = 20 \text{ ms})\big)$

else if $(P \geq \beta \,\&\, n = 2)$, then $\big(mechanoreceptor\,(SA/RA)\,(FS\colon\ pw = 5 \text{ ms})\big)$

else$\big(mechanoreceptor\,(SA/RA)\,(RS\colon\ pw = 1 \text{ ms})\big)$

6.5.8 Prosthesis pain reflex

To mimic biology, we modeled the prosthesis pain withdrawal as a polysynaptic reflex [162, 163] in the prosthesis hardware. In our model, the prosthesis controller was treated as the spinal cord for the polysynaptic reflex. The nociceptor signal was the input, $I(t)$, to an integrating interneuron Γ whose output $I_\Gamma(t)$ was the input to an alpha motor neuron, which triggered the withdrawal reflex through a prosthesis hand open command after 100 ms of pain. Both neurons can be modelled as leaky-integrate-and-fire with a synapse from the alpha motor neuron causing the reflex movement (Eq. 6.4 and 6.5, Fig. 6.10), similar to the EMG signals generated during a nociceptive reflex [168].

$$\text{Interneuron } (\Gamma) : \tau_m \frac{dv_\Gamma}{dt} = E + RI(t) - v_\Gamma(t) \tag{6.4}$$

$$\text{Alpha motor neuron } (\alpha) : \tau_m \frac{dv_\alpha}{dt} = E + RI_\Gamma(t) - v_\alpha(t) \tag{6.5}$$

Both neurons had time constant $\tau_m = 10$ ms, resting potential $E = -60$ mV, membrane resistance $R = 20\Omega$, and a spiking threshold of $v_{th} = -40$ mV. The time step was 5 ms and the nociceptor signal was normalized, enveloped, and scaled by $\beta = 0.2$ mV. The prosthesis reflex

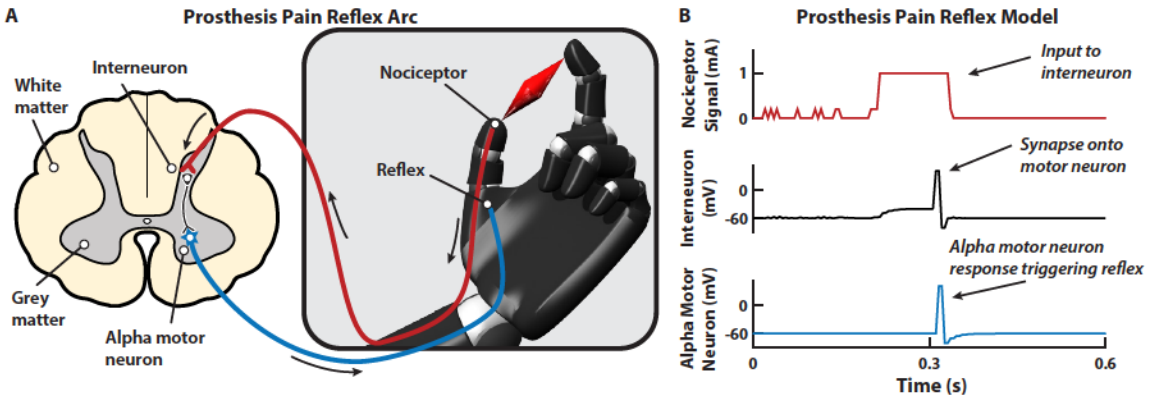

Figure 6.10: Prosthesis pain reflex. (A) The prosthesis pain reflex arc is modeled as a polysynaptic pathway with signal from a nociceptor synapsing on an interneuron in the spinal cord (i.e. the prosthesis controller). The interneuron synapses on an alpha motor neuron, which causes the pain withdrawal reflex. (B) During the Pain Detection Task, the nociceptor signal from the e-dermis on the prosthesis was used as the input to the integrating interneuron on the prosthesis hardware. The alpha motor neuron's input signal is the output signal from the interneuron, which fires after ∼100 ms of continuous pain detection. The prosthesis opens after the alpha motor neuron fires.

parameters were chosen to trigger hand withdrawal after 100 ms of pain to mimic the pain reflex in healthy humans [10]. Fingertip pressure, the rate of contact, and the number of active sensing elements on each fingertip were used as features for an LDA algorithm to detect the different objects. Object 3 was labeled as a painful object. A taxel was considered active if it measured a pressure greater than 10 kPa. The pattern recognition algorithm was trained using sensor data from 5 trials of prosthesis grasping for each object and validated on 10 different trials.

6.5.9 Objects design and fabrication

We created 3 objects of equal size with varying edge curvatures, defined by the edge blend radius, using a Dimension 1200es 3D printer (Stratasys, USA). Each object has a width of 5 cm but differed in curvature. Each object's curvature followed a power law where the leading edge of the protrusions vary in blend radii and range from flat to sharp. The radius of curvature, R_c, of the leading edge can be modified by the body power law exponent, n where

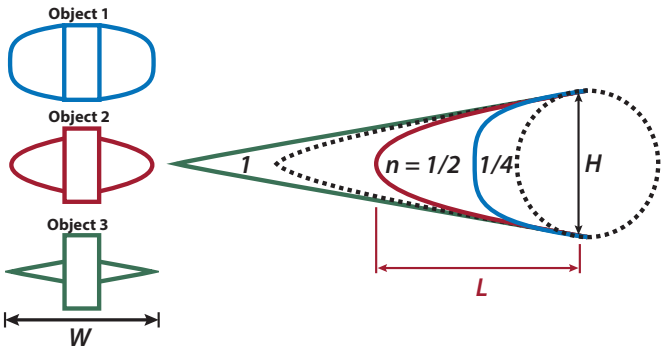

Figure 6.11: Power law object edge radius of curvature. Illustration showing the power law objects and their leading edge. For the three objects used in the pain detection tasks, the width, W, of the entire object was held constant and the length of the leading edge, L, was the same for all objects. The height, H, of each object was different to keep W and L constant across all objects. See [11, 12] for more details.

$$R_c = \frac{1}{|nA(n-1)|}\left[x^{\frac{2(2-n)}{3}} + (nA)^2\, x^{\frac{2(2n-1)}{3}}\right]^{\frac{2}{3}} \tag{6.6}$$

A is the power law constant, which is a function of n, and x is the position along the Cartesian axis in physical space. The objects for this study were designed to maintain a constant width, w (Fig. 6.11) to prevent the ability to discriminate between the objects based on overall width. The three objects used had a power law exponent, n, of $^1/_4$, $^1/_2$, and 1 and were referred to as Object 1, Object 2, and Object 3, respectively. More details and explanation of power law shaped edges can be found in [11, 12].

6.5.10 Experimental design

Finger discrimination: The multilayered e-dermis was placed over the thumb and pinky finger of the prosthesis. Activation of each fingertip sensor corresponded directly to nerve stimulation of the amputee in the corresponding sites of his phantom hand. The participant was seated, and his vision was occluded. The experimenter pressed either the prosthetic thumb, pinky, both, or neither in a random order. Each condition was presented 8 times. The stimulation amplitude was 1.5 mA

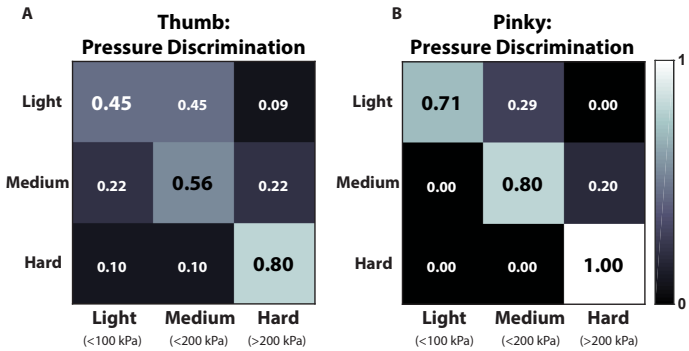

Figure 6.12: Amputee pressure discrimination. Pressure discrimination on the (A) thumb and (B) pinky finger of the amputee subject's phantom hand. The subject could detect appropriate levels of pressure, but with lower accuracy in the case of light touch (<100 kPa) in the thumb.

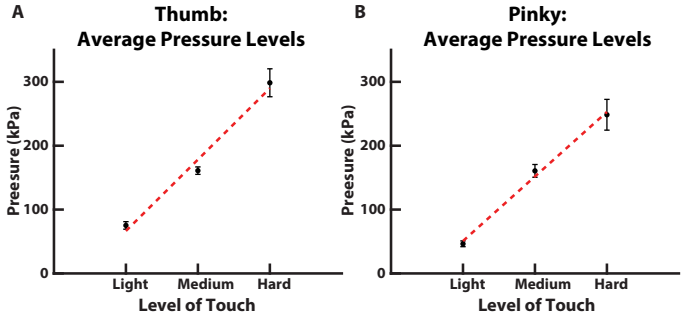

Figure 6.13: Average fingertip pressure. The average pressure on the fingertips of a prosthesis, as recorded from the multilayered e-dermis, during the pressure discrimination experiments with the amputee participant on the (A) thumb and (B) pinky.

and 1.45 mA for the thumb and pinky sites on the amputee's residual limb, respectively. Next, the experimenter pressed the prosthetic thumb or pinky with either a light (< 100 kPa), medium (< 200 kPa), or hard (> 200 kPa) pressure (Fig. 6.12 and 6.13). Each force condition was presented 10 times in a random order for each finger.

Object discrimination: Fingertip sensors were placed on the thumb and index finger of a stationary bebionic prosthetic hand. The participant was seated, and his vision of the prosthesis was occluded. A stimulating electrode was placed over the region of his residual limb that corresponded to his thumb and index fingers on his phantom hand. The experimenter presented one of the 3 objects on the index finger of the prosthetic hand for several seconds. The participant responded with

the perceived object as well as the perceived discomfort based on the tactile sensation. Each block consisted of up to 15 object presentations. The participant performed 3 blocks of this experiment. Each object was presented randomly within each block, and each object was presented the same number of times as the other objects. The participant visually inspected the individual objects before the experiment took place, but he was not given any sample stimulation of what each object would feel like. This was done to allow the participant to create his own expectation of perception of what each object should feel like if he were to receive sensory feedback on his phantom hand.

Pain Detection Task: In the benchtop PDT, the prosthesis was mounted on a stand with the multilayered sensors on the thumb and index finger. The object was placed on a stand and the prosthesis grabbed the object using a closed precision pinch grip. Each object was presented to the prosthesis at least 15 times in a random order. For the user controlled PDT, the participant used his prosthesis to pick up and move one of the three objects. Each object was presented at least 10 times. The instances of prosthesis reflex were recorded. The participant took a survey at the end of the experiments.

6.5.11 Data collection

Each taxel of the multilayered e-dermis was connected to a voltage divider. Sensor data was collected by the customized prosthesis controller and sent through serial communication with a baud rate of 115,200 bps to MATLAB (MathWorks, USA) on a PC for further post-processing and plotting. Each sensing element in the e-dermis was sampled at 200 Hz. Responses from the psychophysical experiments were recorded using MATLAB and stored for processing and plotting. The prosthesis controller communicated with MATLAB through Bluetooth communication with

a baud rate of 468,000 bps. 64 channel EEG data was recorded at 500 Hz by a SynAmp2 system (Neuroscan, UK) and processed in MATLAB using the EEGLab Toolbox (Swartz Center for Computational Neuroscience, UC San Diego, USA). EEG data was downsampled to 256 Hz and band-pass filtered between 0.5 to 40 Hz using a 6th order Chebyshev filter. Muscle artifacts were rejected by the Automatic Artifact Rejection (AAR) blind source separation algorithm using canonical correlation approach. Independent Component Analysis (ICA) was performed for removal of the eye and remnant muscle artifacts to obtain noise-free EEG data. Results from data collected over multiple trials of the same experiment were averaged together. Statistical p-values were calculated using a one-tailed, two-sample t-test. Error bars represent the standard error of the mean, unless otherwise specified

7 | Enhancing Phantom Limb Perception and Control with Sensory Feedback

This chapter is made up of content that is being prepared for submission to a journal.

> L. E. Osborn, M. A. Hays, R. Bose, A. Dragomir, Z. Tayeb, C. Hunt, J. Betthauser, G. M. Lévay, A. Bezerianos, and N. V. Thakor, "Sensory feedback enhances phantom limb perception and prosthesis control," *In Preparation*, 2019

7.1 Overview

In the previous chapters we explored the use of tactile feedback to improve prosthesis grasping and object manipulation. We gave sensations of touch and pain back to a prosthesis user. With the quantity and quality of sensory feedback rapidly improving, we begin looking at what other benefits sensory feedback can provide, namely prosthesis control and embodiment due to enhanced perception of the phantom limb. A major challenge for controlling a prosthetic arm is the disconnection between the device and the user's phantom limb. The lack of sensory feedback to the phantom hand weakens the internal sensorimotor model that drives motion. Here, we show the ability to enhance an amputee's phantom limb perception through targeted transcutaneous electrical nerve stimulation (T^2ENS) to improve prosthesis control from myoelectric signals. Transcutaneous nerve stimulation experiments were performed with three amputee subjects to map and understand their phantom

limb perception. Results show improvements in the amputees' ability to both perceive and move the phantom hand. We discovered that enhanced phantom limb perception leads to improved hand and finger movement decoding performance from myoelectric signals used for control of a prosthetic hand. In an extended study with one amputee, we also found that long-term sensory mapping and prosthesis control success rate remains steady over a period of 2 years and 1 year, respectively, but temporary sensory feedback provides significant improvement in performance. Electroencephalography (EEG) shows increased motor-related neural activity in sensiromotor regions as a result of enhancing phantom limb perception. This work demonstrates the benefit of introducing targeted nerve stimulation in amputees for strengthening the internal sensorimotor control loop to not only improve amputee's perception of the phantom limb but also functional control of a dexterous prosthesis.

7.2 Introduction

Sensory information, specifically touch and proprioception, are essential for palpating and exploring objects in our surroundings. Tactile sensation plays a major role in our ability to manipulate objects [154]. The sensory feedback we receive during object manipulation influences our ability to control [169] and anticipate [170] grasping forces. In fact, we develop sophisticated internal models of sensorimotor integration to enable our bodies to move as intended with volitional control [171]. It is through sensory feedback and errors in our sensory predictions that we continue to update and strengthen our internal sensorimotor models for controlling limb movement [172], indicating the reliance on sensory information for our ability to control limb movements with precision and repeatability. Supplementing or substituting the tactile and proprioceptive senses may also be helpful.

Recently, researchers showed that auditory feedback can help improve internal models and performance in myoelectric control of a virtual prosthesis by able-bodied subjects [173], further indicating the role of feedback in sensorimotor control loops.

In the case of upper limb amputees, the sensorimotor loop is broken or severely disrupted as a result of limb loss; however, perception of the phantom limb persists [174]. Researchers have made profound breakthroughs in recent years by providing naturalistic tactile sensations back to amputees by stimulating peripheral nerves, both invasively [2, 3, 91, 98, 100] and noninvasively [4, 9], in the residual limb. Sensory feedback can provide perceptions of pressure [2, 91], enable discrimination of textures [98], provide proprioceptive perceptions of movement across the surface of the phantom hand [3], improve object manipulation tasks [92], and improve prosthesis use at home [175]. Biomimetic stimulation models can enhance sensation naturalness [176] or be used to provide receptor specific information to enable sensations of pressure or pain [9]. Researchers have also produced a kinesthetic illusion of phantom hand movement through the use of skin vibration in several amputees who had undergone targeted muscle reinnervation (TMR) surgery [97].

While significant efforts have enabled sensory feedback in amputees [2–4, 9, 91, 92, 97, 98, 100, 175, 176], there is an unanswered question of the effect of enhancing phantom limb perception on the internal sensorimotor models for controlling phantom hand movements. More specifically, the question is how perception of the phantom hand affects motor function and the myoelectric signals from the residual limb used for prosthesis control. Pattern recognition techniques aim to create a natural and intuitive control strategy for upper limb amputees through movement decoding from myoelectric signals in the residual limb [60]. The algorithms behind pattern recognition utilize the deterministic structure of myoelectric activity during muscle contractions [177] and have shown the

ability to provide real-time decoding of hand [66] and individual finger movement [37]. Pattern recognition can be utilized for achieving several complicated grip patterns and performance can increase with user training due to better separability of the muscle contractions in the residual limb [67]. More recently, simultaneous and proportional control of multiple degrees of freedom (DOF) has been achieved through other machine learning methods using electrodes implanted on motor nerves [3] and direct control using surface electromyography (EMG) electrodes [62]. Similarly, more advanced decoding algorithms provide enhanced robustness for prosthesis control [14] and even the ability to derive motor unit action potentials from TMR subjects for proportional control of a multiple DOFs of a prosthetic hand [73].

Despite improvements in robust and reliable prosthesis control algorithms, we postulate that an important component of prosthesis control is the ability to perceive and move the phantom hand. A significant amount of research has gone into understanding phantom limb pain (PLP) and emerging research showed that this pain can be reduced through sensory feedback in a prosthesis [178], sensory feedback combined with motor control training [179, 180], and even through augmented and virtual reality prosthesis training [181]. In fact, users with more severe PLP have been shown to have worse motor control over their phantom hand as measured by cortical activity [182], indicating the relationship of phantom hand perception and motor control. Neural signals after TMR suggest that more natural cortical representations of the missing limb can occur in motor cortex as a result of the surgery [183]; however, more recent results show stable somatosensory neural representation of the phantom limb even decades after amputation [184]. It is also known that some movement representations persist in the motor cortex even when an amputee can't voluntarily produce those movements with the phantom hand [185]. Interestingly, sensory feedback through electrical stimu-

lation elicits neural activation of both somatosensory and premotor regions during evoked phantom limb sensations [186].

In this work, we hypothesize that providing sensory feedback to amputees can enhance phantom limb perception, which in turn improves the ability to move the phantom hand and control a prosthesis through EMG pattern recognition. The sensorimotor loop is modulated by strengthening the phantom hand perception through sensory feedback to enable better control of a myoelectric prosthesis. We demonstrate that 1) sensory feedback improves perception of the phantom hand, 2) the ability to perceive the phantom hand affects the ability to control phantom hand and prosthesis movements through myoelectric signals in the residual limb, and 3) electroencephalography (EEG) neural signals show activation of sensorimotor regions during sensory feedback and phantom limb activation.

7.3 Results

7.3.1 Sensory feedback enhances phantom hand perception.

Three amputee participants (male, age: 39 ± 10 years) were recruited for this study. The characteristics of each participant are shown in Table 7.1. Two amputee participants (A01 and A02) underwent elective amputations as a result of nerve injury, and two of the participants (A01 and A03) have transhumeral amputations. Participant A02 has a transradial amputation. A03 also has a right arm transradial amputation but only uses a prosthesis on his left arm, which was the side used for the experiments in this study. Each participant underwent sensory mapping to identify regions of phantom hand activation on their residual limb. Targeted transcutaneous electrical nerve stimulation (T^2ENS) was used to activate underlying peripheral nerves in the residual limb, a method which has

Table 7.1: **Participant characteristics.** Details on the amputee volunteers and their experience.

Participant	Amputation	Cause	Time of Amputation	Prosthesis	Experience
A01	left, transhumeral	brachial plexus injury resulting in paralysis of the arm	nerve injury Jan. 2018, elective amputation March 2018	no prosthesis	no myoelectric control experience
A02	right, transradial	compartment syndrome resulting in paralysis of the arm	nerve injury 2002, elective amputation Nov. 2017	prosthesis, direct myoelectric control	1 month of EMG pattern recognition experience
A03	left, transhumeral right, transradial	septicemia resulting from meningitis	amputation Oct. 2012	left arm prosthesis, pattern recognition control	1 year of EMG pattern recognition experience

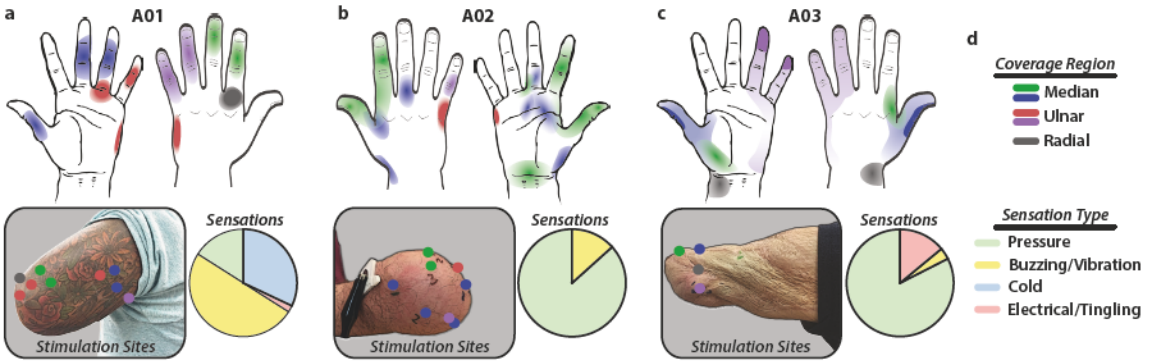

Figure 7.1: **Sensory mapping of amputee subjects. a**, Participant A01 reported sensations of general tactile activation, primarily buzzing or vibration, along with sensations of temperature changes on the palmar side of the middle and ring fingers. **b**, Participant A02, a transradial amputee, reported sensations of pressure in the activated regions. The thumb and index finger, along with a few spots on the ulnar side and palmar side of the hand, were the primary regions of activation. **c**, Participant A03 perceived sensations of pressure and occasional tingling in the thumb, pinky, and wrist regions of his phantom hand. **d**, Colormaps for regions of activation (top) and sensation type (bottom). For all phantom hand sensory maps, regions of strongest to faintest activation are indicated by a gradient of solid to faded color.

been used in previous studies [4, 9, 26]. Tactile sensations were reported in the phantom hand due to stimulation over various regions of the residual limb. Stimulation of the identified regions on the residual limb resulted in perceived sensation primarily in the phantom hand. Each amputee's perception of their phantom limb is different and electrical stimulation provided activation of different regions of their phantom hand (Fig. 7.1). Sensations were reported primarily as tactile and included pressure, buzzing, vibration, and in the case of subject A01, a sensation of cold temperature on the palmar side of the middle and ring fingers (Fig. 7.1a).

7.3.2 Sensory feedback improves EMG.

To understand the effect of sensory feedback on myoelectric activity and phantom hand movements, EMG signals were recorded before and after sensory nerve stimulation. Because sensory feedback provides a heightened sense of the phantom hand, we investigated the effect of this enhanced perception on the ability to make dexterous grasps with the phantom hand. A total of nine movements were presented to the amputee participants (5 hand and 4 wrist movements, Fig. 7.2a). Each movement cue was presented visually to the amputee, who then attempted to mimic the movement with his phantom hand. Each cue was presented 3 times and in a randomized order. Each amputee performed the hand and wrist movements before receiving any sensory feedback. After the first round of EMG collection, regions of the phantom hand were activated via T^2ENS to provide sensory feedback. The sites that provided the most significant coverage of the phantom hand were targeted for the sensory feedback. The stimulation sites activated regions that covered the thumb, index, palm, and ulnar sides of the phantom hand for all subjects (Fig. 7.1). The sensory feedback session lasted between 15 - 30 min and was followed by another round of EMG data collection. The accuracy of the EMG movement classification is shown in Fig. 7.2b-c. Linear discriminant analysis (LDA), a standard EMG pattern recognition algorithm [60], was used to classify the movements. Results indicate at least a 20% relative increase in baseline EMG pattern recognition performance for all subjects (Fig. 7.2d).

7.3.3 Long term sensory feedback.

To better understand the influence of enhanced sensory perception on EMG pattern recognition performance, participant A03 took part in an extended study over 1 year. Stimulation sites on

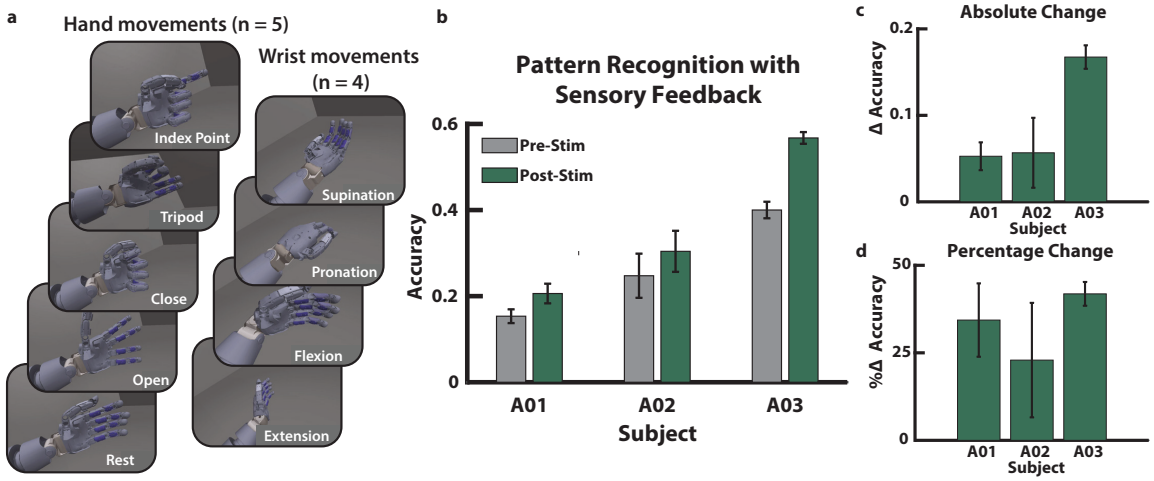

Figure 7.2: **EMG performance of amputee subjects. a**, Five hand movements (rest, open, close, tripod, index point) and four wrist movements (pronation, supination, flexion, extension) were presented, one at a time, to the amputee participant, who attempted to match the movement with his phantom hand. **b**, EMG data from the 9 movements classes before and after sensory feedback. All participants show slight improvements as a result of the sensory feedback. **c**, Absolute and **d**, percent change in performance accuracy for all participants. EMG pattern recognition relative performance increased by at least 20% from baseline as a result of enhanced phantom limb perception.

his residual limb that resulted in activation of the median, ulnar, and radial nerves were targeted for sensory feedback. Anatomical markers and pictures after every session were used to maintain consistency with the sites of stimulation. Perceived activation of the phantom hand remained fairly consistent over the course of the study (Fig. 7.3). The primary regions of activation were the thumb and index finger, the pinky and ulnar side of the hand, and the wrist. With every stimulation session, the participant reported enhanced perception of his phantom hand during sensory feedback.

7.3.4 Long term EMG performance.

In the extended study, we also investigated the effects of sensory feedback on EMG signals due to pattern matching in real-time. The participant identified different regions of activation that best corresponded to particular movements of his phantom hand (Fig. 7.4). For instance, activation of the thumb, index, and pinky were associated with opening, closing, and lateral key grip of his phantom

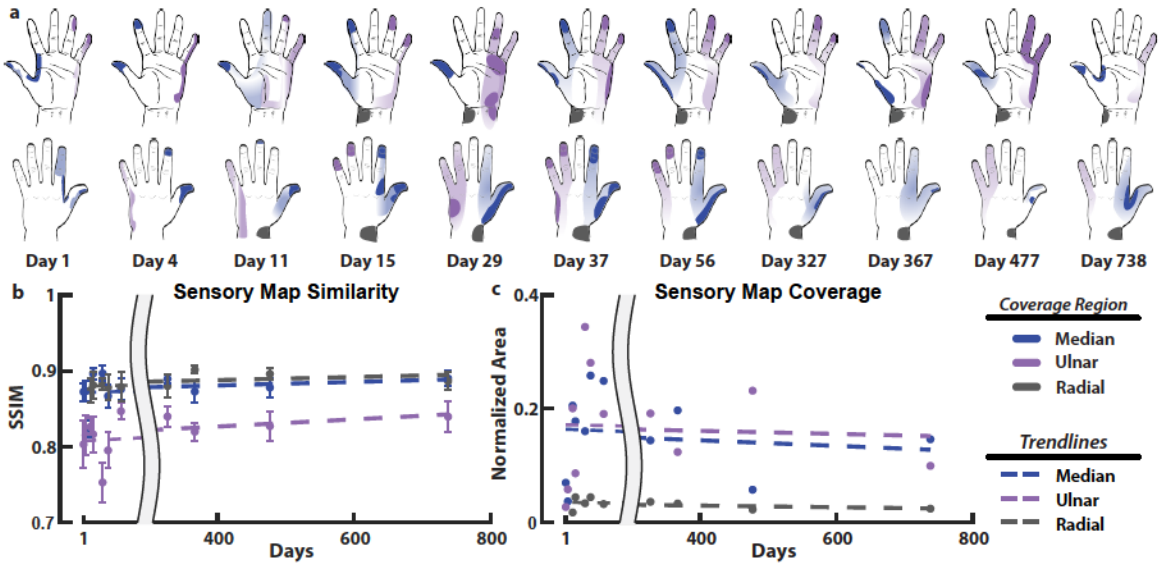

Figure 7.3: **Long term sensory mapping. a**, Sensory mapping from T^{2}ENS of the ulnar, median, and radial nerves was performed on participant A03 over a 2 year period. Activation maps of his phantom hand remained relatively stable over the duration of the study with the primary regions of sensation being on his thumb and index finger, pinky, and wrist. **b**, Structural similarity (SSIM) index of sensory maps for each region (median, ulnar, and radial) compared across days and **c**, normalized coverage area for each region across days.

hand. As is the case for EMG pattern recognition experiments, the participant focused on moving specific fingers of his phantom hand during the different movement classes. The combination of sensory feedback in targeted regions of the phantom hand with movement classes were made based on what the amputee participant saw as most relevant for him. For example, the index point and precision closed hand movements, the participant said he focused on moving the thumb and index fingers but his main focus was on closing his pinky and ring fingers.

A custom prosthetic socket with embedded bipolar electrodes was made for the participant to ensure stable and consistent electrode placement during each EMG signal recording session (Fig. 7.5a). The long term experiment was broken up into three phases of baseline EMG signal recording for pattern recognition decoding. Phase I was 6 weeks long to establish a baseline in performance before additional sensory feedback was provided. Phase II was a 2 week period of sensory feedback

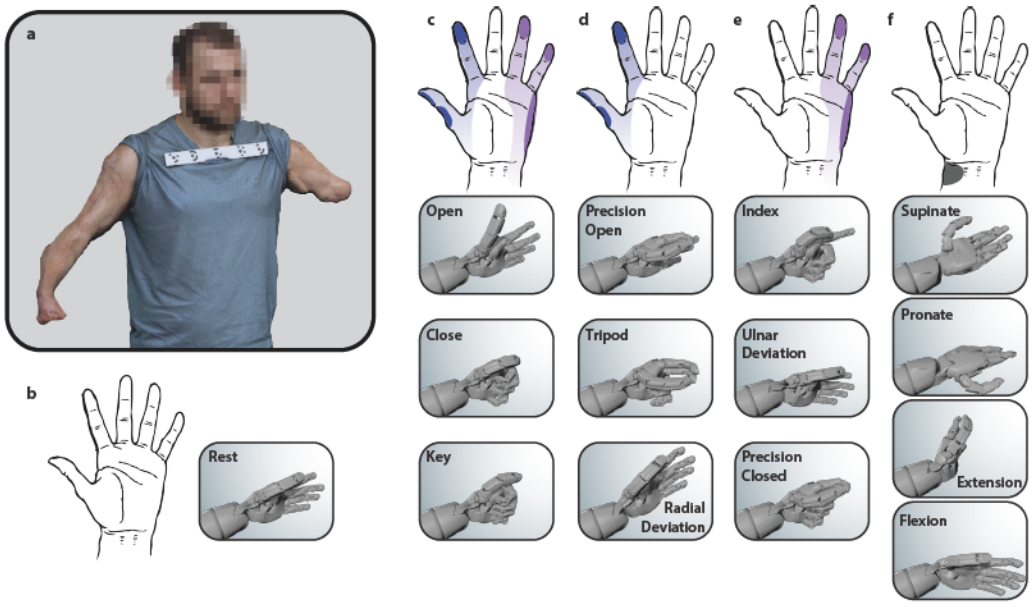

Figure 7.4: **Sensory feedback with phantom hand movements.** **a**, Digital scan of the residual limbs of participant A03. The participant is a bilateral amputee but only his left residual limb (transhumeral) was used for this experiment. The subject associated activation of certain regions of his phantom hand to different grasp patterns. **b**, A hand rest corresponded to no sensory feedback whereas activation in the **c**, median and ulnar regions of his phantom hand were most closely associated with opening, closing, and the lateral key grasp. **d**, Activation of the thumb and index finger was linked to precision open, tripod, and radial deviation of the phantom hand. **e**, Ulnar activation was used for index point, ulnar deviation, and precision closed movements while **f**, sensory activation of the wrist was associated with wrist flexion, extension, pronation, and supination. There was a total of 14 movement classes.

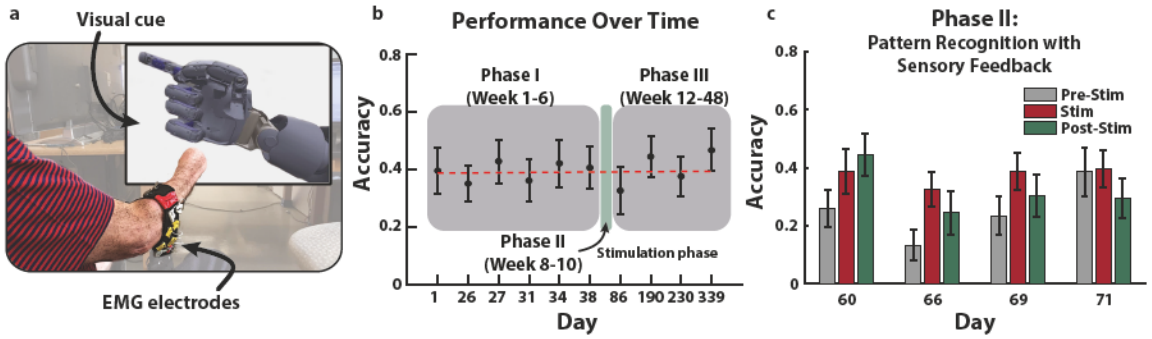

Figure 7.5: **Long term EMG performance.** **a**, The amputee participant used a custom prosthetic socket with embedded bipolar electrodes to ensure consistent electrode placement and secure fit for the extended study. **b**, EMG pattern recognition performance was measured over nearly 1 year. An initial set of baseline data was collected in Phase I, followed by a 2 week period of sensory feedback through T^2ENS (Phase II). Phase III consisted of 4 EMG pattern recognition sessions over a 36 week period. The subject was experienced with pattern recognition and results show a fairly consistent level of performance over time, suggesting no additional improvements as a result of continued training. **c**, The stimulation phase shows improvements in EMG movement decoding of the 14 classes as a result of enhanced phantom limb perception. EMG signal recordings were taken for each movement class before, during, and after sensory feedback. Movement decoding accuracy during trials with sensory feedback were always greater than before stimulation was applied, and persisted after stimulation in most cases.

with EMG recordings. Phase III was a 36 week follow up set of sessions to evaluate any lasting effects of the sensory feedback on the internal sensorimotor loop used by the amputee for moving his phantom hand. There were a total of 14 movement classes (8 hand movements and 6 wrist movements) that the amputee was trying to mimic with his phantom hand. The baseline EMG pattern recognition decoding performance was $\sim$39%, which is not unexpected given the relatively high number of movement classes (Fig. 7.5b). The EMG pattern recognition accuracy remained fairly stable for the 6 week period of Phase I as well as the 36 week period during Phase III. The sensory feedback provided to the phantom hand resulted in improved movement decoding in every case during the stimulation phase (Phase II) of the experiment (Fig. 7.5c). EMG signals were recorded during each movement class before stimulation, during stimulation of regions of the phantom hand, and again after the sensory feedback. There are clear improvements in movement predictions as a direct result of the sensory feedback.

7.3.5 Sensory feedback increases EEG activity in sensorimotor regions.

EEG signals were recorded to capture the neural activity in sensorimotor regions during sensory feedback and phantom hand movement (Fig. 7.6a). The alpha band (8 to 12 Hz) is known to be relevant for motor-related activity [187, 188] and was used to evaluate the influence of sensory feedback in phantom hand movements of participant A03. Stimulation of the thumb, pinky, and wrist regions of the phantom hand were performed during EEG recording and classified (Fig. 7.6b). The relative alpha power from the EEG was analyzed for phantom hand movement before any sensory feedback, sensory feedback with no movement, sensory feedback with movement, and phantom hand movement after sensory feedback (Fig. 7.6c-f). Visual movement cues of either tripod, index point, or wrist flexion were shown to the participant. These grips were chosen by the participant based on mapping results from the long term study (Fig. 7.4. Nerve stimulation was targeted to the median, ulnar, and radial regions of the phantom hand to correspond with the appropriate phantom hand movement (see Methods). There is higher activation in the central and centro-parietal region during phantom hand movement in presence of the sensory feedback compared to movement with no feedback (Fig. 7.6c,e). In the post stimulus condition, the effect of the sensory feedback persists and similar high activation is observed in the central and the centro-parietal region (Fig. 7.6f). We also compared the alpha power for different condition in individual electrodes in the central (C3, C1, Cz, C2 and C4 electrodes) and centro-parietal (CP3, CP1, CPz, CP2, CP4) region as shown in Fig. 7.6g-h. One-way ANOVA followed by post-hoc analysis was performed for each of the electrodes. Significant increase in the relative alpha power was observed for phantom hand movement in absence of sensory feedback stimulus (Pre-Stim) compared to the presence of sensory feedback (Stim-Mov). This difference was also observed in the post stimulus movement (Post-Stim).

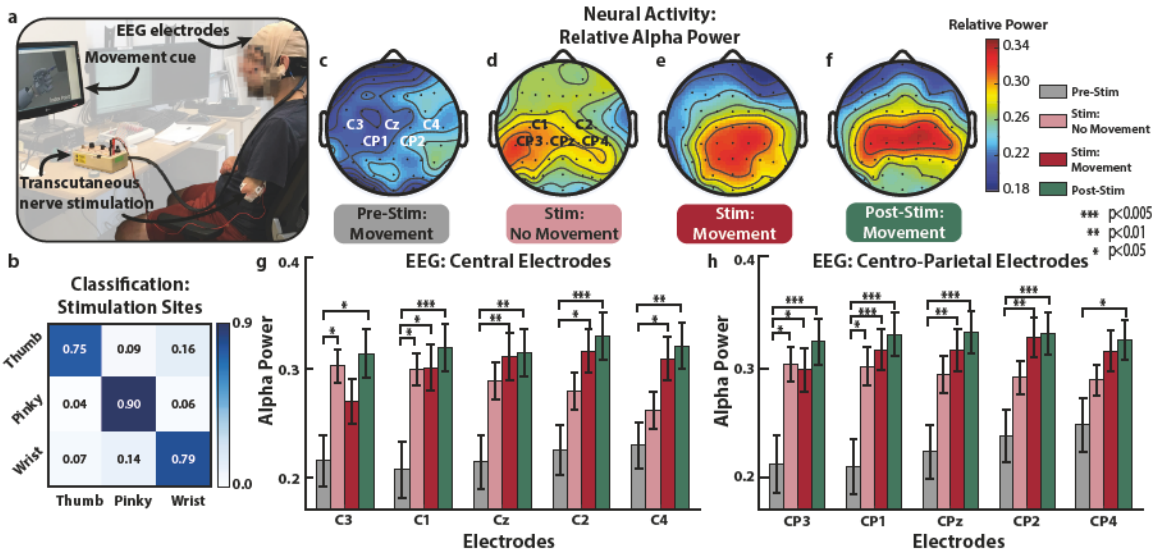

Figure 7.6: **Neural activity in sensorimotor regions.** **a**, The amputee participant received visual cues and performed the corresponding hand movements. In some trials, T^2ENS gave sensory feedback. **b**, Classification of stimulation sites based on the measured EEG signal. **c-f**, Relative alpha power neural activation maps for movements before any sensory feedback (Pre-Stim), sensory feedback with no phantom hand movements (Stim: No Movement), movements with sensory feedback (Stim: Movement), and phantom hand movements (Post-Stim) shortly after (<10 min) after trials with sensory feedback, respectively. **g-h** Relative alpha power in the central and centro-parietal electrodes, respectively.

7.3.6 Sensory feedback improves perceived control of phantom hand.

A user survey was given to each participant after the final EMG recording session. The survey was meant to gauge user perception of the phantom hand and sensory feedback. The questions were modeled after surveys from a previous study [92]. Results from questions targeted specifically at quantifying the enhanced perception and control of the phantom limb as a result of sensory feedback are shown in Fig. 7.7a. In general, participants felt the nerve stimulation as if something was touching the phantom hand. Furthermore, all participants felt as if they could better perceive and better control their phantom hand as a result of the nerve stimulation. The survey was scored using a Likert Scale with answers to questions ranging from “Strongly agree” (+3) to “Strongly disagree” (-3). Individual responses for all survey questions are shown for each participant in Fig. 7.7c. Results vary across participants in several questions, but all participants agree in being able to

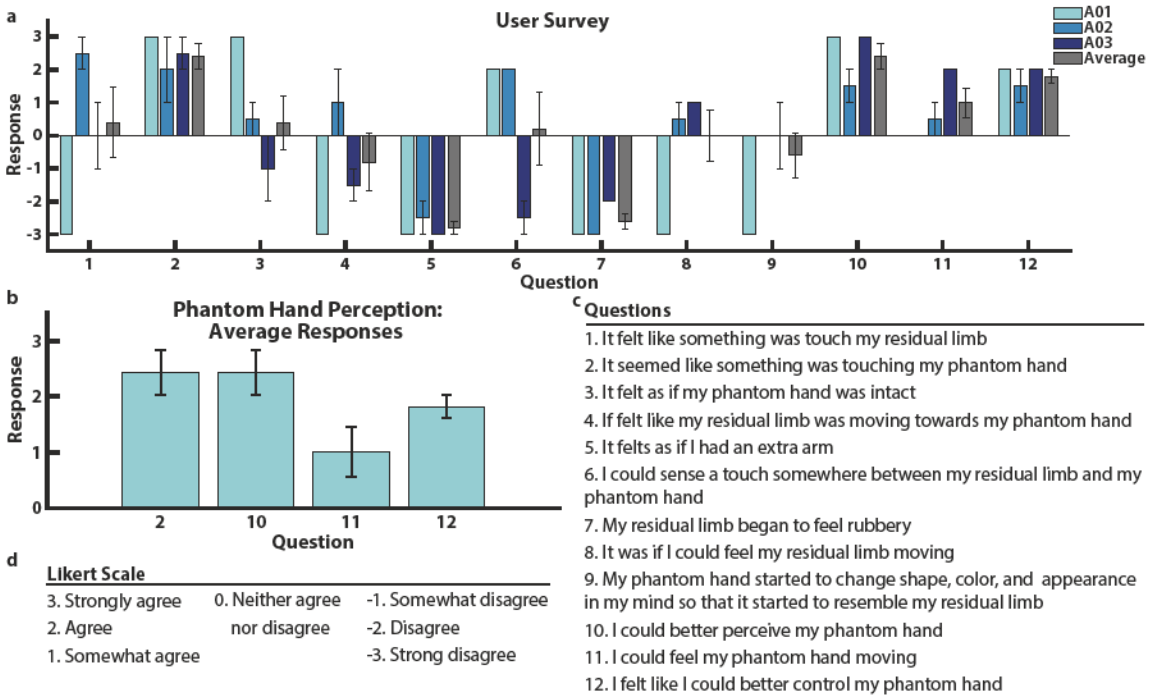

Figure 7.7: **Sensory feedback improves phantom perception and control as reported by user surveys. a**, User survey aimed at understanding subjective perception of sensory feedback. Mixed results for several questions across participants suggest the varying nature of perception due to sensory feedback. However, all participants agreed that heightened perception as well as improved ownership (i.e. control) of the phantom hand were a result of sensory feedback through electrical nerve stimulation. Participants A02 and A03 both took the survey twice, on different days after sensory feedback and prosthesis control experiments. The results were averaged. A01 took the survey once. **b** Averaged user results from survey questions specifically on phantom hand perception as a result of sensory feedback. For all participants, sensory feedback enhanced perception of the phantom hand while also giving the perception of better control over phantom hand movements. **c**, Questions from the user survey. **d**, A Likert Scale was used for all questions on the user surveys.

better perceive and control their phantom hand (Q10 and Q12) as well as disagreeing with unnatural sensations occurring (Q5 and Q7) as a result of nerve stimulation. The user survey results suggest that participants were under the impression that they had better control of their hands because of sensory feedback, despite their being no physiological changes.

7.4 Discussion

7.4.1 Sensory feedback improves perception.

Our results showing enhanced perception of the phantom limb from T^2ENS supports findings from various other studies [4, 9, 26]. Typically this enhancement is used to provide tactile sensations, such as touch, back to the phantom hand. What is interesting in our study here is how this heightened sense of the phantom limb plays into muscle activity during intended movements. Major regions of the phantom hand, such as the thumb and index finger, as well as the pinky and ulnar side of the hand, are activated for every amputee in this study (Fig. 7.1). Various coverage of the palmar and dorsal sides of the metacarpals (i.e. the palm and back of the hand) was also achieved. Because the sensations were reported primarily as being pressure or tactile buzzing, each amputee felt as if the sensations were more or less natural and originating from their phantom hand.

Even over a period of almost 1 year, the sensory perceptions in the phantom hand remained stable for subject A03 (Fig. 7.3). Despite having had an amputation over 5 years prior to the study, the sensory nerves in the residual limb still provided meaningful sensations of touch back to the user indicating both cortical representation of the phantom hand as well as intact neural pathways. The fact that the sensory maps did not significantly change over time suggests that representation of the phantom limb remains even many years after injury and without constant sensory feedback.

7.4.2 Phantom limb perception improves prosthesis control.

Researchers have used sensory feedback as a means to provide realistic tactile information back to amputees [2, 3, 91] and to improve object manipulation tasks with a prosthesis [92, 175]; however,

based on our results it is apparent that the internal sensorimotor pathway is affected by enhanced phantom limb perception as well (Fig. 7.2). It makes sense that a crucial aspect of controlling the phantom hand, and in turn a prosthesis, is the internal perception of the phantom limb. Because there are no physiological changes in the amputee due to the sensory feedback and because the electrodes are placed in approximately the same location, it is reasonable to attribute some of the changes in pattern recognition performance to changes in the internal perception of the ability to physically control the phantom hand.

The long term experiment addresses several interesting questions. One is how does sensory feedback influence real-time myoelectric pattern recognition, and another question is if short term enhancements of the phantom hand improve myoelectric pattern recognition performance several weeks after the stimulation. By working closely with participant A03, we identified the most relevant regions of the phantom hand to enhance perception during certain movements (Fig. 7.4). We also expanded the number of movement classes to 14, an unrealistically high number of classes to achieve reliable control for a prosthesis user, to stretch the limits and see how much improvement was possible due to strengthening the internal sensorimotor control loop of the amputee.

Participant A03 had previous experience with myoelectric pattern recognition and did not show significant signs of improvement as a result of additional training over Phase I of the long term study (Fig. 7.5b); however, there were significant improvements during the sessions with sensory feedback to the phantom hand (Phase II, Fig. 7.5c). Interestingly, these improvements appear to be short-lived in that the ability to perform the 14 movement patterns was the same during Phase III, after the phase with sensory feedback, as it was for Phase I (Fig. 7.5b). These results indicate that the heightened sense of the phantom hand has an immediate ability to strengthen the sensorimotor

loop of the amputee, but that this improvement is lost within a day if the sensory feedback does not persist. This subsiding effect of enhanced phantom perception and control makes sense because our bodies constantly adapt the forward control model based on the sensory inputs we are receiving [172]. Without the sensory feedback and after sensations of the stimulation subside, which can sometimes be several hours after nerve stimulation has ended according to participant A03, the perception of the phantom hand returns to the baseline state. Regardless, the results strongly suggest that enhancing phantom limb perception may be key in improving the control of the phantom hand, which is translated to improved performance during myoelectric pattern recognition.

7.4.3 Sensory feedback activates sensorimotor regions.

The central and the centro-parietal electrodes cover the primary motor cortex and the primary somatosensory cortex. These areas are known to be activated during motor-related tasks [189, 190]. Based on the findings, it can be inferred that the T^2ENS stimulation does not act as a simple sensory stimulus but also improves the perceived control of the phantom hand by the amputee. This inference is also supported by the improvement of the decoding accuracy from the EMG signals (Fig. 7.2 and 7.5). Further, we observed that the sensory feedback effect persists during the Post-Stim phase. Recent studies have shown that the primary sensory cortex (both contralateral and ipsilateral) not only acts as a center for online sensory processing but also as a transient storage site for tactile information [191, 192]. We believe, during the PostStim-Mov condition, the bilateral activation of the primary somatosensory cortex shows the tactile working memory aiding the amputee for better perception of the phantom hand movements even without the feedback stimulus. It should be noted that the above observations were made for all the stimulation sites (median, ulnar and radial). We did not observe significant differences between them owing to the lower spatial resolution of EEG.

We did not observe contralateral activation. Recent literature challenges the idea of functional cortical reorganization of the somatosensory cortex post amputation [193, 194]. There are evidence of disruption of sensorimotor pathways after the amputation of the limbs [195], which showed bilateral activation on presence of electrical sensory stimulus [196] and during phantom movements [197]. Such cortical plasticity mechanisms are not completely understood and vary among different amputees. Deeper insight can be obtained from studying the causal interactions between the two hemispheres focusing on the sensorimotor loop. It will also be interesting to study the effect of the long term T^2ENS stimulation (similar to the long term EMG study with A03) on the sensorimotor pathways and thereby its contribution to improve the prosthesis control by the amputee as observed from the EMG decoding accuracy results.

7.4.4 Subjective perception of enhanced control.

Both the single day and the long term experiments of this study suggest the importance on phantom limb perception on the ability to produce relevant signals for pattern recognition control of a prosthetic hand. We have shown that despite there being no physiological changes, providing sensory feedback to activate the phantom hand enables a greater degree of control of the phantom hand itself, both perceptually by the user as well as quantitatively through performance of the pattern recognition classifier. Subjective feedback from the amputee participants indicated stronger perception of the phantom hand as a result of sensory feedback, which in turn enabled a greater ability to move their phantom hand despite its absence.

Previous research has shown that users tend to perceive greater embodiment of their prosthesis when it is more functional and more lifelike [92] as well as during sensory feedback in an immersive

virtual reality environment [198]. We postulate that in order to create a lifelike prosthesis, it is necessary to develop methods for strengthening the internal sensorimotor models of the amputee's phantom hand. The phantom hand sensation should be utilized in a way that can improve prosthesis control, which in turn will hopefully lead to even better device embodiment by the user. We have shown that sensory feedback to peripheral nerves improves perceptions of the phantom hand, which in turn improves the ability to generate unique myoelectric signals for pattern recognition. The feedback does not change the physiological nature of the amputated limb, yet it seems to be a driving factor in the ability to reliably produce voluntary muscle contractions in the residual limb for mimic complex movements with the phantom hand.

7.5 Methods

7.5.1 Study objectives.

Our objectives were to show that 1) perception of the phantom limb plays a role in prosthesis control through the use of myoelectric pattern recognition of complex movements and 2) that enhancing the perception of the phantom limb can directly improve the ability to control a prosthesis through pattern recognition as a result of improved internal sensorimotor models.

7.5.2 Participant recruitment.

All experiments were approved by the Johns Hopkins Medicine Institutional Review Board. The three amputee participants were recruited from previous studies at Johns Hopkins University in Baltimore, MD or through referrals from local prosthetists.

7.5.3 Sensory feedback.

The sensory feedback experiments consisted of T^2ENS of the median and ulnar nerves using monophasic square wave pulses. We performed mapping of the phantom hand using a 1 mm beryllium copper (BeCu) probe connected to an isolated current stimulator (DS3, Digitimer Ltd., UK). An amplitude of 0.8 – 3.0 mA and frequency of 2 – 4 Hz were used while mapping the phantom hand. Anatomical and ink markers were used, along with photographs of the amputee's limbs, to map the areas of the residual limb to the phantom hand. For all other stimulation experiments, we used a 5 mm disposable Ag-Ag/Cl electrode.

The structural similarity (SSIM) index [199] was used to compare similarity of sensory mapping regions of the phantom hand across different days. We cropped each sensory mapping image to the region of interest (median, ulnar, or radial) and removed the background so that only the colored regions remained. We used the SSIM function in MATLAB (Natick, USA) and compared each sensory mapping image to all other images with the same region of interest. This was done for every image and the results were averaged together to generate a single value for each day (Fig. 7.3b). To calculate the sensory coverage area, we removed the background from every sensory mapping image and converted the image to grayscale. The percentage area was calculated by summing the number of elements with color and dividing by the total number of elements in the image of the hand.

7.5.4 EMG recording.

For participants A01 and A02, eight channels of raw EMG signals were collected using bipolar Ag/Ag-Cl electrodes placed approximately equidistant around the circumference of the residual

limb. No specific muscle groups or locations were targeted for electrode placemenet. Raw EMG signals were amplified using 13E200 Myobock amplifiers (Ottobock, Plymouth, MN). The output of the amplifiers was captured by a NI USB-6009 (National Instruments, Austin, TX) at 1024 Hz and filtered with a 60 Hz digital notch filter as well as a 20 – 500 Hz bandpass digital filter.

Participant A03 used a custom socket manufactured by the participant's prosthetist (Dankmeyer, Linthicum, MD). Bipolar Ag/Ag-Cl electrodes (Infinite Biomedical Technologies, Baltimore, MD) were embedded within the socket. Eight electrodes were used in the socket and each one was targeted to a specific location on the residual limb by the prosthetist. These locations did not change during the duration of this study. The bipolar electrodes in the custom socket were amplified and filtered with a 20 – 500 Hz bandpass filter and a 60 Hz digital notch filter using on-board signal processing hardware.

7.5.5 EEG recording and analysis.

A 64-channel EEG cap with Ag-Ag/Cl electrodes was used for the EEG experiment. Participant A03 was seated, and stimulation electrodes were placed on the median, ulnar, and radial nerve sites of his residual limb. Each site was stimulated individually for a period of 2 s, followed by a 4 s delay with 25% jitter before the next stimulation. There was a total of 60 stimulation presentations with varying pulse width (1 to 20ms) and frequencies (4 to 45 Hz) with an amplitude of 1.6 mA.

The EEG data was band-pass filtered from 1 to 50 Hz and re-referenced to both of the mastoids. Automatic artifact Removal (AAR) was used to remove the muscle (canonical correlation approach, 5 sec window size) and ocular (blind source separation sobi algorithm, 256 sec window size) artifacts [200]. Further, Independent Component Analysis (ICA) was used to remove any other

additional artifacts. Continuous EEG data was then epoched from the start of each trial till 2 secs after the stimulus presentation. All preprocessing steps were carried out using the EEGLAB toolbox in MATLAB [201].

The epoched data was band-pass filtered from 8 Hz to 12 Hz to obtain the alpha band which is reported to be more relevant for motor-related activity [187, 188]. We further epoched the data from 450 – 850 ms to remove the early activations due to the TENS and visual stimulation from analysis and focusing on the motor-related activity in the brain [202]. We evaluated the alpha band power in all the electrodes for each condition and each trial. All the three phantom hand movement conditions (thumb, pinky and wrist) were combined for rest of the analysis. The band power analysis was performed in MATLAB.

Classification of stimulation sites from the EEG data was performed using the gumpy toolbox [203]. Multi-class spatial patterns (CSP) [204] were used as features for classification with a support vector machine (SVM). A 100 ms sliding window was used and 80% of the trials were used for training and 20% were used for testing. A grid search was performed to select the best hyper parameters for the SVM classifier.

7.5.6 Experimental protocol.

Phantom Movements with Feedback: We used a modified Virtual Integration Environment (VIE) (Johns Hopkins University Applied Physics Lab, Laurel, MD) with MATLAB to display movement cues in a random order. The subjects were seated comfortably in front of a screen that displayed the 9 individual movement classes. The skin of the residual limb was cleaned with an alcohol wipe before placing the electrodes on the arm. The electrodes were allowed to settle for up to 10 minutes.

The subjects performed three repetitions of each movement. After EMG data collection, the subject underwent T^2ENS for sensory feedback and phantom hand mapping. The sensory feedback lasted between 30 – 60 min with stimulation of each site of the phantom hand for up to 10 s at a time. If the subject began to feel a constant buzzing or tingling in the phantom hand as a result of the nerve stimulation, then the sensory feedback was stopped until the residual sensations subsided. After the sensory feedback, the participants performed another round of EMG data collection. Anatomical markers and photographs were used to ensure the electrodes were positioned in approximately the same location for subjects A01 and A02. Subject A03 used a customized socket, which ensured consistent electrode placement for ever session. The total experiment lasted between 2 – 3 hr.

Long Term Sensory Feedback and EMG: For the long term study, participant A03 performed 3 different sets of pattern recognition data collection. In this case, 14 movement patterns were used. Over the course of 6 weeks, A03 came in for an EMG recording session on average once per week. For the following 2 weeks, he came in for EMG recording sessions on 4 different days. There were 3 separate rounds of EMG data collection on each of those days. During this 2 week period, a pre-stimulation set of EMG signals were recorded for each movement with each movement being repeated 3 times. Next, EMG signals were recorded simultaneously while sensory feedback was being given to the relevant parts of his phantom hand. The motivation of this was to see what role active sensory feedback plays in the sensorimotor control loop of the amputee. After the session with both EMG recording and nerve stimulation, a final EMG recording session was performed without stimulation. There was up to a 30 min break between each of the 3 recording sessions. The total experiment lasted between 2.5 – 3.5 hr each day.

Neural Recording: The purpose of the EEG experiment was to collect neural signals from par-

ticipant A03 during various phantom hand movements with and without sensory feedback. The participant was seated comfortably and was shown visual movement cues. The movement cues chosen by the participant were tripod, index point, and wrist flexion with corresponding nerve stimulation in median, ulnar, and radial regions, respectively (Fig. 7.4). Two trials of baseline activity were recorded for up to 1 min. In the first trial, the movement cues were shown to the participant who mimicked the movements with his phantom hand. Next, the participant received TENS on the residual limb to activate the median, ulnar, and radial regions of the phantom hand, but he did not perform the movements with his phantom hand. In the next trial, the subject received sensory feedback while also performing the corresponding movements with his phantom hand. Finally, the subject repeated another trial of only phantom hand movements but with no sensory feedback. Each movement cue was presented up to 20 times for each trial.

7.5.7 Movement pattern recognition and classification.

Features of the EMG signals were extracted using a 200 ms sliding window with new feature vectors computed every 50 ms. The EMG signal features used were mean absolute value (Eq. 7.1), waveform length (Eq. 7.2), and variance (Eq. 7.3). For subject's A01 and A02, the raw EMG signals were recorded with the NI USB-6009 and the features extracted in MATLAB (Mathworks, Natick, MA). For subject A03, the EMG signal features were extracted on the electrodes themselves and sent via Bluetooth from a custom prosthesis controller (Infinite Biomedical Technologies, Baltimore, MD) to MATLAB at 100 Hz. Movements were decoded using the extracted EMG features with an LDA classifier [205].

$$MAV = \frac{1}{N}\sum_{k=1}^{N}|x_k| \tag{7.1}$$

$$WL = \sum_{k=2}^{N}|x_k - x_{k-1}| \tag{7.2}$$

$$var(x) = E\left[(x-\mu)^2\right] \tag{7.3}$$

N is the number of samples, x_k is the k^{th} sample, and μ is the mean of x.

7.5.8 Stimulation noise removal and statistics.

The surface EMG electrodes used with participant A03 stream feature extracted data to a PC via Bluetooth. To mitigate the effects of electrical stimulation on the EMG signal features, we implemented a noise filtering technique to remove unwanted stimulation effects in the EMG signal. To establish a baseline for the noise source, all possible combinations of electrical stimulation were provided to the residual limb of A03 while he was resting his phantom hand (i.e. no movement). The noise signal from the surface EMG electrodes was smoothed and used as a noise baseline. This noise baseline was subtracted from the actual EMG signal collected during trials with phantom hand movement and nerve stimulation.

Results from data collected over multiple trials of the same experiment were averaged together. Error bars represent the standard error of the mean, unless otherwise specified.

Acknowledgments

The Virtual Integration Environment (VIE) was developed and made available by the Johns Hopkins Applied Physics Laboratory (JHU/APL) under the Revolutionizing Prosthetics program (Defense Advanced Research Projects Agency (DARPA), Contract No. N66001-10-C-4056). The VIE was developed by Robert Armiger and the virtual prosthesis model used with the VIE was developed by Brock Wester, Tim Gion, Ken Fischer, and Scott Swetz. R.B., A.D., and A.B. performed the signal analysis of the EEG data in this chapter. Z.T. performed classification of stimulation site from the EEG signals. C.H., J.B., and G.L. developed software for the EMG experiments and analysis in this chapter.

8 | Conclusion

8.1 Summary of results

Hopefully the work contained in this thesis progressed in a logical and straight forward fashion that was easy to follow. If you started at the beginning and have finally reached this chapter then congratulations on navigating the numerous pages of technical details and results, and thank you for reading. If you jumped straight to this chapter then kudos for trying to be efficient with your time. In either case, hopefully a brief summary of my work will help you grasp the big picture and potential impact of this work.

8.1.1 Tactile sensing

We showed that local tactile feedback can improve prosthesis grasping and object manipulation. Our hands are capable of making small, yet extremely fast, adjustments to ensure objects we are handling don't break or drop. We showed that similar functionality can be given to a prosthetic hand by providing information of grip force during object manipulation [16]. Furthermore, we showed for the first time that a neuromorphic tactile signal can be used to provide meaningful information in real-time to a prosthetic hand for improving object grasping and manipulation [25].

8.1.2 Sensory feedback

The question persists though as to why use a neuromorphic representation of a tactile signal for a prosthesis. The answer is because we want to now provide sensory information back to the prosthesis, so that it can make automated and fast grip adjustments, as well as the user. The tactile information we provide to an amputee needs to follow some spiking activity, similar to what may be found from healthy receptors in the skin. First, we showed that we are able to provide tactile sensations to the phantom hand of several amputees through transcutaneous (i.e. noninvasive) electrical nerve stimulation on the residual limb. Electrical spikes pass through the skin and activate the underlying sensory nerves. This process requires several hours of sensory mapping of the residual limb, but results in the ability to provide sensations of touch back to an amputee [26].

8.1.3 Touch and pain

Our tactile sensation is fairly complicated and extends beyond perceptions of pressure to temperature, proprioception, and even pain. We showed that by using a neuromorphic model to drive stimulation, we could reliably provide sensations of either touch or pain in an amputee using the same stimulation modality. We accomplished this by creating a multilayered electronic dermis (e-dermis) that translates pressure into sensations of touch or pain to both the prosthesis and the user. We showed that sensations of pain could be perceived by the user but also the prosthesis, which used an automatic pain reflex to release objects that were sharp and thus perceived as painful.

8.1.4 Phantom perception and control

Finally, we investigated the effect of sensory feedback not only on its ability to provide tactile sensations but also in enhancing perception of the phantom limb. We found, in multiple amputees, that providing sensory feedback enhanced not only their perception of their phantom limb but also their ability to mimic complicated hand movements. EMG signal pattern recognition showed that the amputees were better able to perform movements with their phantom hand after having received sensory feedback. An extended experiment also showed that these effects are limited to short term improvements, typically within the same day. This suggests that sensory feedback and perception of the phantom hand play a major role in the internal sensorimotor models of amputees.

8.2 Future directions

8.2.1 Advanced materials

Recently, researchers have investigated more advanced materials for creating sensors and synthetic skins. One area of continued improvement will be in creating realistic, sophisticated e-skins that will cover prosthetic limbs. Sensations will likely include pressure as well as things like temperature and position, much like the receptors throughout our bodies [89]. Additionally, other skinlike properties such as stretchability and compliance [79, 159] as well as self-healing [85, 160] will be leveraged in making more sophisticated and lifelike sensing devices.

8.2.2 Stimulating electrodes

Currently, electrodes for peripheral nerve stimulation enable targeting of nerve fasicles within nerve bundles. As a result, it is likely that a small population of sensory fibers are being stimulated as

opposed to individual afferents. To fully recreate sensations of natural touch, it may be necessary to selectively stimulate sensory nerve fibers based on receptor type. To do so, more sophisticated neural stimulation techniques will need to be developed. Already, there are several techniques that improve electrodes by using advanced materials [48].

8.2.3 Neuromorphic stimulation

When finer resolution for stimulating sensory nerves is achieved, there will be a larger interest in using more realistic neuromorphic models to provide sensory feedback. Researchers have developed sophisticated models that can mimic the behavior of different slowly adapting and rapidly adapting mechanoreceptors [99]. We have shown that using a neuromorphic model to provide sensations of touch and pain can be achieved. In future work, researchers will undoubtedly investigate the effects of different biomimetic stimulation patterns on the perceptual qualities and naturalness of the perceived sensations.

8.2.4 Sensorimotor integration

Finally, it is important to further investigate the role sensory feedback plays in the ability of amputees to control their prosthesis. We rely on sensory feedback for understanding our surrounding environment and the objects we interact with, but that information is constantly being monitored by our cortex to update how we model and predict our limb movements through space [172]. Researchers have already shown the benefit of providing sensory feedback for prosthesis use during object manipulation [92, 175], but a lifelike prosthetic limb requires sophisticated levels of dexterous and reliable control. This control could be further improved by developing techniques to strengthen the internal sensorimotor control models of amputee users.

Bibliography

[1] L. E. Osborn, J. L. Betthauser, and N. V. Thakor, "Neural prostheses," in *Wiley Encyclopedia of Electrical and Electronics Engineering*. John Wiley & Sons, 2019, ch. *in press*, pp. 1–15. [Cited on pages xiii, xiv, 2, 6, 8, 9, 14, 15, and 17]

[2] D. W. Tan, M. A. Schiefer, M. W. Keith, J. R. Anderson, J. Tyler, and D. J. Tyler, "A neural interface provides long-term stable natural touch perception," *Science Translational Medicine*, vol. 6, no. 257, p. 257ra138, 10/08 2014. [doi] [Cited on pages xiv, 7, 19, 20, 56, 80, 113, and 125]

[3] S. Wendelken, D. M. Page, T. Davis, H. A. C. Wark, D. T. Kluger, C. Duncan, D. J. Warren, D. T. Hutchinson, and G. A. Clark, "Restoration of motor control and proprioceptive and cutaneous sensation in humans with prior upper-limb amputation via multiple utah slanted electrode arrays (useas) implanted in residual peripheral arm nerves," *Journal of Neuroengineering and Rehabilitation*, vol. 14, no. 1, p. 121, Nov 2017. [doi] [Cited on pages xiv, 14, 16, 20, 21, 24, 80, 113, 114, and 125]

[4] E. D'Anna, F. M. Petrini, F. Artoni, I. Popovic, I. Simanić, S. Raspopovic, and S. Micera, "A somatotopic bidirectional hand prosthesis with transcutaneous electrical nerve stimulation based sensory feedback," *Scientific Reports*, vol. 7, no. 1, p. 10930, 2017. [doi] [Cited on pages xiv, 20, 24, 113, 116, and 125]

[5] R. S. Johansson and Å. B. Vallbo, "Tactile sensory coding in the glabrous skin of the human hand," *Trends in Neurosciences*, vol. 6, no. 0, pp. 27 – 32, 1983. [doi] [Cited on pages xiv, 27, and 28]

[6] B. Matulevich, G. E. Loeb, and J. A. Fishel, "Utility of contact detection reflexes in prosthetic hand control," in *IEEE/RSJ International Conference on Intelligent Robots and Systems (IROS)*, 2013, pp. 4741–4746. [Cited on pages xv, 27, 38, 51, 62, and 64]

[7] N. Wettels, A. R. Parnandi, J.-H. Moon, G. E. Loeb, and G. S. Sukhatme, "Grip control using biomimetic tactile sensing systems," *IEEE/ASME Transactions on Mechatronics*, vol. 14, no. 6, pp. 718–723, 2009. [Cited on pages xv, 38, 47, and 48]

[8] J. M. Romano, K. Hsiao, G. Niemeyer, S. Chitta, and K. J. Kuchenbecker, "Human-inspired robotic grasp control with tactile sensing," *IEEE Transactions on Robotics*, vol. 27, no. 6, pp. 1067–1079, 2011. [Cited on pages xv and 38]

[9] L. E. Osborn, A. Dragomir, J. L. Betthauser, C. L. Hunt, H. H. Nguyen, R. R. Kaliki, and N. V. Thakor, "Prosthesis with neuromorphic multilayered e-dermis perceives touch and pain," *Science Robotics*, vol. 3, no. 19, p. eaat3818, 2018. [doi] [Cited on pages xvii, xviii, 2, 77, 82, 84, 86, 90, 91, 92, 94, 113, 116, and 125]

[10] V. Skljarevski and N. Ramadan, "The nociceptive flexion reflex in humans – review article," *Pain*, vol. 96, no. 1, pp. 3 – 8, 2002. [doi] [Cited on pages xviii, 81, 91, 92, and 106]

[11] W. F. N. Santos and M. J. Lewis, "Aerothermodynamic performance analysis of hypersonic flow on power law leading edges," *Journal of Spacecraft and Rockets*, vol. 42, no. 4, pp. 588–597, 2005. [doi] [Cited on pages xix and 107]

[12] ——, "Power-law shaped leading edges in rarefied hypersonic flow," *Journal of Spacecraft and Rockets*, vol. 39, no. 6, pp. 917–925, 2002. [doi] [Cited on pages xix and 107]

[13] L. E. Osborn, M. A. Hays, R. Bose, A. Dragomir, Z. Tayeb, C. Hunt, J. Betthauser, G. M. Lévay, A. Bezerianos, and N. V. Thakor, "Sensory feedback enhances phantom limb perception and prosthesis control," *In Preparation*, 2019. [Cited on pages 2 and 111]

[14] J. Betthauser, C. Hunt, L. Osborn, M. Masters, G. Lévay, R. Kaliki, and N. Thakor, "Limb position tolerant pattern recognition for myoelectric prosthesis control with adaptive sparse representations from extreme learning," *IEEE Transactions on Biomedical Engineering*, vol. 65, no. 4, pp. 770–778, 2018. [doi] [Cited on pages 2, 14, and 114]

[15] D. Yang, Y. Gu, L. Jiang, L. Osborn, and H. Liu, "Dynamic training protocol improves the robustness of pr-based myoelectric control," *Biomedical Signal Processing and Control*, vol. 31, pp. 249–256, 2017. [doi] [Cited on page 2]

[16] L. Osborn, R. Kaliki, A. Soares, and N. Thakor, "Neuromimetic event-based detection for closed-loop tactile feedback control of upper limb prostheses," *IEEE Transactions on Haptics*, vol. 9, no. 2, pp. 196–206, 2016. [doi] [Cited on pages 2, 25, 56, 57, 59, 61, 62, 64, 66, 80, 101, and 137]

[17] L. E. Osborn, M. Iskarous, and N. V. Thakor, "Sensing and control for prosthetic hands in clinical and research applications," in *Wearable Robotics*. Elsevier, 2019, ch. *under review*. [Cited on pages 2, 6, and 15]

[18] M. Hays, L. Osborn, R. Ghosh, M. Iskarous, C. Hunt, and N. V. Thakor, "Neuromorphic vision and tactile fusion for upper limb prosthesis control," in *IEEE Neural Engineering (NER)*, 2019, pp. 1–4. [Cited on page 2]

[19] M. M. Iskarous, H. H. Nguyen, L. E. Osborn, J. L. Betthauser, and N. V. Thakor, "Unsupervised learning and adaptive classification of neuromorphic tactile encoding of textures," in *IEEE Biomedical Circuits and Systems Conference (BioCAS)*, 2018, pp. 1–4. [Cited on page 2]

[20] H. Nguyen, L. Osborn, M. Iskarous, C. Shallal, C. Hunt, J. Betthauser, and N. V. Thakor, "Dynamic texture decoding using a neuromorphic multilayer tactile sensor," in *IEEE Biomedical Circuits and Systems Conference (BioCAS)*, 2018, pp. 1–4. [Cited on page 2]

[21] C. L. Hunt, A. Sharma, L. E. Osborn, R. R. Kaliki, and N. V. Thakor, "Predictive trajectory estimation during rehabilitative tasks in augmented reality using inertial sensors," in *IEEE*

Biomedical Circuits and Systems Conference (BioCAS), 2018, pp. 1–4. [Cited on page 2]

[22] A. Sharma, C. L. Hunt, A. Maheshwari, L. Osborn, G. Lévay, R. R. Kaliki, A. B. Soares, and V. Thakor, "A mixed-reality training environment for upper limb prosthesis control," in *IEEE Biomedical Circuits and Systems Conference (BioCAS)*, 2018, pp. 1–4. [Cited on page 2]

[23] J. Costacurta, , L. Osborn, N. Thakor, and S. Sarma, "Designing feedback controllers for human-prosthetic systems using h-infinity model matching," in *2018 40th Annual International Conference of the IEEE Engineering in Medicine and Biology Society (EMBC)*, 2018, pp. 2316 – 2319. [doi] [Cited on page 2]

[24] J. Fu, H. Nguyen, D. Kim, C. Shallal, S. Cho, , L. Osborn, and N. Thakor, "Dynamically mapping socket loading conditions during real time operation of an upper limb prosthesis," in *2018 40th Annual International Conference of the IEEE Engineering in Medicine and Biology Society (EMBC)*, 2018, pp. 3930 – 3933. [doi] [Cited on page 2]

[25] L. Osborn, H. Nguyen, R. Kaliki, and N. Thakor, "Prosthesis grip force modulation using neuromorphic tactile sensing," in *Myoelectric Controls Symposium (MEC)*, 2017, pp. 188–191. [Cited on pages 2, 54, 66, 67, 72, 80, and 137]

[26] L. Osborn, M. Fifer, C. Moran, J. Betthauser, R. Armiger, R. Kaliki, and N. Thakor, "Targeted transcutaneous electrical nerve stimulation for phantom limb sensory feedback," in *IEEE Biomedical Circuits and Systems (BioCAS)*, 2017, pp. 1–4. [doi] [Cited on pages 2, 65, 80, 83, 85, 98, 101, 116, 125, and 138]

[27] J. L. Betthauser, L. E. Osborn, R. R. Kaliki, and N. V. Thakor, "Electrode-shift tolerant myoelectric movement-pattern classification using extreme learning for adaptive sparse representations," in *IEEE Biomedical Circuits and Systems Conference (BioCAS)*, 2017, pp. 1–4. [doi] [Cited on pages 2 and 66]

[28] C. Hunt, R. Yerrabelli, C. Clancy, L. Osborn, R. Kaliki, and N. Thakor, "Pham: prosthetic hand assessment measure," in *Proceedings of Myoelectric Controls Symposium*, 2017, pp. 221–224. [Cited on page 2]

[29] D. Candrea, A. Sharma, L. Osborn, Y. Gu, and N. Thakor, "An adaptable prosthetic socket: Regulating independent air bladders through closed-loop control," in *IEEE International Symposium on Circuits and Systems (ISCAS)*, May 2017, pp. 1–4. [doi] [Cited on page 2]

[30] L. Osborn, H. Nguyen, J. Betthauser, R. Kaliki, and N. Thakor, "Biologically inspired multilayered synthetic skin for tactile feedback in prosthetic limbs," in *IEEE Engineering in Medicine and Biology Society (EMBC)*, 2016, pp. 4622–4625. [doi] [Cited on pages 2, 57, and 66]

[31] J. L. Betthauser, C. L. Hunt, L. E. Osborn, R. R. Kaliki, and N. V. Thakor, "Limb-position robust classification of myoelectric signals for prosthesis control using sparse representations," in *2016 38th Annual International Conference of the IEEE Engineering in Medicine and Biology Society (EMBC)*, 2016, pp. 6373–6376. [doi] [Cited on pages 2 and 56]

[32] M. Masters, L. Osborn, N. Thakor, and A. Soares, "Real-time arm tracking for hmi applications," in *2015 IEEE 12th International Conference on Wearable and Implantable Body Sensor Networks (BSN)*, 2015, pp. 1–4. [doi] [Cited on page 2]

[33] K. Ziegler-Graham, E. J. MacKenzie, P. L. Ephraim, T. G. Travison, and R. Brookmeyer, "Estimating the prevalence of limb loss in the united states: 2005 to 2050," *Archives of Physical Medicine and Rehabilitation*, vol. 89, no. 3, pp. 422–429, 2014/12 2008. [doi] [Cited on page 7]

[34] B. S. Armour, E. A. Courtney-Long, M. H. Fox, H. Fredine, and A. Cahill, "Prevalence and causes of paralysis - united states, 2013," *American Journal of Public Health*, vol. 106, no. 10, pp. 1855–1857, 2016. [doi] [Cited on page 7]

[35] S. Acharya, M. S. Fifer, H. L. Benz, N. E. Crone, and N. V. Thakor, "Electrocorticographic amplitude predicts finger positions during slow grasping motions of the hand," *Journal of Neural Engineering*, vol. 7, no. 4, p. 046002, 2010. [Cited on page 7]

[36] V. Aggarwal, S. Acharya, F. Tenore, H. C. Shin, R. Etienne-Cummings, M. H. Schieber, and N. V. Thakor, "Asynchronous decoding of dexterous finger movements using m1 neurons," *IEEE Transactions on Neural Systems and Rehabilitation Engineering*, vol. 16, no. 1, pp. 3–14, 2008. [doi] [Cited on page 7]

[37] F. V. G. Tenore, A. Ramos, A. Fahmy, S. Acharya, R. Etienne-Cummings, and N. V. Thakor, "Decoding of individuated finger movements using surface electromyography," *IEEE Transactions on Biomedical Engineering*, vol. 56, no. 5, pp. 1427–1434, 2009. [doi] [Cited on pages 7 and 114]

[38] B. S. Wilson and M. F. Dorman, "Cochlear implants: current designs and future possibilities," *Journal Rehabilitation Research and Development*, vol. 45, no. 5, pp. 695–730, 2008. [Cited on page 7]

[39] J. D. Weiland and M. S. Humayun, "Visual prosthesis," *Proceedings of the IEEE*, vol. 96, no. 7, pp. 1076–1084, 2008. [doi] [Cited on page 7]

[40] A. Prasad and M. Sahin, "Can motor volition be extracted from the spinal cord?" *Journal of NeuroEngineering and Rehabilitation*, vol. 9, no. 1, p. 41, Jun 2012. [doi] [Cited on page 10]

[41] J. B. Zimmermann, K. Seki, and A. Jackson, "Reanimating the arm and hand with intraspinal microstimulation," *Journal of Neural Engineering*, vol. 8, no. 5, p. 054001, 2011. [doi] [Cited on page 10]

[42] C. E. Bouton, A. Shaikhouni, N. V. Annetta, M. A. Bockbrader, D. A. Friedenberg, D. M. Nielson, G. Sharma, P. B. Sederberg, B. C. Glenn, W. J. Mysiw, A. G. Morgan, M. Deogaonkar, and A. R. Rezai, "Restoring cortical control of functional movement in a human with quadriplegia," *Nature*, vol. 533, no. 7602, p. 247, May 12, 2016. [doi] [Cited on page 10]

[43] H. A. C. Wark, R. Sharma, K. S. Mathews, E. Fernandez, J. Yoo, B. Christensen, P. Tresco, L. Rieth, F. Solzbacher, R. A. Normann, and P. Tathireddy, "A new high-density (25 electrodes/mm^2) penetrating microelectrode array for recording and stimulating sub-millimeter neuroanatomical structures," *Journal of Neural Engineering*, vol. 10, no. 4, p. 045003, Aug 2013. [Cited on page 10]

[44] X. Zheng, J. Zhang, T. Chen, and Z. Chen, "Longitudinally implanted intrafascicular electrodes for stimulating and recording fascicular physioelectrical signals in the sciatic nerve of

rabbits," *Microsurgery*, vol. 23, no. 3, pp. 268–273, 2003. [doi] [Cited on page 11]

[45] T. Boretius, J. Badia, A. Pascual-Font, M. Schuettler, X. Navarro, K. Yoshida, and T. Stieglitz, "A transverse intrafascicular multichannel electrode (time) to interface with the peripheral nerve," *Biosensors and Bioelectronics*, vol. 26, no. 1, pp. 62–69, 9/15 2010. [doi] [Cited on page 11]

[46] D. J. Tyler and D. M. Durand, "Functionally selective peripheral nerve stimulation with a flat interface nerve electrode," *IEEE Transactions on Neural Systems and Rehabilitation Engineering*, vol. 10, no. 4, pp. 294–303, 2002. [Cited on page 11]

[47] S. F. Cogan, "Neural stimulation and recording electrodes," *Annual Review of Biomedical Engineering*, vol. 10, pp. 275–309, 2008. [doi] [Cited on page 11]

[48] A. Patil and N. Thakor, "Implantable neurotechnologies: a review of micro- and nanoelectrodes for neural recording," *Medical & Biological Engineering & Computing*, vol. 54, no. 1, pp. 23–44, Jan 2016. [doi] [Cited on pages 11 and 140]

[49] S. Nag and N. Thakor, "Implantable neurotechnologies: electrical stimulation and applications," *Medical & Biological Engineering & Computing*, vol. 54, no. 1, pp. 63–76, Jan 2016. [doi] [Cited on page 11]

[50] D. R. Merrill, M. Bikson, and J. G. R. Jefferys, "Electrical stimulation of excitable tissue: design of efficacious and safe protocols," *Journal of Neuroscience Methods*, vol. 141, no. 2, pp. 171–198, February 15, 2005. [doi] [Cited on page 11]

[51] T. A. Kuiken, P. D. Marasco, B. A. Lock, R. N. Harden, and J. P. A. Dewald, "Redirection of cutaneous sensation from the hand to the chest skin of human amputees with targeted reinnervation," *Proceedings of the National Academy of Sciences USA*, vol. 104, no. 50, pp. 20 061–20 066, 12/11 2007. [Cited on pages 11, 20, and 67]

[52] N. V. Thakor, "Translating the brain-machine interface," *Science Translational Medicine*, vol. 5, no. 210, p. 210ps17, Nov 6, 2013. [doi] [Cited on page 11]

[53] M. Johannes, J. Bigelow, J. Burck, S. Harshbarger, M. Kozlowski, and T. V. Doren, "An overview of the development process for the modular prosthetic limb," *JHU APL Technical Digest*, vol. 30, no. 3, pp. 207–216, 2011. [Cited on page 12]

[54] G. Hotson, D. P. McMullen, M. S. Fifer, M. S. Johannes, K. D. Katyal, M. P. Para, R. Armiger, W. S. Anderson, N. V. Thakor, and B. A. Wester, "Individual finger control of a modular prosthetic limb using high-density electrocorticography in a human subject," *Journal of Neural Engineering*, vol. 13, no. 2, p. 026017, 2016. [doi] [Cited on page 12]

[55] M. S. Fifer, G. Hotson, B. A. Wester, D. P. McMullen, Y. Wang, M. S. Johannes, K. D. Katyal, J. B. Helder, M. P. Para, R. J. Vogelstein, W. S. Anderson, N. V. Thakor, and N. E. Crone, "Simultaneous neural control of simple reaching and grasping with the modular prosthetic limb using intracranial eeg," *IEEE Transactions on Neural Systems and Rehabilitation Engineering*, vol. 22, no. 3, pp. 695–705, 2014. [doi] [Cited on page 12]

[56] J. Collinger, B. Wodlinger, J. Downey, W. Wang, E. Tyler-Kabara, D. Weber, A. McMorland, M. Velliste, M. Boninger, and A. Schwartz, "High-performance neuroprosthetic control by an individual with tetraplegia," *Lancet*, vol. 381, p. 8, 2012. [doi] [Cited on page 12]

[57] S. N. Flesher, J. L. Collinger, S. T. Foldes, J. M. Weiss, J. E. Downey, E. C. Tyler-Kabara, S. J. Bensmaia, A. B. Schwartz, M. L. Boninger, and R. A. Gaunt, "Intracortical microstimulation of human somatosensory cortex," *Science Translational Medicine*, vol. 8, no. 361, p. 361ra141, Oct 19, 2016. [doi] [Cited on pages 12, 21, and 24]

[58] G. A. Tabot, J. F. Dammann, J. A. Berg, F. V. Tenore, J. L. Boback, R. J. Vogelstein, and S. J. Bensmaia, "Restoring the sense of touch with a prosthetic hand through a brain interface," *Proceedings of the National Academy of Sciences*, vol. 110, no. 45, pp. 18 279–18 284, 2013. [doi] [Cited on page 12]

[59] K. Østlie, I. M. Lesjø, R. J. Franklin, B. Garfelt, O. H. Skjeldal, and P. Magnus, "Prosthesis use in adult acquired major upper-limb amputees: patterns of wear, prosthetic skills and the actual use of prostheses in activities of daily life," *Disability and Rehabilitation: Assistive Technology*, vol. 7, no. 6, pp. 479–493, 2012. [doi] [Cited on page 12]

[60] E. Scheme and K. Englehart, "Electromyogram pattern recognition for control of powered upper-limb prostheses: State of the art and challenges for clinical use," *Journal of Rehabilitation Research and Development*, vol. 48, no. 6, pp. 643–659, 2011. [doi] [Cited on pages 14, 15, 113, and 117]

[61] V. Gilja, P. Nuyujukian, C. A. Chestek, J. P. Cunningham, M. Y. Byron, J. M. Fan, M. M. Churchland, M. T. Kaufman, J. C. Kao, S. I. Ryu *et al.*, "A high-performance neural prosthesis enabled by control algorithm design," *Nature Neuroscience*, vol. 15, no. 12, pp. 1752–1757, 2012. [doi] [Cited on page 14]

[62] J. M. Hahne, M. A. Schweisfurth, M. Koppe, and D. Farina, "Simultaneous control of multiple functions of bionic hand prostheses: Performance and robustness in end users," *Science Robotics*, vol. 3, no. 19, p. eaat3630, 2018. [doi] [Cited on pages 14, 15, 16, and 114]

[63] T. Tsuji, R. O. Fukuda, M. Kaneko, and K. Ito, "Pattern classification of time-series emg signals using neural networks," *Int. J. Adapt. Control Signal Process*, vol. 14, no. 8, pp. 829–848, 2000. [doi] [Cited on page 14]

[64] H. C. Shin, V. Aggarwal, S. Acharya, M. H. Schieber, and N. V. Thakor, "Neural decoding of finger movements using skellam-based maximum-likelihood decoding," *IEEE Transactions on Biomedical Engineering*, vol. 57, no. 3, pp. 754–760, 2010. [doi] [Cited on page 14]

[65] L. J. Hargrove, E. J. Scheme, K. B. Englehart, and B. S. Hudgins, "Multiple binary classifications via linear discriminant analysis for improved controllability of a powered prosthesis," *IEEE Transactions on Neural Systems and Rehabilitation Engineering*, vol. 18, no. 1, pp. 49–57, 2010. [doi] [Cited on page 14]

[66] K. Englehart and B. Hudgins, "A robust, real-time control scheme for multifunction myoelectric control," *IEEE Transactions on Biomedical Engineering*, vol. 50, no. 7, pp. 848–854, 2003. [doi] [Cited on pages 14, 26, and 114]

[67] M. A. Powell, R. R. Kaliki, and N. V. Thakor, "User training for pattern recognition-based myoelectric prostheses: improving phantom limb movement consistency and distinguishability," *IEEE Transactions on Neural Systems and Rehabilitation Engineering*, vol. 22, no. 3, pp. 522–532, 2014. [doi] [Cited on pages 15, 26, 56, 66, and 114]

[68] W. Geng, Y. Du, W. Jin, W. Wei, Y. Hu, and J. Li, "Gesture recognition by instantaneous surface emg images," *Scientific Reports*, vol. 6, p. 36571, 2016. [Cited on page 15]

[69] T. A. Kuiken, L. A. Miller, R. D. Lipschutz, B. A. Lock, K. Stubblefield, P. D. Marasco, P. Zhou, and G. A. Dumanian, "Targeted reinnervation for enhanced prosthetic arm function in a woman with a proximal amputation: a case study," *Lancet*, vol. 369, no. 9559, pp. 371–380, Feb 3 2007. [doi] [Cited on pages 15 and 67]

[70] T. A. Kuiken, G. Li, B. A. Lock, R. D. Lipschutz, L. A. Miller, K. A. Stubblefield, and K. B. Englehart, "Targeted muscle reinnervation for real-time myoelectric control of multifunction artificial arms," *Journal of the American Medical Association*, vol. 301, no. 6, pp. 619–628, Feb 11 2009. [doi] [Cited on page 15]

[71] L. J. Hargrove, L. A. Miller, K. Turner, and T. A. Kuiken, "Myoelectric pattern recognition outperforms direct control for transhumeral amputees with targeted muscle reinnervation: a randomized clinical trial," *Scientific Reports*, vol. 7, p. 1, 2017. [doi] [Cited on page 15]

[72] M. Ortiz-Catalan, B. Håkansson, and R. Brånemark, "An osseointegrated human-machine gateway for long-term sensory feedback and motor control of artificial limbs," *Science Translational Medicine*, vol. 6, no. 257, p. 257re6, 2014. [doi] [Cited on pages 15 and 19]

[73] D. Farina, I. Vujaklija, M. Sartori, T. Kapelner, F. Negro, N. Jiang, K. Bergmeister, A. Andalib, J. Principe, and O. C. Aszmann, "Man/machine interface based on the discharge timings of spinal motor neurons after targeted muscle reinnervation," *Nature Biomedical Engineering*, vol. 1, p. 0025, 02/06 2017. [doi] [Cited on pages 15, 66, 79, and 114]

[74] V. E. Abraira and D. D. Ginty, "The sensory neurons of touch," *Neuron*, vol. 79, no. 4, pp. 618–639, 8/21 2013. [doi] [Cited on pages 17, 18, 78, 79, and 82]

[75] A. E. Dubin and A. Patapoutian, "Nociceptors: the sensors of the pain pathway," *The Journal of Clinical Investigation*, vol. 120, no. 11, pp. 3760–3772, Nov 2010. [doi] [Cited on pages 17 and 79]

[76] A. Vallbo and R. Johansson, "Properties of cutaneous mechanoreceptors in the human hand related to touch sensation," *Human Neurobiology*, vol. 3, no. 1, pp. 3–14, 1984. [Cited on pages 18 and 79]

[77] R. S. Johansson and K. J. Cole, "Sensory-motor coordination during grasping and manipulative actions," *Current Opinion in Neurobiology*, vol. 2, no. 6, pp. 815–823, 12 1992. [doi] [Cited on pages 18 and 56]

[78] J. A. Pruszynski and R. S. Johansson, "Edge-orientation processing in first-order tactile neurons," *Nature Neuroscience*, vol. 17, no. 10, pp. 1404–1409, Oct 2014. [doi] [Cited on pages 18 and 79]

[79] J. Kim, M. Lee, H. J. Shim, R. Ghaffari, H. R. Cho, D. Son, Y. H. Jung, M. Soh, C. Choi, S. Jung, K. Chu, D. Jeon, S.-T. Lee, J. H. Kim, S. H. Choi, T. Hyeon, and D.-H. Kim, "Stretchable silicon nanoribbon electronics for skin prosthesis," *Nature Communications*, vol. 5, p. 5747, 12/09 2014. [doi] [Cited on pages 18, 80, and 139]

[80] J. Park, M. Kim, Y. Lee, H. S. Lee, and H. Ko, "Fingertip skin–inspired microstructured ferroelectric skins discriminate static/dynamic pressure and temperature stimuli," *Science*

Advances, vol. 1, no. 9, 2015. [doi] [Cited on page 18]

[81] H. Zhao, K. O'Brien, S. Li, and R. F. Shepherd, "Optoelectronically innervated soft prosthetic hand via stretchable optical waveguides," *Science Robotics*, vol. 1, no. 1, p. eaai7529, 2016. [doi] [Cited on pages 18 and 80]

[82] J. Byun, Y. Lee, J. Yoon, B. Lee, E. Oh, S. Chung, T. Lee, K.-J. Cho, J. Kim, and Y. Hong, "Electronic skins for soft, compact, reversible assembly of wirelessly activated fully soft robots," *Science Robotics*, vol. 3, no. 18, p. eaas9020, 2018. [doi] [Cited on page 18]

[83] Z. Zou, C. Zhu, Y. Li, X. Lei, W. Zhang, and J. Xiao, "Rehealable, fully recyclable, and malleable electronic skin enabled by dynamic covalent thermoset nanocomposite," *Science Advances*, vol. 4, no. 2, p. eaaq0508, 2018. [doi] [Cited on pages 18 and 80]

[84] B. C. Tee, C. Wang, R. Allen, and Z. Bao, "An electrically and mechanically self-healing composite with pressure- and flexion-sensitive properties for electronic skin applications," *Nature Nanotechnology*, vol. 7, no. 12, pp. 825–832, Dec 2012. [doi] [Cited on pages 19 and 80]

[85] S. Terryn, J. Brancart, D. Lefeber, G. Van Assche, and B. Vanderborght, "Self-healing soft pneumatic robots," *Science Robotics*, vol. 2, no. 9, p. eaan4268, 2017. [doi] [Cited on pages 19, 94, and 139]

[86] T. Yokota, P. Zalar, M. Kaltenbrunner, H. Jinno, N. Matsuhisa, H. Kitanosako, Y. Tachibana, W. Yukita, M. Koizumi, and T. Someya, "Ultraflexible organic photonic skin," *Science Advances*, vol. 2, no. 4, p. e1501856, 2016. [doi] [Cited on page 19]

[87] R. Di Giacomo, L. Bonanomi, V. Costanza, B. Maresca, and C. Daraio, "Biomimetic temperature-sensing layer for artificial skins," *Science Robotics*, vol. 2, no. 3, p. eaai9251, 2017. [doi] [Cited on page 19]

[88] B. C. K. Tee, A. Chortos, A. Berndt, A. K. Nguyen, A. Tom, A. McGuire, Z. C. Lin, K. Tien, W.-G. Bae, H. Wang, P. Mei, H.-H. Chou, B. Cui, K. Deisseroth, T. N. Ng, and Z. Bao, "A skin-inspired organic digital mechanoreceptor," *Science*, vol. 350, no. 6258, pp. 313–316, 10/16 2015. [doi] [Cited on pages 19 and 80]

[89] Y. Kim, A. Chortos, W. Xu, Y. Liu, J. Y. Oh, D. Son, J. Kang, A. M. Foudeh, C. Zhu, Y. Lee, S. Niu, J. Liu, R. Pfattner, Z. Bao, and T.-W. Lee, "A bioinspired flexible organic artificial afferent nerve," *Science*, vol. 360, no. 6392, pp. 998–1003, 2018. [doi] [Cited on pages 19 and 139]

[90] A. Chortos, J. Liu, and Z. Bao, "Pursuing prosthetic electronic skin," *Nature Materials*, vol. 15, no. 9, pp. 937–950, 2016. [doi] [Cited on page 19]

[91] S. Raspopovic, M. Capogrosso, F. M. Petrini, M. Bonizzato, J. Rigosa, G. D. Pino, J. Carpaneto, M. Controzzi, T. Boretius, E. Fernandez, G. Granata, C. M. Oddo, L. Citi, A. L. Ciancio, C. Cipriani, M. C. Carrozza, W. Jensen, E. Guglielmelli, T. Stieglitz, P. M. Rossini, and S. Micera, "Restoring natural sensory feedback in real-time bidirectional hand prostheses," *Science Translational Medicine*, vol. 6, no. 222, p. 222ra19, Feb 5 2014. [doi] [Cited on pages 19, 56, 80, 113, and 125]

[92] M. Schiefer, D. Tan, S. M. Sidek, and D. J. Tyler, "Sensory feedback by peripheral nerve

stimulation improves task performance in individuals with upper limb loss using a myoelectric prosthesis," *Journal of Neural Engineering*, vol. 13, no. 1, p. 016001, 2016. [doi] [Cited on pages 19, 56, 66, 113, 123, 125, 128, and 140]

[93] H. Shin, Z. Watkins, H. H. Huang, Y. Zhu, and X. Hu, "Evoked haptic sensations in the hand via non-invasive proximal nerve stimulation," *Journal of Neural Engineering*, vol. 15, no. 4, p. 046005, 2018. [doi] [Cited on page 20]

[94] A. Akhtar, J. Sombeck, B. Boyce, and T. Bretl, "Controlling sensation intensity for electrotactile stimulation in human-machine interfaces," *Science Robotics*, vol. 3, no. 17, p. eaap9770, 2018. [doi] [Cited on page 20]

[95] J. S. Hebert, J. L. Olson, M. J. Morhart, M. R. Dawson, P. D. Marasco, T. A. Kuiken, and K. M. Chan, "Novel targeted sensory reinnervation technique to restore functional hand sensation after transhumeral amputation," *IEEE Transactions on Neural Systems and Rehabilitation Engineering*, vol. 22, no. 4, pp. 765–773, 2014. [doi] [Cited on pages 20 and 67]

[96] P. D. Marasco, A. E. Schultz, and T. A. Kuiken, "Sensory capacity of reinnervated skin after redirection of amputated upper limb nerves to the chest," *Brain*, vol. 132, no. 6, pp. 1441–1448, 03/08 2009. [doi] [Cited on page 20]

[97] P. D. Marasco, J. S. Hebert, J. W. Sensinger, C. E. Shell, J. S. Schofield, Z. C. Thumser, R. Nataraj, D. T. Beckler, M. R. Dawson, D. H. Blustein, S. Gill, B. D. Mensh, R. Granja-Vazquez, M. D. Newcomb, J. P. Carey, and B. M. Orzell, "Illusory movement perception improves motor control for prosthetic hands," *Science Translational Medicine*, vol. 10, no. 432, p. eaao6990, 2018. [doi] [Cited on pages 21, 22, and 113]

[98] C. M. Oddo, S. Raspopovic, F. Artoni, A. Mazzoni, G. Spigler, F. Petrini, F. Giambattistelli, F. Vecchio, F. Miraglia, L. Zollo, G. D. Pino, D. Camboni, M. C. Carrozza, E. Guglielmelli, P. M. Rossini, U. Faraguna, and S. Micera, "Intraneural stimulation elicits discrimination of textural features by artificial fingertip in intact and amputee humans," *eLife*, vol. 5, p. e09148, 03/08 2016. [doi] [Cited on pages 23, 56, 57, 66, 80, 88, 104, and 113]

[99] H. P. Saal, B. P. Delhaye, B. C. Rayhaun, and S. J. Bensmaia, "Simulating tactile signals from the whole hand with millisecond precision," *Proceedings of the National Academy of Sciences USA*, 2017. [doi] [Cited on pages 23, 80, 97, and 140]

[100] E. L. Graczyk, M. A. Schiefer, H. P. Saal, B. P. Delhaye, S. J. Bensmaia, and D. J. Tyler, "The neural basis of perceived intensity in natural and artificial touch," *Science Translational Medicine*, vol. 8, no. 362, p. 362ra142, 10/26 2016. [doi] [Cited on pages 23, 66, 80, and 113]

[101] E. L. Graczyk, B. P. Delhaye, M. A. Schiefer, S. J. Bensmaia, and D. J. Tyler, "Sensory adaptation to electrical stimulation of the somatosensory nerves," *Journal of Neural Engineering*, vol. 15, no. 4, p. 046002, 2018. [doi] [Cited on page 23]

[102] R. S. Johansson, "Sensory input and control of grip," *Novartis Foundation symposium*, vol. 218, pp. 45–63, 1998. [Cited on pages 26 and 27]

[103] S. S. Hsiao and M. Gomez-Ramirez, "Neural mechanisms of tactile perception," in *Comprehensive Handbook of Psychology: Volume 3: Behavioral Neuroscience*, 2nd ed., M. Gallagher and R. Nelson, Eds. John Wiley and Sons, Inc, 01/01 2012. [doi] [Cited on pages

26 and 29]

[104] P. Parker and R. Scott, "Myoelectric control of prostheses," *Critical Reviews in Biomedical Engineering*, vol. 13, no. 4, pp. 283–310, 1986. [Cited on page 26]

[105] P. Parker, K. Englehart, and B. Hudgins, "Myoelectric signal processing for control of powered limb prostheses," *Journal of Electromyography and Kinesiology*, vol. 16, no. 6, pp. 541–548, 12 2006. [doi] [Cited on page 26]

[106] A. Fougner, O. Stavdahl, P. J. Kyberd, Y. G. Losier, and P. A. Parker, "Control of upper limb prostheses: Terminology and proportional myoelectric control a review," *IEEE Transactions on Neural Systems and Rehabilitation Engineering*, vol. 20, no. 5, pp. 663–677, 2012. [doi] [Cited on page 26]

[107] S. M. Wurth and L. J. Hargrove, "A real-time comparison between direct control, sequential pattern recognition control and simultaneous pattern recognition control using a fitts' law style assessment procedure," *Journal of neuroengineering and rehabilitation*, vol. 11, pp. 3–11, May 30 2014. [Cited on pages 26, 40, and 56]

[108] L. H. Smith, T. A. Kuiken, and L. J. Hargrove, "Real-time simultaneous and proportional myoelectric control using intramuscular emg," *Journal of Neural Engineering*, vol. 11, no. 6, p. 066013, Dec 2014. [Cited on page 26]

[109] T. L. Gibo, A. J. Bastian, and A. M. Okamura, "Grip force control during virtual object interaction: Effect of force feedback, accuracy demands, and training," *IEEE Transactions on Haptics*, vol. 7, no. 1, pp. 37–47, 2014. [Cited on page 27]

[110] C. King, M. O. Culjat, M. L. Franco, C. E. Lewis, E. P. Dutson, W. S. Grundfest, and J. W. Bisley, "Tactile feedback induces reduced grasping force in robot-assisted surgery," *IEEE Transactions on Haptics*, vol. 2, no. 2, pp. 103–110, 2009. [Cited on page 27]

[111] D. Prattichizzo, C. Pacchierotti, and G. Rosati, "Cutaneous force feedback as a sensory subtraction technique in haptics," *IEEE Transactions on Haptics*, vol. 5, no. 4, pp. 289–300, 2012. [Cited on page 27]

[112] J. Walker, A. Blank, P. Shewokis, and M. O'Malley, "Tactile feedback of object slip facilitates virtual object manipulation," *IEEE Transactions on Haptics*, Apr 6 2015. [Cited on pages 27, 45, and 51]

[113] T. D'Alessio and R. Steindler, "Slip sensors for the control of the grasp in functional neuromuscular stimulation," *Medical Engineering & Physics*, vol. 17, no. 6, pp. 466–470, 9 1995. [Cited on page 27]

[114] P. J. Kyberd and P. H. Chappell, "Object-slip detection during manipulation using a derived force vector," *Mechatronics*, vol. 2, no. 1, pp. 1–13, 2 1992. [Cited on page 27]

[115] E. D. Engeberg and S. Meek, "Improved grasp force sensitivity for prosthetic hands through force-derivative feedback," *IEEE Transactions on Biomedical Engineering*, vol. 55, no. 2, pp. 817–821, 2008. [Cited on pages 27, 45, and 46]

[116] E. D. Engeberg and S. G. Meek, "Adaptive sliding mode control for prosthetic hands to simultaneously prevent slip and minimize deformation of grasped objects," *IEEE/ASME Transactions on Mechatronics*, vol. 18, no. 1, pp. 376–385, 2013. [Cited on pages 27, 56, and 66]

[117] A. Ajoudani, S. B. Godfrey, M. Bianchi, M. G. Catalano, G. Grioli, N. Tsagarakis, and A. Bicchi, "Exploring teleimpedance and tactile feedback for intuitive control of the pisa/iit softhand," *IEEE Transactions on Haptics*, vol. 7, no. 2, pp. 203–215, 2014. [Cited on page 27]

[118] C. F. Pasluosta, H. Tims, and A. W. L. Chiu, "Slippage sensory feedback and nonlinear force control system for a low-cost prosthetic hand," *American Journal of Biomedical Science*, vol. 1, no. 4, pp. 295–302, 2009. [Cited on page 27]

[119] E. D. Engeberg, S. G. Meek, and M. A. Minor, "Hybrid force-velocity sliding mode control of a prosthetic hand," *IEEE Transactions on Biomedical Engineering*, vol. 55, no. 5, pp. 1572–1581, 2008. [Cited on page 27]

[120] E. D. Engeberg and S. Meek, "Enhanced visual feedback for slip prevention with a prosthetic hand," *Prosthetics and Orthotics International*, vol. 36, no. 4, pp. 423–429, Dec 2012. [Cited on pages 27, 45, and 46]

[121] G. Westling and R. S. Johansson, "Responses in glabrous skin mechanoreceptors during precision grip in humans," *Experimental Brain Research*, vol. 66, no. 1, pp. 128–140, 1987. [Cited on page 27]

[122] T. J. Prescott, M. E. Diamond, and A. M. Wing, "Active touch sensing," *Philosophical Transactions of the Royal Society B: Biological Sciences*, vol. 366, no. 1581, pp. 2989–2995, Nov 2011. [Cited on pages 27 and 49]

[123] F. Grassia, L. Buhry, T. Lévi, J. Tomas, A. Destexhe, and S. Saïghi, "Tunable neuromimetic integrated system for emulating cortical neuron models," *Frontiers in Neuroscience*, vol. 5, pp. 1–12, 2011. [Cited on pages 28 and 56]

[124] C. Mead, *Analog VLSI and Neural Systems*. Boston, MA, USA: Addison-Wesley Longman Publishing Co., Inc, 1989. [Cited on page 28]

[125] R. J. Vogelstein, U. Mallik, E. Culurciello, G. Cauwenberghs, and R. Etienne-Cummings, "A multichip neuromorphic system for spike-based visual information processing," *Neural Computation*, vol. 19, no. 9, pp. 2281–2300, 09/01; 2015/03 2007. [doi] [Cited on pages 28 and 56]

[126] G. Orchard, J. G. Martin, R. J. Vogelstein, and R. Etienne-Cummings, "Fast neuromimetic object recognition using fpga outperforms gpu implementations," *IEEE Transactions on Neural Networks and Learning Systems*, vol. 24, no. 8, pp. 1239–1252, 2013. [Cited on page 28]

[127] S. D. Ha, J. Shi, Y. Meroz, L. Mahadevan, and S. Ramanathan, "Neuromimetic circuits with synaptic devices based on strongly correlated electron systems," *Physics Review Applied*, vol. 2, no. 6, pp. 064 003, 1–11, 12 2014. [doi] [Cited on page 28]

[128] P. M. Daye, L. M. Optican, E. Roze, B. Gaymard, and P. Pouget, "Neuromimetic model of saccades for localizing deficits in an atypical eye-movement pathology," *Journal of Translational Medicine*, vol. 11, p. 125, May 2013. [Cited on pages 28 and 56]

[129] L. L. Bologna, J. Pinoteau, J.-B. Passot, J. A. Garrido, J. Vogel, E. R. Vidal, and A. Arleo, "A closed-loop neurobotic system for fine touch sensing," *Journal of Neural Engineering*, vol. 10, no. 4, pp. 1–17, 2013. [Cited on page 28]

[130] F. Corradi, D. Zambrano, M. Raglianti, G. Passetti, C. Laschi, and G. Indiveri, "Towards a

neuromorphic vestibular system," *IEEE Transactions on Biomedical Circuits and Systems*, vol. 8, no. 5, pp. 669–680, Oct 2014. [Cited on pages 28 and 56]

[131] D. D. Damian, A. H. Arita, H. Martinez, and R. Pfeifer, "Slip speed feedback for grip force control," *IEEE Transactions on Biomedical Engineering*, vol. 59, no. 8, pp. 2200–2210, 2012. [doi] [Cited on pages 28, 47, 51, and 96]

[132] K. J. Cole and J. H. Abbs, "Grip force adjustments evoked by load force perturbations of a grasped object," *Journal of Neurophysiology*, vol. 60, no. 4, pp. 1513–1522, 1988. [Cited on pages 28, 29, 34, and 47]

[133] M. De Gregorio and V. Santos, "Human grip responses to perturbations of objects during precision grip," in *The Human Hand as an Inspiration for Robot Hand Development*, ser. Springer Tracts in Advanced Robotics, R. Balasubramanian and V. J. Santos, Eds. Springer International Publishing, 2014, vol. 95, pp. 159–188. [doi] [Cited on page 28]

[134] R. Johansson and G. Westling, "Roles of glabrous skin receptors and sensorimotor memory in automatic control of precision grip when lifting rougher or more slippery objects," *Experimental Brain Research*, vol. 56, no. 3, pp. 550–564, 1984. [doi] [Cited on page 29]

[135] W. W. Lee, J. J. Cabibihan, and N. V. Thakor, "Biomimetic strategies for tactile sensing," in *IEEE Sensors International Conference*, 2013, pp. 1–4. [Cited on page 30]

[136] L. Osborn, W. W. Lee, R. Kaliki, and N. V. Thakor, "Tactile feedback in upper limb prosthetic devices using flexible textile force sensors," in *5th IEEE RAS & EMBS International Conference on Biomedical Robotics and Biomechatronics (BioRob)*, 2014, pp. 114–119. [doi] [Cited on pages 30, 32, 59, 66, 71, and 101]

[137] L. N. Kachanov, *Plastic deformation, principles and theories*, H. H. Hausner, Ed. Brooklyn: Mapleton House, 1948. [Cited on pages 38 and 40]

[138] K. O. Phillips JR FAU Johnson and J. KO, "Tactile spatial resolution. iii. a continuum mechanics model of skin predicting mechanoreceptor responses to bars, edges, and gratings." [Cited on page 51]

[139] Q. Wang and V. Hayward, "In vivo biomechanics of the fingerpad skin under local tangential traction," *Journal of Biomechanics*, vol. 40, no. 4, pp. 851–860, 2007. [Cited on page 51]

[140] B. Delhaye, P. Lefèvre, and J.-L. Thonnard, "Dynamics of fingertip contact during the onset of tangential slip," *Journal of The Royal Society Interface*, vol. 11, no. 100, November 06 2014. [Cited on page 51]

[141] K. O. Johnson and S. S. Hsiao, "Neural mechanisms of tactual form and texture perception," *Annual Review of Neuroscience*, vol. 15, no. 1, pp. 227–250, 1992. [Cited on page 55]

[142] E. A. Lumpkin and M. J. Caterina, "Mechanisms of sensory transduction in the skin," *Nature*, vol. 445, no. 7130, pp. 858–865, 02/22 2007. [Cited on pages 55 and 66]

[143] E. Biddiss, D. Beaton, and T. Chau, "Consumer design priorities for upper limb prosthetics," *Disability and Rehabilitation: Assistive Technology*, vol. 2, no. 6, pp. 346–357, 2007. [Cited on page 56]

[144] E. D. Engeberg, "A physiological basis for control of a prosthetic hand," *Biomedical Signal*

Processing and Control, vol. 8, no. 1, pp. 6–15, 1 2013. [Cited on page 56]

[145] J. J. Cabibihan, R. Pradipta, and S. S. Ge, "Prosthetic finger phalanges with lifelike skin compliance for low-force social touching interactions," *Journal of Neuroengineering and Rehabilitation*, vol. 8, no. 16, 2011. [Cited on page 56]

[146] E. M. Izhikevich, "Simple model of spiking neurons," *IEEE Transactions on Neural Networks*, vol. 14, no. 6, pp. 1569–1572, 2003. [doi] [Cited on pages 56, 88, 97, 102, and 104]

[147] U. B. Rongala, A. Mazzoni, and C. M. Oddo, "Neuromorphic artificial touch for categorization of naturalistic textures," *IEEE Transactions on Neural Networks and Learning Systems*, vol. 28, no. 4, pp. 819–829, 2015. [Cited on page 56]

[148] S.-C. Liu and T. Delbruck, "Neuromorphic sensory systems," *Current Opinion in Neurobiology*, vol. 20, no. 3, pp. 288–295, 6// 2010. [Cited on page 56]

[149] D. Rager, D. Alvares, I. Birznieks, S. Redmond, J. Morley, N. Lovell, and R. Vickery, "Generating tactile afferent stimulation patterns for slip and touch feedback in neural prosthetics," in *International Conference of the IEEE Engineering in Medicine and Biology Society (EMBC)*, July 2013, pp. 5922–5925. [doi] [Cited on page 57]

[150] A. F. Russell, R. S. Armiger, R. J. Vogelstein, S. J. Bensmaia, and R. Etienne-Cummings, "Real-time implementation of biofidelic sa1 model for tactile feedback," in *International Conference of the IEEE Engineering in Medicine and Biology Society (EMBC)*, 2009, pp. 185–188. [Cited on page 57]

[151] S. S. Kim, A. Sripati, R. Vogelstein, R. Armiger, A. Russell, and S. Bensmaia, "Conveying tactile feedback in sensorized hand neuroprostheses using a biofidelic model of mechanotransduction," *IEEE Transactions on Biomedical Circuits and Systems*, vol. 3, no. 6, pp. 398–404, Dec 2009. [Cited on page 57]

[152] W. W. Lee, C. H. Yeow, H. Ren, S. L. Kukreja, and N. V. Thakor, "Fpga implementation of a fa-1 mechanoreceptor model for efficient representation of tactile features," in *2016 6th IEEE International Conference on Biomedical Robotics and Biomechatronics (BioRob)*, 2016, pp. 243–246. [doi] [Cited on page 57]

[153] W. Gerstner and W. Kistler, *Spiking Neuron Models: Single Neurons, Populations, Plasticity*. Cambridge University Press, 2002. [Cited on pages 57 and 58]

[154] R. S. Johansson and J. R. Flanagan, "Coding and use of tactile signals from the fingertips in object manipulation tasks," *Nature Reviews Neuroscience*, vol. 10, no. 5, pp. 345–359, 2009. [doi] [Cited on pages 78, 79, and 112]

[155] J. Scheibert, S. Leurent, A. Prevost, and G. Debregeas, "The role of fingerprints in the coding of tactile information probed with a biomimetic sensor," *Science*, vol. 323, no. 5920, pp. 1503–1506, Mar 13 2009. [Cited on page 79]

[156] E. S. J. Smith and G. R. Lewin, "Nociceptors: a phylogenetic view," *Journal of Comparative Physiology A*, vol. 195, no. 12, pp. 1089–1106, 2009. [doi] [Cited on page 79]

[157] E. Perl, "Myelinated afferent fibres innervating the primate skin and their response to noxious stimuli," *The Journal of Physiology*, vol. 197, no. 3, pp. 593–615, 1968. [doi] [Cited on pages 79 and 104]

[158] D. H. Kim, J. H. Ahn, W. M. Choi, H. S. Kim, T. H. Kim, J. Song, Y. Y. Huang, Z. Liu, C. Lu, and J. A. Rogers, "Stretchable and foldable silicon integrated circuits," *Science*, vol. 320, no. 5875, pp. 507–511, Apr 25 2008. [doi] [Cited on page 80]

[159] C. Larson, B. Peele, S. Li, S. Robinson, M. Totaro, L. Beccai, B. Mazzolai, and R. Shepherd, "Highly stretchable electroluminescent skin for optical signaling and tactile sensing," *Science*, vol. 351, no. 6277, pp. 1071–1074, 03/03 2016. [doi] [Cited on pages 80 and 139]

[160] C.-H. Li, C. Wang, C. Keplinger, J.-L. Zuo, L. Jin, Y. Sun, P. Zheng, Y. Cao, F. Lissel, C. Linder *et al.*, "A highly stretchable autonomous self-healing elastomer," *Nature Chemistry*, vol. 8, no. 6, pp. 618–624, 2016. [doi] [Cited on pages 80, 94, and 139]

[161] C. Kyoung-Yong, S. Y. Jun, J. Eun-Seok, L. Sehan, and H. Chang-Soo, "A self-powered sensor mimicking slow- and fast-adapting cutaneous mechanoreceptors," *Advanced Materials*, vol. 30, no. 12, p. 1706299, 2018. [doi] [Cited on page 80]

[162] B. Bussel, A. Roby-Brami, P. Azouvi, A. Biraben, A. Yakovleff, and J. Held, "Myoclonus in a patient with spinal cord transection: possible involvement of the spinal stepping generator," *Brain*, vol. 111, no. 5, pp. 1235–1245, 1988. [doi] [Cited on pages 81 and 105]

[163] A. Latremoliere and C. J. Woolf, "Central sensitization: a generator of pain hypersensitivity by central neural plasticity," *The Journal of Pain*, vol. 10, no. 9, pp. 895–926, 2009. [doi] [Cited on pages 81 and 105]

[164] G. Chai, X. Sui, S. Li, L. He, and N. Lan, "Characterization of evoked tactile sensation in forearm amputees with transcutaneous electrical nerve stimulation," *Journal of Neural Engineering*, vol. 12, no. 6, p. 066002, 2015. [doi] [Cited on page 85]

[165] G. Schalk and J. Mellinger, "Brain–computer interfaces," in *A Practical Guide to Brain–Computer Interfacing with BCI2000*. Springer, London, 2010, ch. 2, pp. 9–35. [doi] [Cited on page 86]

[166] C. Hartley, E. P. Duff, G. Green, G. S. Mellado, A. Worley, R. Rogers, and R. Slater, "Nociceptive brain activity as a measure of analgesic efficacy in infants," *Science Translational Medicine*, vol. 9, no. 388, p. eaah6122, 2017. [doi] [Cited on page 100]

[167] F. Mancini, C. F. Sambo, J. D. Ramirez, D. L. Bennett, P. Haggard, and G. D. Iannetti, "A fovea for pain at the fingertips," *Current Biology*, vol. 23, no. 6, pp. 496 – 500, 2013. [doi] [Cited on page 101]

[168] M. Serrao, F. Pierelli, R. Don, A. Ranavolo, A. Cacchio, A. Currà, G. Sandrini, M. Frascarelli, and V. Santilli, "Kinematic and electromyographic study of the nociceptive withdrawal reflex in the upper limbs during rest and movement," *Journal of Neuroscience*, vol. 26, no. 13, pp. 3505–3513, 2006. [doi] [Cited on page 105]

[169] H. Forssberg, A. C. Eliasson, H. Kinoshita, R. S. Johansson, and G. Westling, "Development of human precision grip i: Basic coordination of force," *Experimental Brain Research*, vol. 85, no. 2, pp. 451–457, 1991. [Cited on page 112]

[170] H. Forssberg, H. Kinoshita, A. C. Eliasson, R. S. Johansson, G. Westling, and A. M. Gordon, "Development of human precision grip ii: Anticipatory control of isometric forces targeted for object's weight," *Experimental Brain Research*, vol. 90, no. 2, pp. 393–398, 1992. [doi]

[Cited on page 112]

[171] D. Wolpert, Z. Ghahramani, and M. Jordan, "An internal model for sensorimotor integration," *Science*, vol. 269, no. 5232, pp. 1880–1882, 1995. [doi] [Cited on page 112]

[172] R. Shadmehr, M. A. Smith, and J. W. Krakauer, "Error correction, sensory prediction, and adaptation in motor control," *Annual Review of Neuroscience*, vol. 33, no. 1, pp. 89–108, 2010. [doi] [Cited on pages 112, 127, and 140]

[173] A. W. Shehata, L. F. Engels, M. Controzzi, C. Cipriani, E. J. Scheme, and J. W. Sensinger, "Improving internal model strength and performance of prosthetic hands using augmented feedback," *Journal of NeuroEngineering and Rehabilitation*, vol. 15, no. 1, p. 70, Jul 2018. [doi] [Cited on page 113]

[174] V. S. Ramachandran and W. Hirstein, "The perception of phantom limbs," *Brain*, vol. 121, no. 9, pp. 1603–1630, 1998. [doi] [Cited on page 113]

[175] E. L. Graczyk, L. Resnik, M. A. Schiefer, M. S. Schmitt, and D. J. Tyler, "Home use of a neural-connected sensory prosthesis provides the functional and psychosocial experience of having a hand again," *Scientific Reports*, vol. 8, no. 1, p. 9866, 2018. [doi] [Cited on pages 113, 125, and 140]

[176] G. Valle, A. Mazzoni, F. Iberite, E. D'Anna, I. Strauss, G. Granata, M. Controzzi, F. Clemente, G. Rognini, C. Cipriani, T. Stieglitz, F. M. Petrini, P. M. Rossini, and S. Micera, "Biomimetic intraneural sensory feedback enhances sensation naturalness, tactile sensitivity, and manual dexterity in a bidirectional prosthesis," *Neuron*, vol. 100, no. 1, pp. 37 – 45.e7, 2018. [doi] [Cited on page 113]

[177] B. Hudgins, P. Parker, and R. N. Scott, "A new strategy for multifunction myoelectric control," *IEEE Transactions on Biomedical Engineering*, vol. 40, no. 1, pp. 82–94, 1993. [doi] [Cited on page 113]

[178] C. Dietrich, K. Walter-Walsh, S. Preißler, G. O. Hofmann, O. W. Witte, W. H. Miltner, and T. Weiss, "Sensory feedback prosthesis reduces phantom limb pain: Proof of a principle," *Neuroscience Letters*, vol. 507, no. 2, pp. 97 – 100, 2012. [doi] [Cited on page 114]

[179] A. M. D. Nunzio, M. A. Schweisfurth, N. Ge, D. Falla, J. Hahne, K. Gödecke, F. Petzke, M. Siebertz, P. Dechent, T. Weiss, H. Flor, B. Graimann, O. C. Aszmann, and D. Farina, "Relieving phantom limb pain with multimodal sensory-motor training," *Journal of Neural Engineering*, vol. 15, no. 6, p. 066022, 2018. [doi] [Cited on page 114]

[180] D. M. Page, J. A. George, D. T. Kluger, C. Duncan, S. Wendelken, T. Davis, D. T. Hutchinson, and G. A. Clark, "Motor control and sensory feedback enhance prosthesis embodiment and reduce phantom pain after long-term hand amputation," *Frontiers in Human Neuroscience*, vol. 12, p. 352, 2018. [doi] [Cited on page 114]

[181] M. Ortiz-Catalan, R. A. Guðmundsdóttir, M. B. Kristoffersen, A. Zepeda-Echavarria, K. Caine-Winterberger, K. Kulbacka-Ortiz, C. Widehammar, K. Eriksson, A. Stockselius, C. Ragnö, Z. Pihlar, H. Burger, and L. Hermansson, "Phantom motor execution facilitated by machine learning and augmented reality as treatment for phantom limb pain: a single group, clinical trial in patients with chronic intractable phantom limb pain," *The Lancet*, vol. 388,

no. 10062, pp. 2885 – 2894, 2016. [doi] [Cited on page 114]

[182] S. Kikkert, M. Mezue, D. H. Slater, H. Johansen-Berg, I. Tracey, and T. R. Makin, "Motor correlates of phantom limb pain," *Cortex*, vol. 95, pp. 29 – 36, 2017. [doi] [Cited on page 114]

[183] A. Chen, J. Yao, T. A. Kuiken, and J. P. A. Dewald, "Cortical motor activity and reorganization following upper-limb amputation and subsequent targeted reinnervation," *NeuroImage: Clinical*, vol. 3, pp. 498 – 506, 2013. [doi] [Cited on page 114]

[184] S. Kikkert, J. Kolasinski, S. Jbabdi, I. Tracey, C. F. Beckmann, H. Johansen-Berg, and T. R. Makin, "Revealing the neural fingerprints of a missing hand," *eLife*, vol. 5, p. e15292, aug 2016. [doi] [Cited on page 114]

[185] C. Mercier, K. T. Reilly, C. D. Vargas, A. Aballea, and A. Sirigu, "Mapping phantom movement representations in the motor cortex of amputees," *Brain*, vol. 129, no. 8, pp. 2202–2210, 2006. [doi] [Cited on page 114]

[186] J. Andoh, M. Diers, C. Milde, C. Frobel, D. Kleinböhl, and H. Flor, "Neural correlates of evoked phantom limb sensations," *Biological Psychology*, vol. 126, pp. 89 – 97, 2017. [doi] [Cited on page 115]

[187] C. Neuper, R. Scherer, M. Reiner, and G. Pfurtscheller, "Imagery of motor actions: Differential effects of kinesthetic and visual–motor mode of imagery in single-trial eeg," *Cognitive Brain Research*, vol. 25, no. 3, pp. 668 – 677, 2005. [doi] [Cited on pages 122 and 132]

[188] C. Neuper, R. Scherer, S. Wriessnegger, and G. Pfurtscheller, "Motor imagery and action observation: Modulation of sensorimotor brain rhythms during mental control of a brain–computer interface," *Clinical Neurophysiology*, vol. 120, no. 2, pp. 239 – 247, 2009. [doi] [Cited on pages 122 and 132]

[189] C. A. Porro, M. P. Francescato, V. Cettolo, M. E. Diamond, P. Baraldi, C. Zuiani, M. Bazzocchi, and P. E. di Prampero, "Primary motor and sensory cortex activation during motor performance and motor imagery: A functional magnetic resonance imaging study," *Journal of Neuroscience*, vol. 16, no. 23, pp. 7688–7698, 1996. [doi] [Cited on page 127]

[190] G. Pfurtscheller and C. Neuper, "Motor imagery activates primary sensorimotor area in humans," *Neuroscience Letters*, vol. 239, no. 2, pp. 65 – 68, 1997. [doi] [Cited on page 127]

[191] D. Zhao, Y.-D. Zhou, M. Bodner, and Y. Ku, "The causal role of the prefrontal cortex and somatosensory cortex in tactile working memory," *Cerebral Cortex*, vol. 28, no. 10, pp. 3468–3477, 2018. [doi] [Cited on page 127]

[192] J. A. Harris, C. Miniussi, I. M. Harris, and M. E. Diamond, "Transient storage of a tactile memory trace in primary somatosensory cortex," *Journal of Neuroscience*, vol. 22, no. 19, pp. 8720–8725, 2002. [doi] [Cited on page 127]

[193] T. R. Makin, J. Scholz, D. Henderson Slater, H. Johansen-Berg, and I. Tracey, "Reassessing cortical reorganization in the primary sensorimotor cortex following arm amputation," *Brain*, vol. 138, no. 8, pp. 2140–2146, 2015. [doi] [Cited on page 128]

[194] B. Philip, K. Valyear, C. Cirstea, and S. Frey, "Reorganization of primary somatosensory cortex after upper limb amputation may lack functional significance," *Archives of Physical*

Medicine and Rehabilitation, vol. 98, no. 10, p. e103, 2017. [doi] [Cited on page 128]

[195] M. Gomez-Rodriguez, J. Peters, J. Hill, B. Schölkopf, A. Gharabaghi, and M. Grosse-Wentrup, "Closing the sensorimotor loop: haptic feedback facilitates decoding of motor imagery," *Journal of Neural Engineering*, vol. 8, no. 3, p. 036005, 2011. [doi] [Cited on page 128]

[196] J. Yao, A. Chen, T. Kuiken, C. Carmona, and J. Dewald, "Sensory cortical re-mapping following upper-limb amputation and subsequent targeted reinnervation: A case report," *NeuroImage: Clinical*, vol. 8, pp. 329 – 336, 2015. [doi] [Cited on page 128]

[197] G. Lundborg, A. Waites, A. Björkman, B. Rosén, and E.-M. Larsson, "Functional magnetic resonance imaging shows cortical activation on sensory stimulation of an osseointegrated prosthetic thumb." *Scandinavian Journal of Plastic Surgery and Hand Surgery*, vol. 40, no. 4, pp. 234–239, 2006. [doi] [Cited on page 128]

[198] G. Rognini, F. M. Petrini, S. Raspopovic, G. Valle, G. Granata, I. Strauss, M. Solcà, J. Bello-Ruiz, B. Herbelin, R. Mange, E. D'Anna, R. Di Iorio, G. Di Pino, D. Andreu, D. Guiraud, T. Stieglitz, P. M. Rossini, A. Serino, S. Micera, and O. Blanke, "Multisensory bionic limb to achieve prosthesis embodiment and reduce distorted phantom limb perceptions," *Journal of Neurology, Neurosurgery & Psychiatry*, vol. 0, no. 0, pp. 1–3, 2018. [doi] [Cited on page 129]

[199] Z. Wang, A. C. Bovik, H. R. Sheikh, and E. P. Simoncelli, "Image quality assessment: from error visibility to structural similarity," *IEEE Transactions on Image Processing*, vol. 13, no. 4, pp. 600–612, 2004. [doi] [Cited on page 130]

[200] G. Gómez-Herrero, "Automatic artifact removal (aar) toolbox v1. 3 (release 09.12. 2007) for matlab," 2007. [Cited on page 131]

[201] A. Delorme and S. Makeig, "Eeglab: an open source toolbox for analysis of single-trial eeg dynamics including independent component analysis," *Journal of Neuroscience Methods*, vol. 134, no. 1, pp. 9 – 21, 2004. [doi] [Cited on page 132]

[202] S. J. Luck, "Event-related potentials," *APA handbook of research methods in psychology*, vol. 1, pp. 523–546, 2012. [Cited on page 132]

[203] Z. Tayeb, N. Waniek, J. Fedjaev, N. Ghaboosi, L. Rychly, C. Widderich, C. Richter, J. Braun, M. Saveriano, G. Cheng, and J. Conradt, "Gumpy: a python toolbox suitable for hybrid brain–computer interfaces," *Journal of Neural Engineering*, vol. 15, no. 6, p. 065003, 2018. [doi] [Cited on page 132]

[204] M. Grosse-Wentrup and M. Buss, "Multiclass common spatial patterns and information theoretic feature extraction," *IEEE Transactions on Biomedical Engineering*, vol. 55, no. 8, pp. 1991–2000, 2008. [doi] [Cited on page 132]

[205] K. Englehart, B. Hudgins, P. Parker, and M. Stevenson, "Classification of the myoelectric signal using time-frequency based representations," *Medical Engineering & Physics*, vol. 21, no. 6, pp. 431 – 438, 1999. [doi] [Cited on page 134]

Vita

Luke Emmett Osborn was born in Little Rock, AR in 1989 and was homeschooled up until his junior year of high school when he attended Little Rock Central High School. He received a B.S. from the Department of Mechanical Engineering and a minor in physics from the University of Arkansas in 2012. He received an M.S.E. from the Department of Biomedical Engineering at Johns Hopkins University in 2014. He enrolled in the Ph.D. program in the Department of Biomedical Engineering at Johns Hopkins School of Medicine in 2014. He was inducted into the Tau Beta Pi and Pi Tau Sigma honor societies in 2011, was awarded the Mechanical Engineering Department's Senior Scholar Award in 2012 at the University of Arkansas, received a National Science Foundation Research Undergraduate Fellowship in 2011, and received two undergraduate research fellowships from 2011 - 2012. He received the TA of the Year Award from the Department of Biomedical Engineering in 2016. He received the award for Best Live Demonstration at the 2017 IEEE International Biomedical Circuits and Sys-

tems Conference. He was named a Siebel Scholar for 2018 - 2019 and was selected as a member of the Forbes 30 Under 30 in Science for 2019. His research focuses on biologically inspired sensors for prosthetic limbs as well as using neuromorphic techniques for providing sensory feedback to amputees. His work has been featured in several media outlets including Wired, National Public Radio, The Atlantic, IEEE Spectrum, Reuters, World Economic Forum, The Times, and Le Monde. To date, he is an author on 5 journal papers, 1 book chapter, and 17 peer-reviewed conference papers. He plans to continue working in the neuroengineering field to develop new technologies for rehabilitation, neuroprostheses, and human augmentation.